lattice QCD and the hadron spectrum

Jozef Dudek

hadron spectrum collaboration
hadspec.org

WILLIAM & MARY
CHARTERED 1693

Jefferson Lab
Thomas Jefferson National Accelerator Facility

contents

meson spectroscopy *"illustrating the problem"*

- resonances, scattering, elastic phase-shifts

lattice QCD *"introducing the tool"*

- discrete spectrum, finite volume, computing the spectrum

elastic scattering *"solving the simplest problem"*

- lattice QCD phase-shift results

coupled-channel scattering *"a more realistic situation"*

- mapping the discrete spectrum to the t-matrix
- lattice QCD calculation results

the complex energy plane *"well-defined quantities"*

- rigorously determining resonances

producing meson resonances

some example processes:

heavy flavour decays

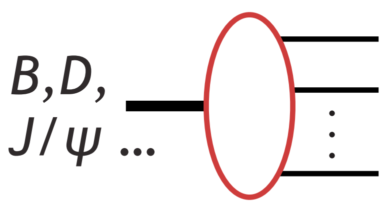

e.g. LHCb

peripheral meson hadroproduction

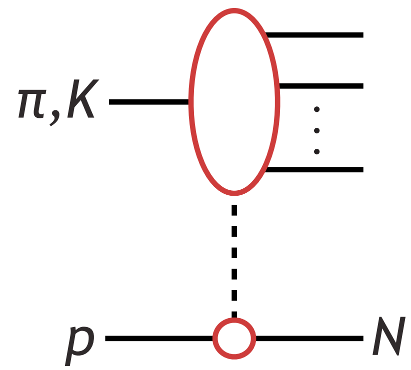

e.g. COMPASS

peripheral meson photoproduction

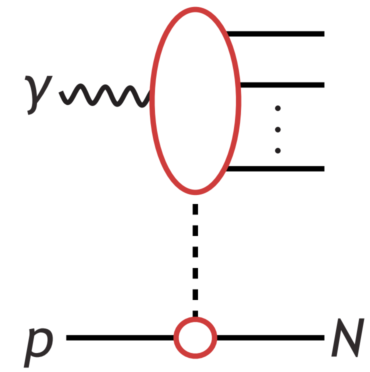

e.g. GlueX

two photon fusion

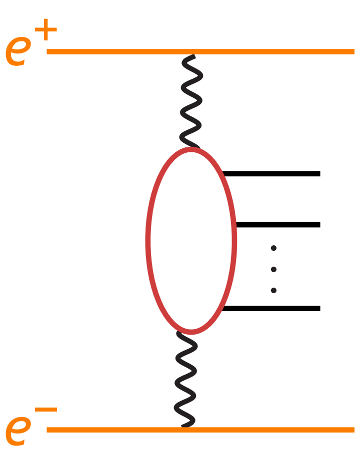

e.g. Belle

e^+e^- annihilation

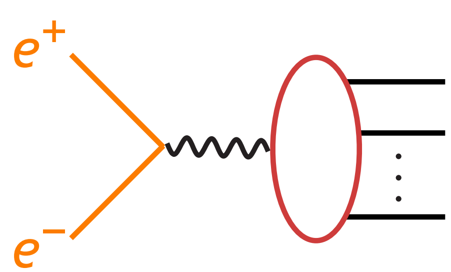

e.g. BES III

central production

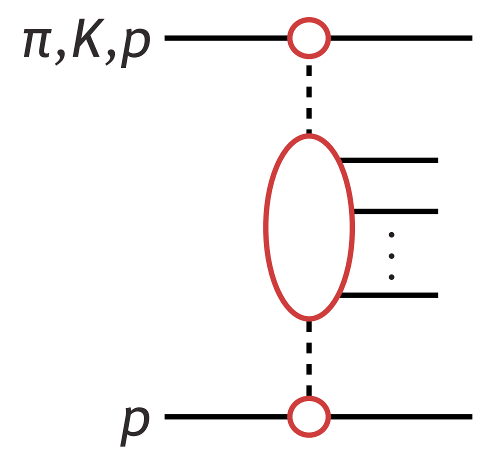

e.g. WA102

$p\bar{p}$ annihilation

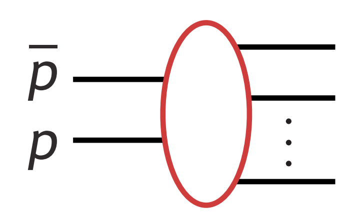

e.g. Crystal Barrel

many decades of accumulated data ...

'straightforward' coupled-channel resonances

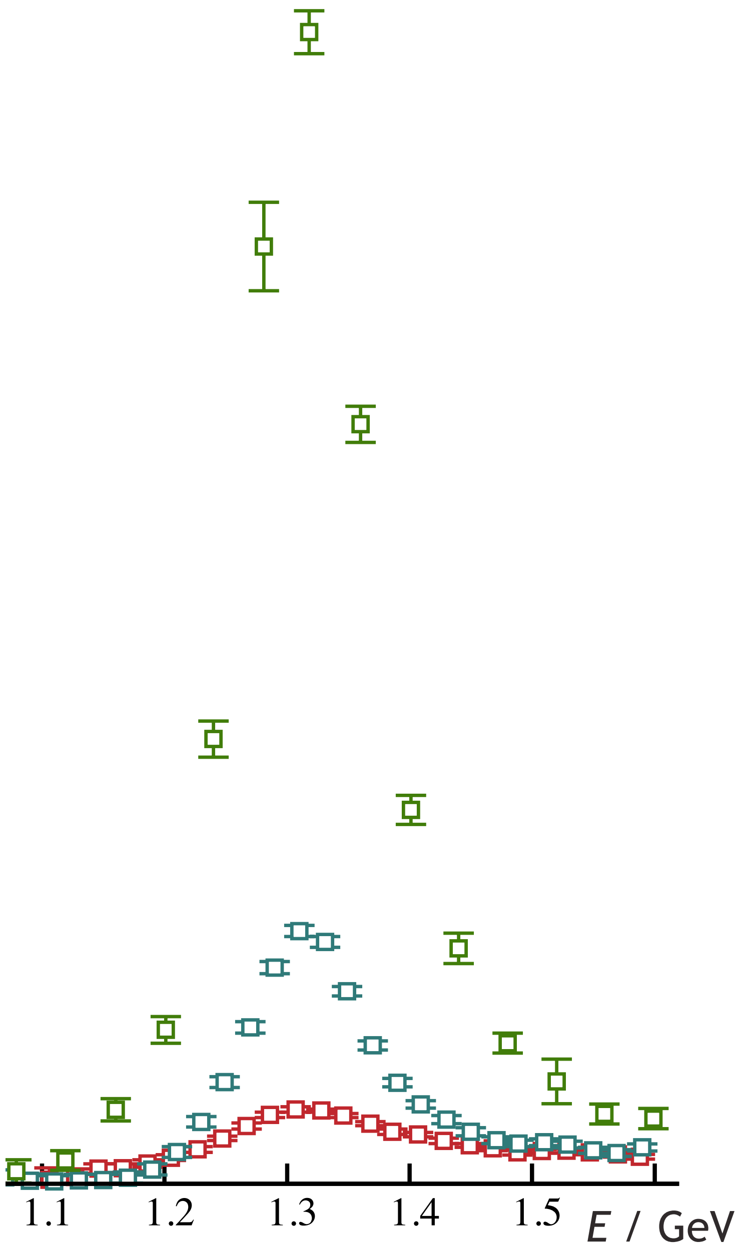

$\pi\,\mathrm{Pb} \to \pi\rho\,\mathrm{Pb}$ COMPASS

$\gamma\gamma \to \pi\eta$ Belle

$\pi p \to K\overline{K}\,p$ CERN SPS

same 'bump' appears in multiple different processes

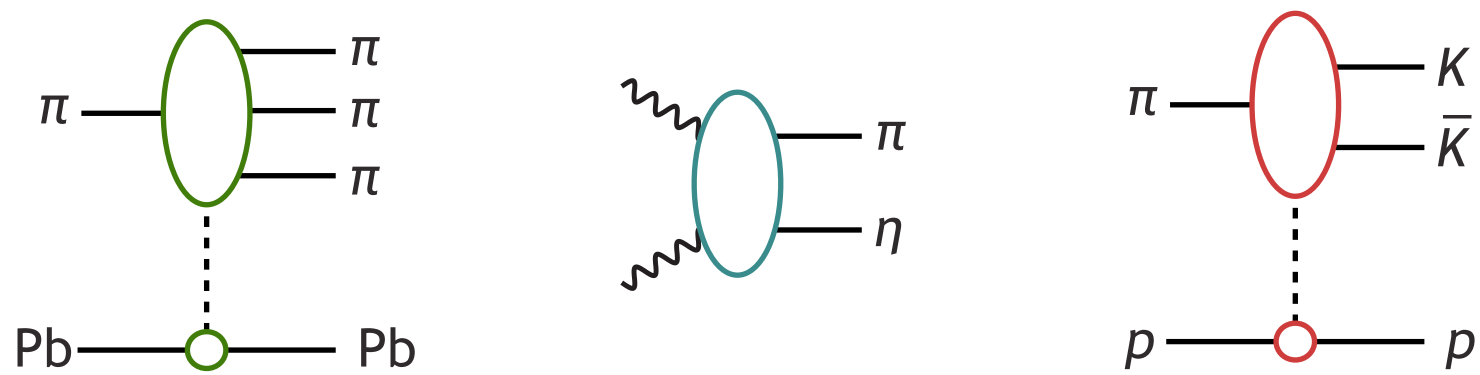

‘straightforward’ **coupled-channel** resonances

$a_2(1320)$

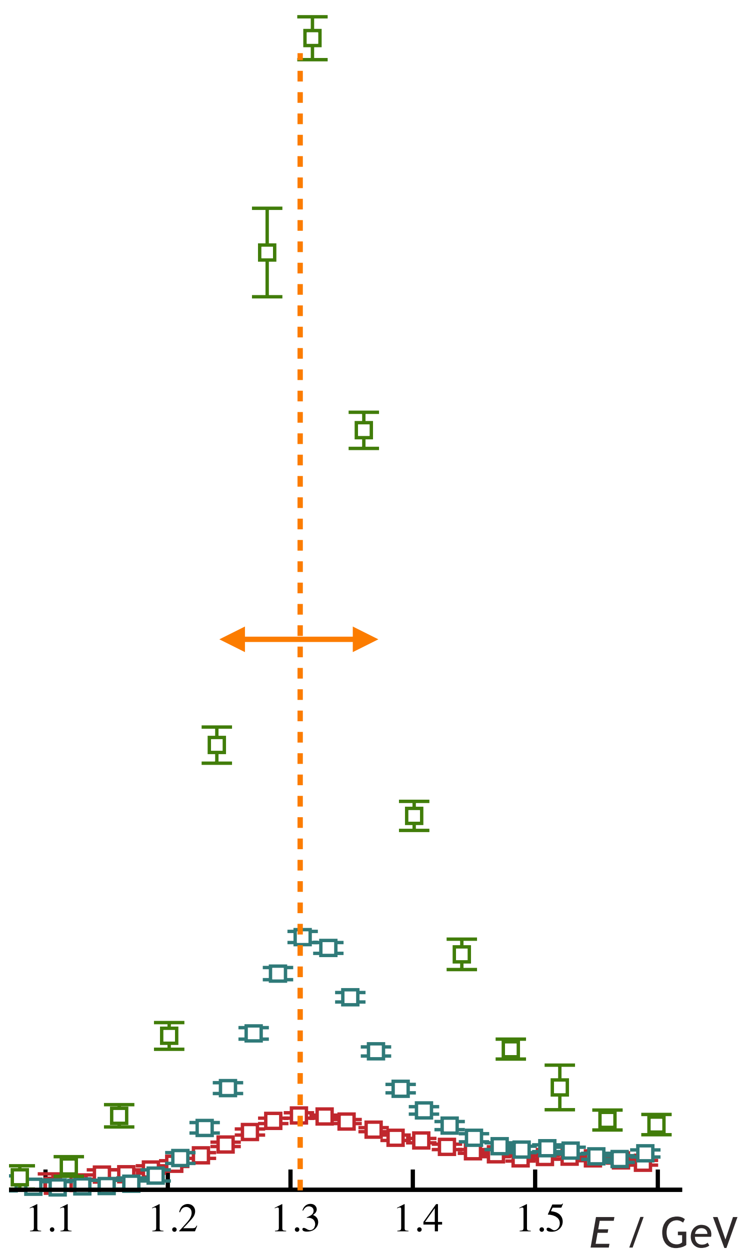

$\pi\,\mathrm{Pb} \to \pi\rho\,\mathrm{Pb}$ COMPASS

$\gamma\gamma \to \pi\eta$ Belle

$\pi p \to K\overline{K}\, p$ CERN SPS

same ‘bump’ appears in multiple different processes …

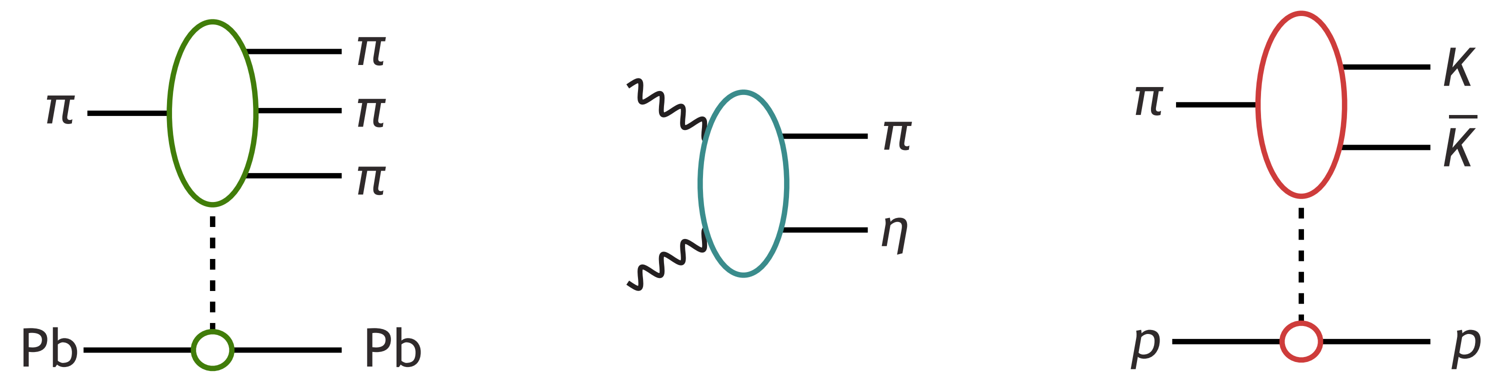

… due to same **a_2 resonance**

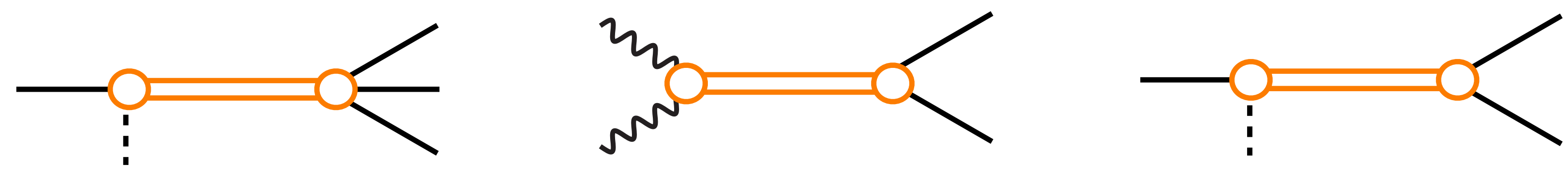

pdg summary entry

$a_2(1320)$ $I^G(J^{PC}) = 1^-(2^{++})$

Mass $m = 1318.3^{+0.5}_{-0.6}$ MeV

Full width $\Gamma = 107 \pm 5$ MeV

$a_2(1320)$ DECAY MODES	Fraction (Γ_i/Γ)
3π	(70.1 ± 2.7) %
$\eta\pi$	(14.5 ± 1.2) %
$\omega\pi\pi$	(10.6 ± 3.2) %
$K\overline{K}$	(4.9 ± 0.8) %
$\eta'(958)\pi$	$(5.5 \pm 0.9) \times 10^{-3}$
$\pi^\pm\gamma$	$(2.91 \pm 0.27) \times 10^{-3}$
$\gamma\gamma$	$(9.4 \pm 0.7) \times 10^{-6}$

the experimental excited meson spectrum

pdg meson listings

LIGHT UNFLAVORED ($S = C = B = 0$)

	$I^G(J^{PC})$		$I^G(J^{PC})$
• $\pi^\pm$	$1^-(0^-)$	• $\rho_3(1690)$	$1^+(3^{--})$
• π^0	$1^-(0^{-+})$	• $\rho(1700)$	$1^+(1^{--})$
• η	$0^+(0^{-+})$	$a_2(1700)$	$1^-(2^{++})$
• $f_0(500)$	$0^+(0^{++})$	• $f_0(1710)$	$0^+(0^{++})$
• $\rho(770)$	$1^+(1^{--})$	$\eta(1760)$	$0^+(0^{-+})$
• $\omega(782)$	$0^-(1^{--})$	• $\pi(1800)$	$1^-(0^{-+})$
• $\eta'(958)$	$0^+(0^{-+})$	$f_2(1810)$	$0^+(2^{++})$
• $f_0(980)$	$0^+(0^{++})$	$X(1835)$	$?^?(0^{-+})$
• $a_0(980)$	$1^-(0^{++})$	$X(1840)$	$?^?(?^{??})$
• $\phi(1020)$	$0^-(1^{--})$	$a_1(1420)$	$1^-(1^{++})$
• $h_1(1170)$	$0^-(1^{+-})$	• $\phi_3(1850)$	$0^-(3^{--})$
• $b_1(1235)$	$1^+(1^{+-})$	$\eta_2(1870)$	$0^+(2^{-+})$
• $a_1(1260)$	$1^-(1^{++})$	• $\pi_2(1880)$	$1^-(2^{-+})$
• $f_2(1270)$	$0^+(2^{++})$	$\rho(1900)$	$1^+(1^{--})$
• $f_1(1285)$	$0^+(1^{++})$	$f_2(1910)$	$0^+(2^{++})$
• $\eta(1295)$	$0^+(0^{-+})$	$a_0(1950)$	$1^-(0^{++})$
• $\pi(1300)$	$1^-(0^{-+})$	• $f_2(1950)$	$0^+(2^{++})$
• $a_2(1320)$	$1^-(2^{++})$	$\rho_3(1990)$	$1^+(3^{--})$
• $f_0(1370)$	$0^+(0^{++})$	• $f_2(2010)$	$0^+(2^{++})$
$h_1(1380)$	$?^-(1^{+-})$	$f_0(2020)$	$0^+(0^{++})$
• $\pi_1(1400)$	$1^-(1^{-+})$	• $a_4(2040)$	$1^-(4^{++})$
• $\eta(1405)$	$0^+(0^{-+})$	• $f_4(2050)$	$0^+(4^{++})$
• $f_1(1420)$	$0^+(1^{++})$	$\pi_2(2100)$	$1^-(2^{-+})$
• $\omega(1420)$	$0^-(1^{--})$	$f_0(2100)$	$0^+(0^{++})$
$f_2(1430)$	$0^+(2^{++})$	$f_2(2150)$	$0^+(2^{++})$

STRANGE ($S = \pm 1$, $C = B = 0$)

	$I(J^P)$
• $K^\pm$	$1/2(0^-)$
• K^0	$1/2(0^-)$
• K^0_S	$1/2(0^-)$
• K^0_L	$1/2(0^-)$
$K_0^*(800)$	$1/2(0^+)$
• $K^*(892)$	$1/2(1^-)$
• $K_1(1270)$	$1/2(1^+)$
• $K_1(1400)$	$1/2(1^+)$
• $K^*(1410)$	$1/2(1^-)$
• $K_0^*(1430)$	$1/2(0^+)$
• $K_2^*(1430)$	$1/2(2^+)$
$K(1460)$	$1/2(0^-)$
$K_2(1580)$	$1/2(2^-)$
$K(1630)$	$1/2(?^?)$
$K_1(1650)$	$1/2(1^+)$
• $K^*(1680)$	$1/2(1^-)$
• $K_2(1770)$	$1/2(2^-)$
• $K_3^*(1780)$	$1/2(3^-)$
• $K_2(1820)$	$1/2(2^-)$
$K(1830)$	$1/2(0^-)$
$K_0^*(1950)$	$1/2(0^+)$
$K_2^*(1980)$	$1/2(2^+)$
• $K_4^*(2045)$	$1/2(4^+)$
$K_2(2250)$	$1/2(2^-)$

CHARMED, STRANGE ($C = S = \pm 1$)

	$I(J^P)$
• $D_s^\pm$	$0(0^-)$
• $D_s^{*\pm}$	$0(?^?)$
• $D_{s0}^*(2317)^\pm$	$0(0^+)$
• $D_{s1}(2460)^\pm$	$0(1^+)$
• $D_{s1}(2536)^\pm$	$0(1^+)$
• $D_{s2}(2573)$	$0(2^+)$
• $D_{s1}^*(2700)^\pm$	$0(1^-)$
$D_{s1}^*(2860)^\pm$	$0(1^-)$
$D_{s3}^*(2860)^\pm$	$0(3^-)$
$D_{sJ}(3040)^\pm$	$0(?^?)$

BOTTOM ($B = \pm 1$)

• $B^\pm$	$1/2(0^-)$
• B^0	$1/2(0^-)$
• $B^\pm/B^0$ ADMIXTURE	
• $B^\pm/B^0/B^0_s/b$-baryon ADMIXTURE	
V_{cb} and V_{ub} CKM Matrix Elements	
• B^*	$1/2(1^-)$
• $B_1(5721)^+$	$1/2(1^+)$
• $B_1(5721)^0$	$1/2(1^+)$
$B_J^*(5732)$	$?(?^?)$
• $B_2^*(5747)^+$	$1/2(2^+)$
• $B_2^*(5747)^0$	$1/2(2^+)$

$c\bar{c}$

	$I^G(J^{PC})$
• $\eta_c(1S)$	$0^+(0^{-+})$
• $J/\psi(1S)$	$0^-(1^{--})$
• $\chi_{c0}(1P)$	$0^+(0^{++})$
• $\chi_{c1}(1P)$	$0^+(1^{++})$
• $h_c(1P)$	$?^?(1^{+-})$
• $\chi_{c2}(1P)$	$0^+(2^{++})$
• $\eta_c(2S)$	$0^+(0^{-+})$
• $\psi(2S)$	$0^-(1^{--})$
• $\psi(3770)$	$0^-(1^{--})$
• $\psi(3823)$	$?^?(2^{--})$
• $X(3872)$	$0^+(1^{++})$
• $X(3900)$	$1^+(1^{+-})$
• $X(3915)$	$0^+(0/2^{++})$
• $\chi_{c2}(2P)$	$0^+(2^{++})$
$X(3940)$	$?^?(?^{??})$
• $X(4020)$	$1(?^?)$
• $\psi(4040)$	$0^-(1^{--})$
$X(4050)^\pm$	$?(?^?)$
$X(4055)^\pm$	$?(?^?)$
• $X(4140)$	$0^+(1^{++})$
• $\psi(4160)$	$0^-(1^{--})$
$X(4160)$	$?^?(?^{??})$
$X(4200)^\pm$	$?(1^+)$
$X(4230)$	$?^?(1^{--})$
$X(4240)^\pm$	$?^?(0^-)$
$X(4250)^\pm$	$?(?^?)$

pdg.lbl.gov

coupled-channel scattering

evolution from scattering ‘*in*’ state to scattering ‘*out*’ state given by *S*-matrix elements $S_{ij} = \langle \mathrm{out}, i \,|\, \mathrm{in}, j \rangle$

e.g. in coupled $\pi\pi$, $K\overline{K}$ scattering $\mathbf{S} = \begin{pmatrix} S_{\pi\pi,\pi\pi} & S_{\pi\pi,K\overline{K}} \\ S_{K\overline{K},\pi\pi} & S_{K\overline{K},K\overline{K}} \end{pmatrix}$

coupled-channel scattering

evolution from scattering '*in*' state to scattering '*out*' state given by *S*-matrix elements $S_{ij} = \big\langle \mathrm{out}, i \,\big|\, \mathrm{in}, j \big\rangle$

e.g. in coupled *ππ*, *KK̄* scattering $\mathbf{S} = \begin{pmatrix} S_{\pi\pi,\pi\pi} & S_{\pi\pi,K\overline{K}} \\ S_{K\overline{K},\pi\pi} & S_{K\overline{K},K\overline{K}} \end{pmatrix}$

more convenient to work with *t*-matrix $\mathbf{S} = \mathbf{1} + 2i\sqrt{\boldsymbol{\rho}}\cdot\mathbf{t}\cdot\sqrt{\boldsymbol{\rho}}$ typically in partial-waves $t^{(\ell)}_{ij}(E)$

in time-reversal invariant theories, ***t*** is symmetric $\Rightarrow \frac{1}{2}N(N+1)$ *complex* numbers at each energy?

coupled-channel scattering

evolution from scattering '*in*' state to scattering '*out*' state given by *S*-matrix elements $S_{ij} = \langle \mathrm{out}, i \,|\, \mathrm{in}, j \rangle$

e.g. in coupled *ππ*, *KK̅* scattering $\mathbf{S} = \begin{pmatrix} S_{\pi\pi,\pi\pi} & S_{\pi\pi,K\overline{K}} \\ S_{K\overline{K},\pi\pi} & S_{K\overline{K},K\overline{K}} \end{pmatrix}$

more convenient to work with *t*-matrix $\mathbf{S} = \mathbf{1} + 2i\sqrt{\boldsymbol{\rho}} \cdot \mathbf{t} \cdot \sqrt{\boldsymbol{\rho}}$ typically in partial-waves $t^{(\ell)}_{ij}(E)$

in time-reversal invariant theories, ***t*** is symmetric $\Rightarrow \frac{1}{2}N(N+1)$ *complex* numbers at each energy?

conservation of probability, a.k.a. **unitarity** is an important constraint

$$\left(S^\dagger S\right)_{ij} = \sum_k \langle \mathrm{in}, i \,|\, \mathrm{out}, k \rangle \langle \mathrm{out}, k \,|\, \mathrm{in}, j \rangle = \delta_{ij}$$

completeness of outgoing states $1 = \sum_k |\, \mathrm{out}, k \rangle \langle \mathrm{out}, k \,|$

$$\mathrm{Im}\, t_{ij} = \sum_k t^*_{ik}\, \rho_k\, t_{kj}$$

sum over channels kinematically open

or $\boxed{\mathrm{Im}\left(t^{-1}(E)\right)_{ij} = -\delta_{ij}\, \rho_i(E)\, \Theta(E - E_i^{\mathrm{thr.}})}$

$\Rightarrow \frac{1}{2}N(N+1)$ ***real*** numbers at each energy

$\pi\pi$, $K\bar{K}$, $\eta\eta$ S-wave scattering

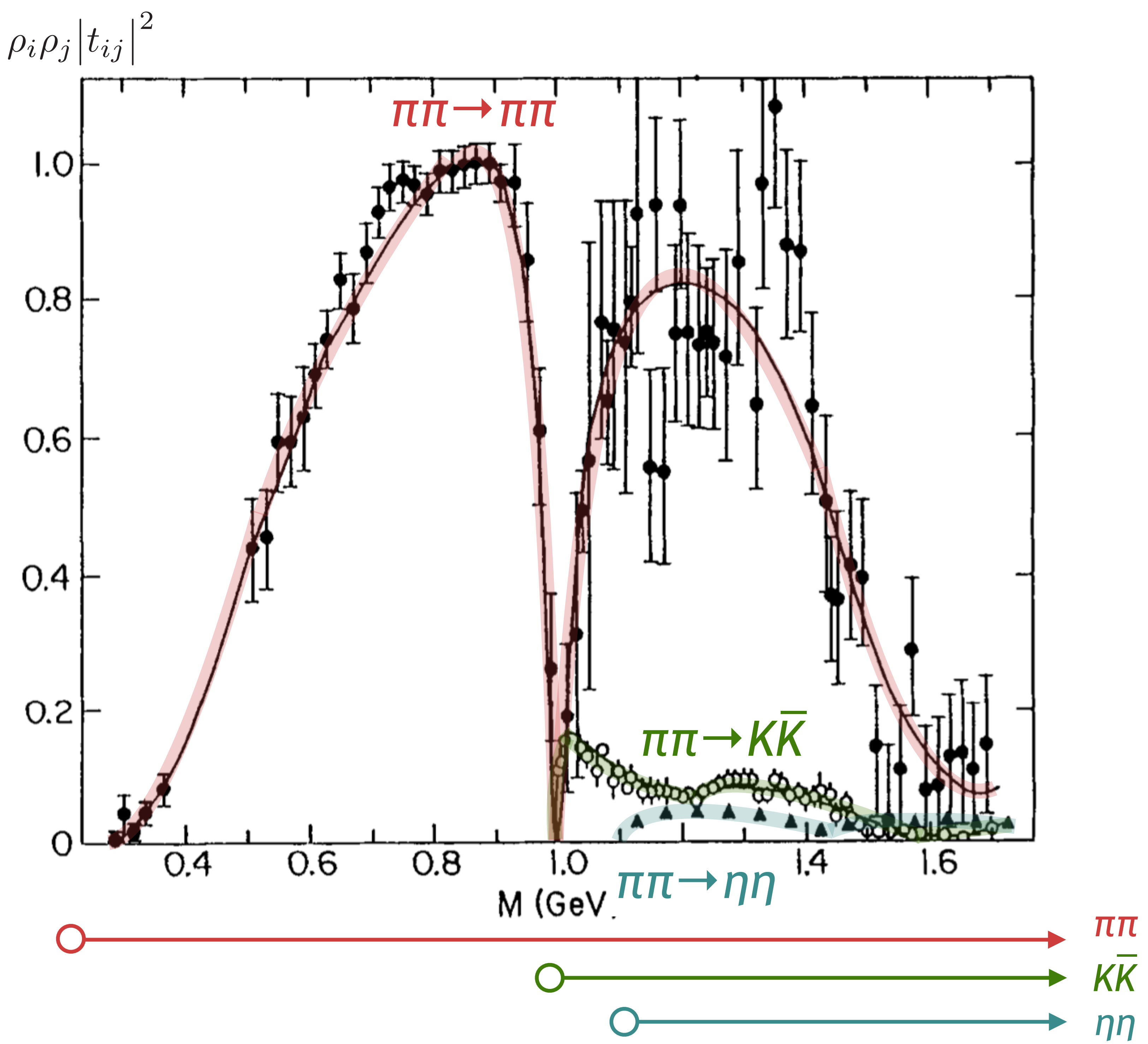

experimentally
quite difficult to fill out
the whole matrix

$$
\begin{array}{cc}
 & \begin{array}{ccc} \pi\pi & K\bar{K} & \eta\eta \end{array} \\
\mathbf{t} = & \begin{pmatrix} \blacksquare & \blacksquare & \blacksquare \\ & \square & \square \\ & & \square \end{pmatrix}
\end{array}
\begin{array}{c} \pi\pi \\ K\bar{K} \\ \eta\eta \end{array}
$$

isolating kaon exchange hard
& η beams don't exist

normalization of $\pi\pi \to K\bar{K}$
also slightly uncertain ...

coupled-channel scattering — a simple resonance model

Flatté form — coupled-channel generalisation of Breit-Wigner

m_π = 300 MeV
m_K = 500 MeV

$$t_{ij}(E) = \frac{g_i\, g_j}{m^2 - E^2 - i g_1^2\, \rho_1 - i g_2^2\, \rho_2}$$

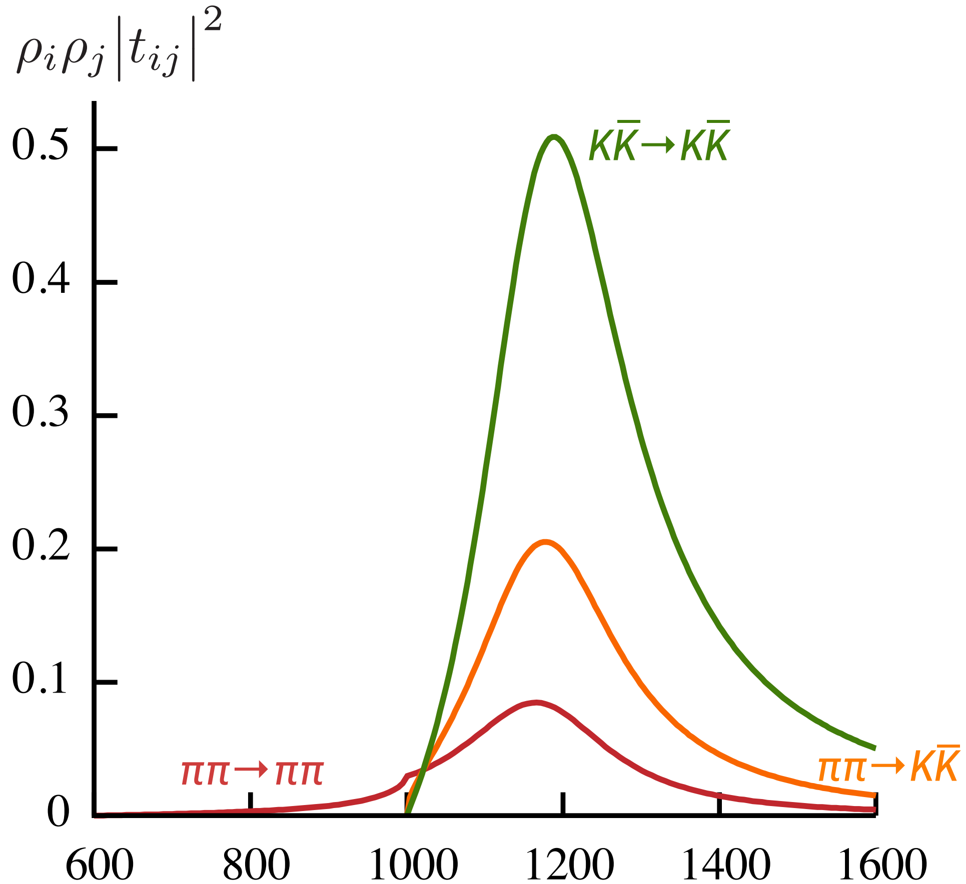

m = 1182 MeV
$g_{\pi\pi}$ = 296 MeV
g_{KK} = 592 MeV

coupled-channel scattering — a simple resonance model

Flatté form — coupled-channel generalisation of Breit-Wigner

m_π = 300 MeV
m_K = 500 MeV

$$t_{ij}(E) = \frac{g_i\, g_j}{m^2 - E^2 - i g_1^2\, \rho_1 - i g_2^2\, \rho_2}$$

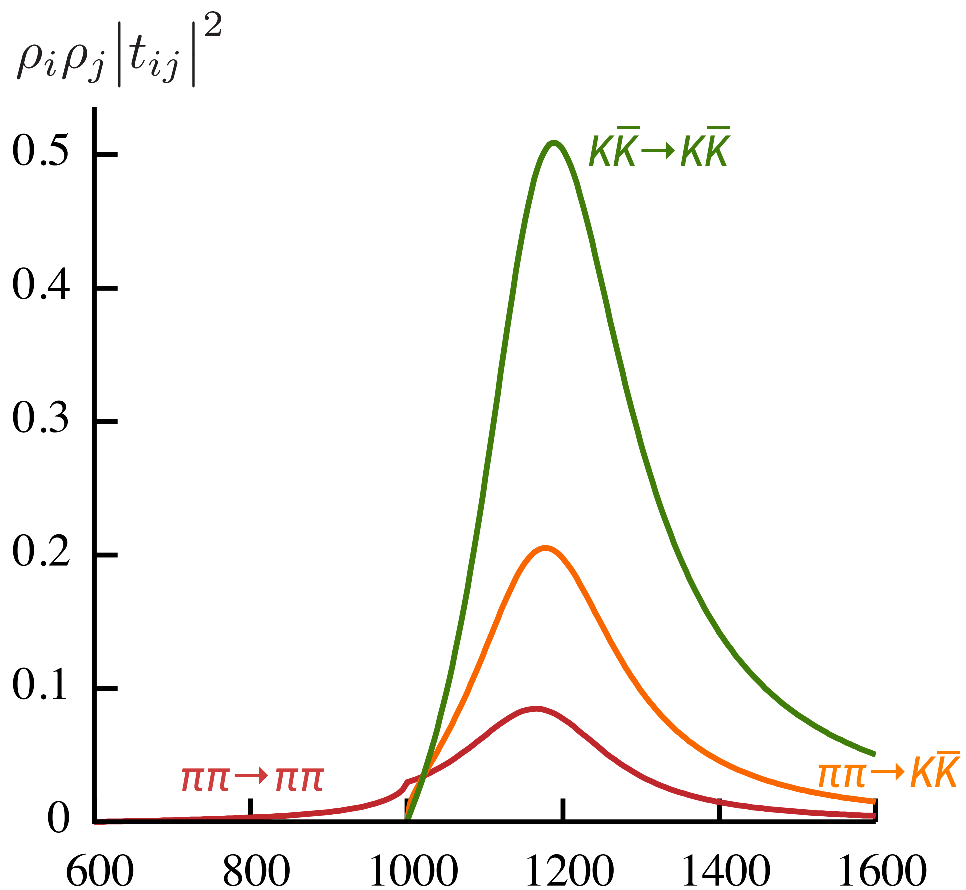

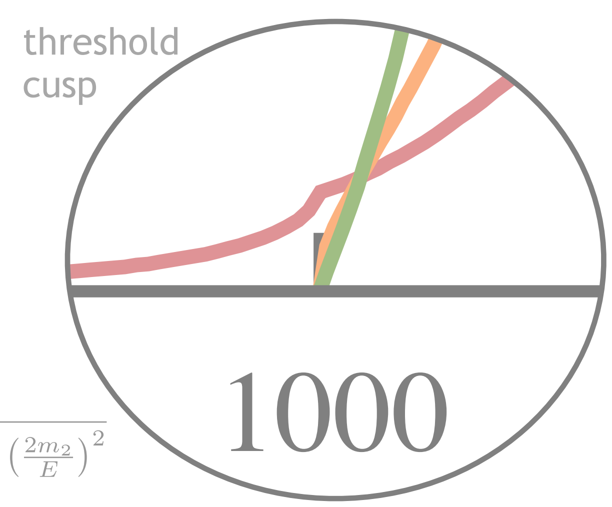

m = 1182 MeV
$g_{\pi\pi}$ = 296 MeV
g_{KK} = 592 MeV

$\rho_2(E) = \sqrt{1 - \left(\frac{2m_2}{E}\right)^2}$

Flatté form — coupled-channel generalisation of Breit-Wigner

m_π = 300 MeV
m_K = 500 MeV

$$t_{ij}(E) = \frac{g_i\, g_j}{m^2 - E^2 - i g_1^2\, \rho_1 - i g_2^2\, \rho_2}$$

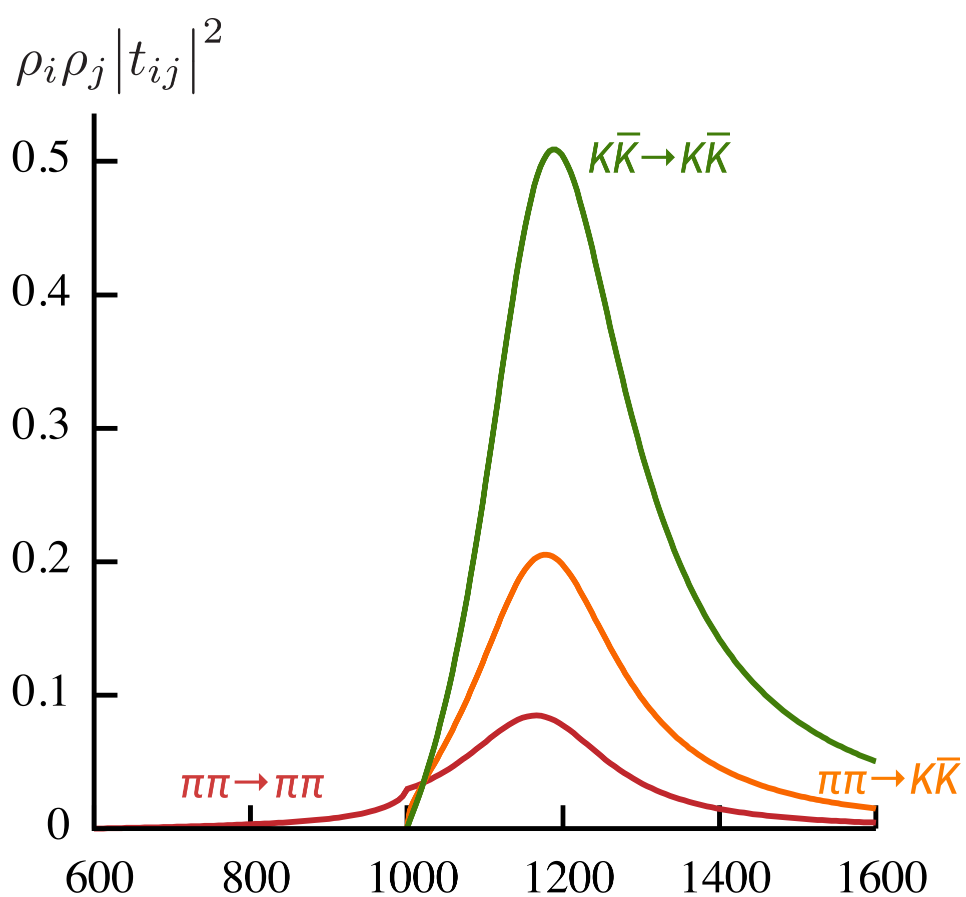

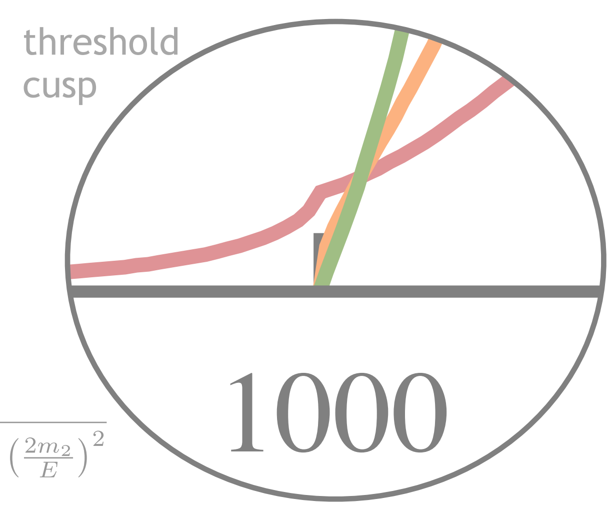

$\rho_2(E) = \sqrt{1 - \left(\frac{2m_2}{E}\right)^2}$

m = 1182 MeV
$g_{\pi\pi}$ = 296 MeV
g_{KK} = 592 MeV

‘phase-shifts’

$$S = \begin{pmatrix} \eta\, e^{2i\delta_1} & i\sqrt{1-\eta^2}\, e^{i(\delta_1+\delta_2)} \\ i\sqrt{1-\eta^2}\, e^{i(\delta_1+\delta_2)} & \eta\, e^{2i\delta_2} \end{pmatrix}$$

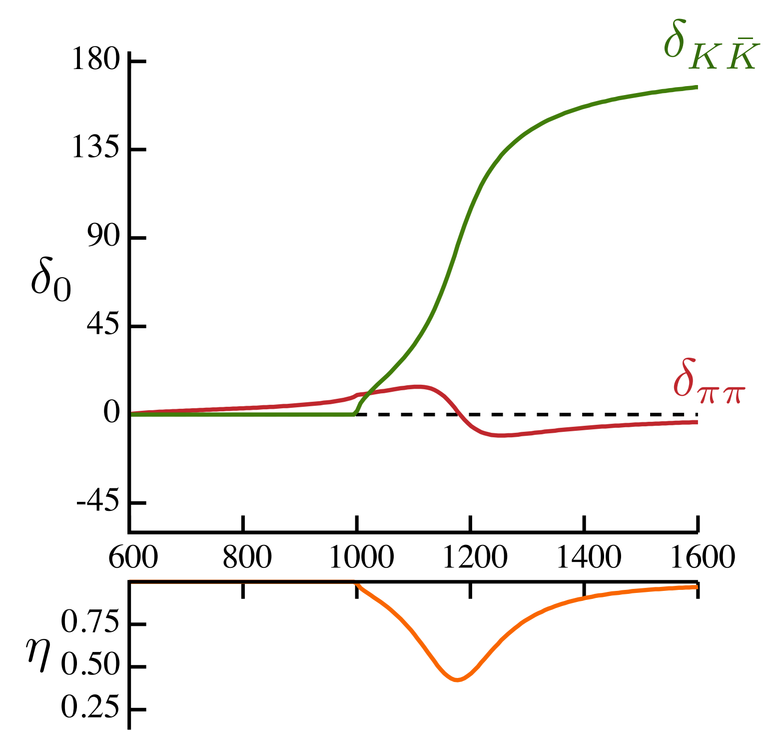

coupled-channel scattering in a finite-volume

the quantization condition generalizes to

$$\boxed{0 = \det\left[\mathbf{1} + i\boldsymbol{\rho}\cdot\mathbf{t}\cdot\left(\mathbf{1} + i\boldsymbol{\mathcal{M}}\right)\right]}$$

coupled-channel scattering in a finite-volume

the quantization condition generalizes to $$\boxed{0 = \det\left[\mathbf{1} + i\boldsymbol{\rho}\cdot\mathbf{t}\cdot\left(\mathbf{1} + i\boldsymbol{\mathcal{M}}\right)\right]}$$

e.g. in $A_1{}^+$ irrep (ℓ = 0, 4 …)

$$\mathbf{t} = \begin{pmatrix} \begin{pmatrix} t_{11}^{(0)} & t_{12}^{(0)} \\ t_{12}^{(0)} & t_{22}^{(0)} \end{pmatrix} & \mathbf{0} & \cdots \\ \mathbf{0} & \begin{pmatrix} t_{11}^{(4)} & t_{12}^{(4)} \\ t_{12}^{(4)} & t_{22}^{(4)} \end{pmatrix} & \cdots \\ \vdots & \vdots & \ddots \end{pmatrix}$$

dense in channel space
– infinite-volume dynamics mixes channels

diagonal in angular momentum space
– ℓ good q.n. in infinite-volume

coupled-channel scattering in a finite-volume

the quantization condition generalizes to $$\boxed{0 = \det\left[\mathbf{1} + i\boldsymbol{\rho}\cdot\mathbf{t}\cdot\left(\mathbf{1} + i\boldsymbol{\mathcal{M}}\right)\right]}$$

e.g. in A_1^+ irrep ($\ell = 0, 4 \ldots$)

$$\mathbf{t} = \begin{pmatrix} \begin{pmatrix} t_{11}^{(0)} & t_{12}^{(0)} \\ t_{12}^{(0)} & t_{22}^{(0)} \end{pmatrix} & \mathbf{0} & \cdots \\ \mathbf{0} & \begin{pmatrix} t_{11}^{(4)} & t_{12}^{(4)} \\ t_{12}^{(4)} & t_{22}^{(4)} \end{pmatrix} & \cdots \\ \vdots & \vdots & \ddots \end{pmatrix}$$

dense in channel space
— infinite-volume dynamics mixes channels

diagonal in angular momentum space
— ℓ good q.n. in infinite-volume

$$\boldsymbol{\mathcal{M}} = \begin{pmatrix} \begin{pmatrix} \mathcal{M}_{00}^{A_1^+}(k_1) & 0 \\ 0 & \mathcal{M}_{00}^{A_1^+}(k_2) \end{pmatrix} & \begin{pmatrix} \mathcal{M}_{04}^{A_1^+}(k_1) & 0 \\ 0 & \mathcal{M}_{04}^{A_1^+}(k_2) \end{pmatrix} & \cdots \\ \begin{pmatrix} \mathcal{M}_{40}^{A_1^+}(k_1) & 0 \\ 0 & \mathcal{M}_{40}^{A_1^+}(k_2) \end{pmatrix} & \begin{pmatrix} \mathcal{M}_{44}^{A_1^+}(k_1) & 0 \\ 0 & \mathcal{M}_{44}^{A_1^+}(k_2) \end{pmatrix} & \cdots \\ \vdots & \vdots & \ddots \end{pmatrix}$$

diagonal in channel space
— no dynamics in $\boldsymbol{\mathcal{M}}$

dense in angular momentum
— cubic symmetry lives here

$$k_1 = \tfrac{1}{2}\sqrt{E^2 - 4m_1^2}$$

$$k_2 = \tfrac{1}{2}\sqrt{E^2 - 4m_2^2}$$

coupled-channel scattering in a finite-volume

the quantization condition generalizes to $$\boxed{0 = \det\left[\mathbf{1} + i\boldsymbol{\rho}\cdot\mathbf{t}\cdot\big(\mathbf{1}+i\boldsymbol{\mathcal{M}}\big)\right]}$$

can also be expressed as $0 = \det\left[\mathbf{t}^{-1} + i\boldsymbol{\rho} - \boldsymbol{\mathcal{M}}\cdot\boldsymbol{\rho})\right]$

which exposes the role of unitarity $\mathrm{Im}\left(t^{-1}(E)\right)_{ij} = -\delta_{ij}\,\rho_i(E)\,\Theta(E-E_i^{\mathrm{thr.}})$

the quantization condition is a **single real condition**:

the zeroes $E=E_n(\mathrm{L})$ of the function $\det\left[\mathbf{1} + i\boldsymbol{\rho}(E)\cdot\mathbf{t}(E)\cdot\big(\mathbf{1}+i\boldsymbol{\mathcal{M}}(E,L)\big)\right]$

correspond to the spectrum in an $L\times L\times L$ volume

zeroes of the determinant

e.g. previously presented two-channel Flatté form — [000] A_1^+ irrep in L=2.4 fm box

m_π = 300 MeV
m_K = 500 MeV

$$\det\left[\mathbf{1} + i\boldsymbol{\rho}(E)\cdot\mathbf{t}(E)\cdot\left(\mathbf{1}+i\boldsymbol{\mathcal{M}}(E,L)\right)\right]$$

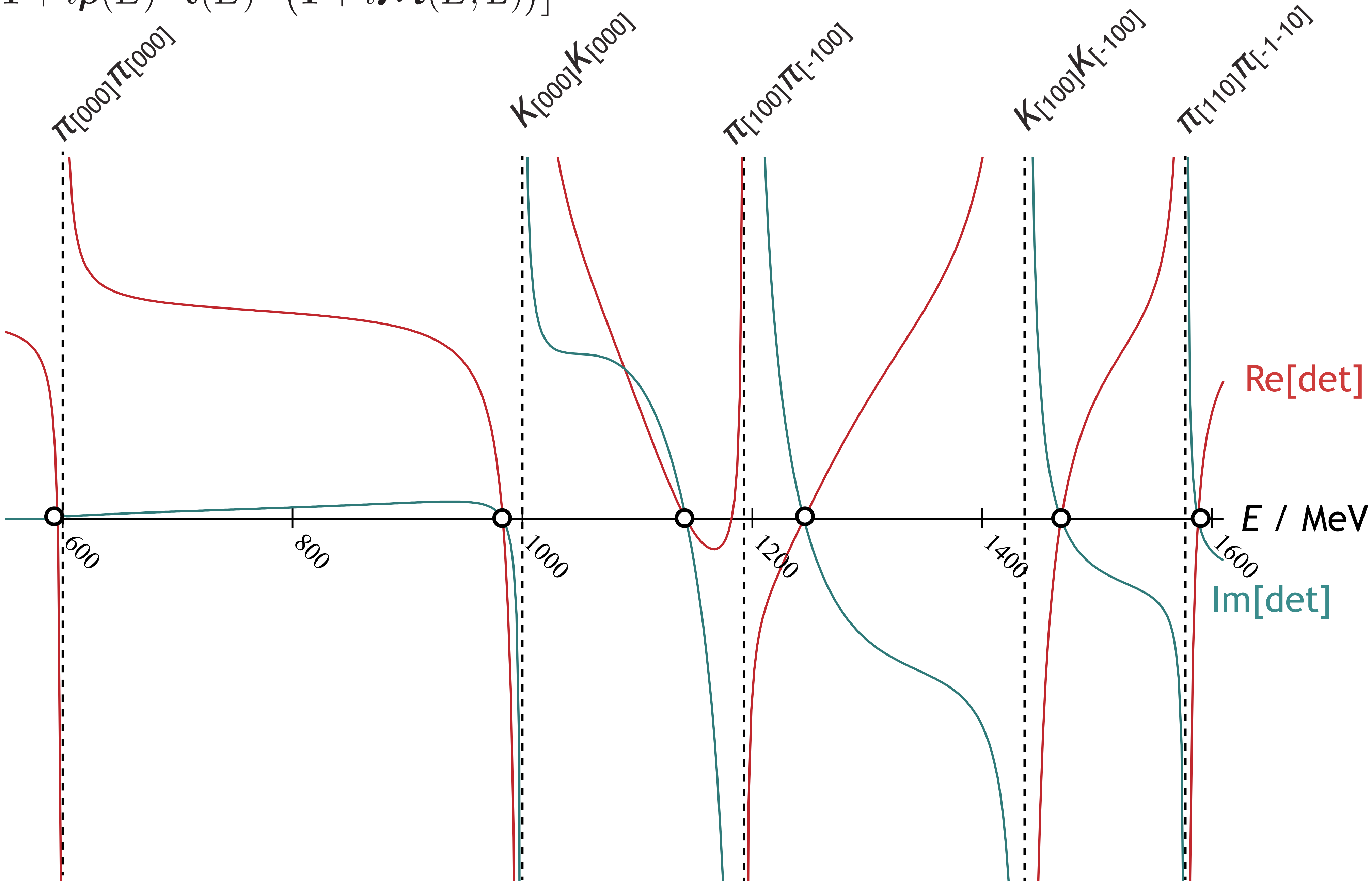

numerical root-finding exercise in practice

zeroes of the determinant

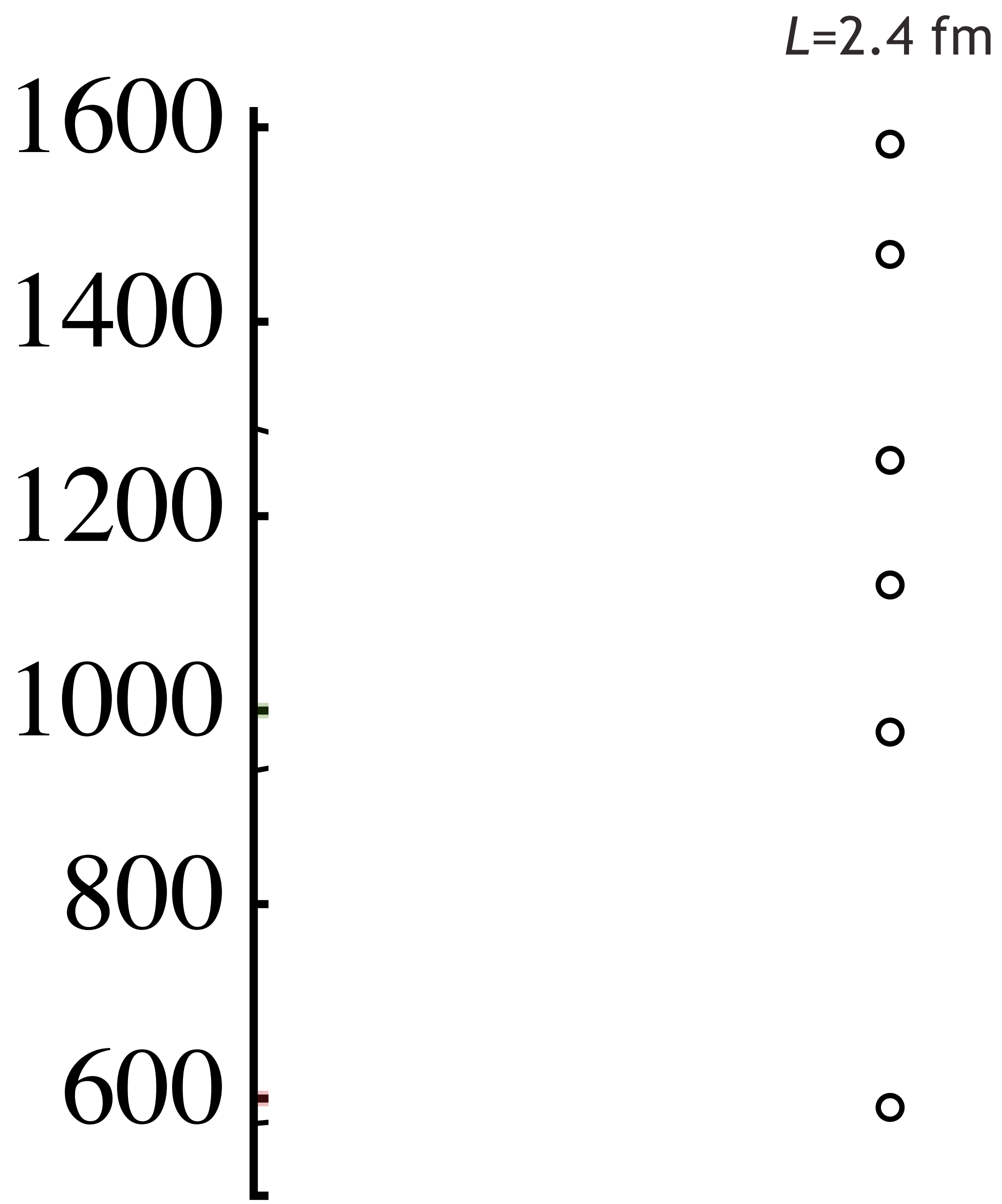

zeroes of the determinant

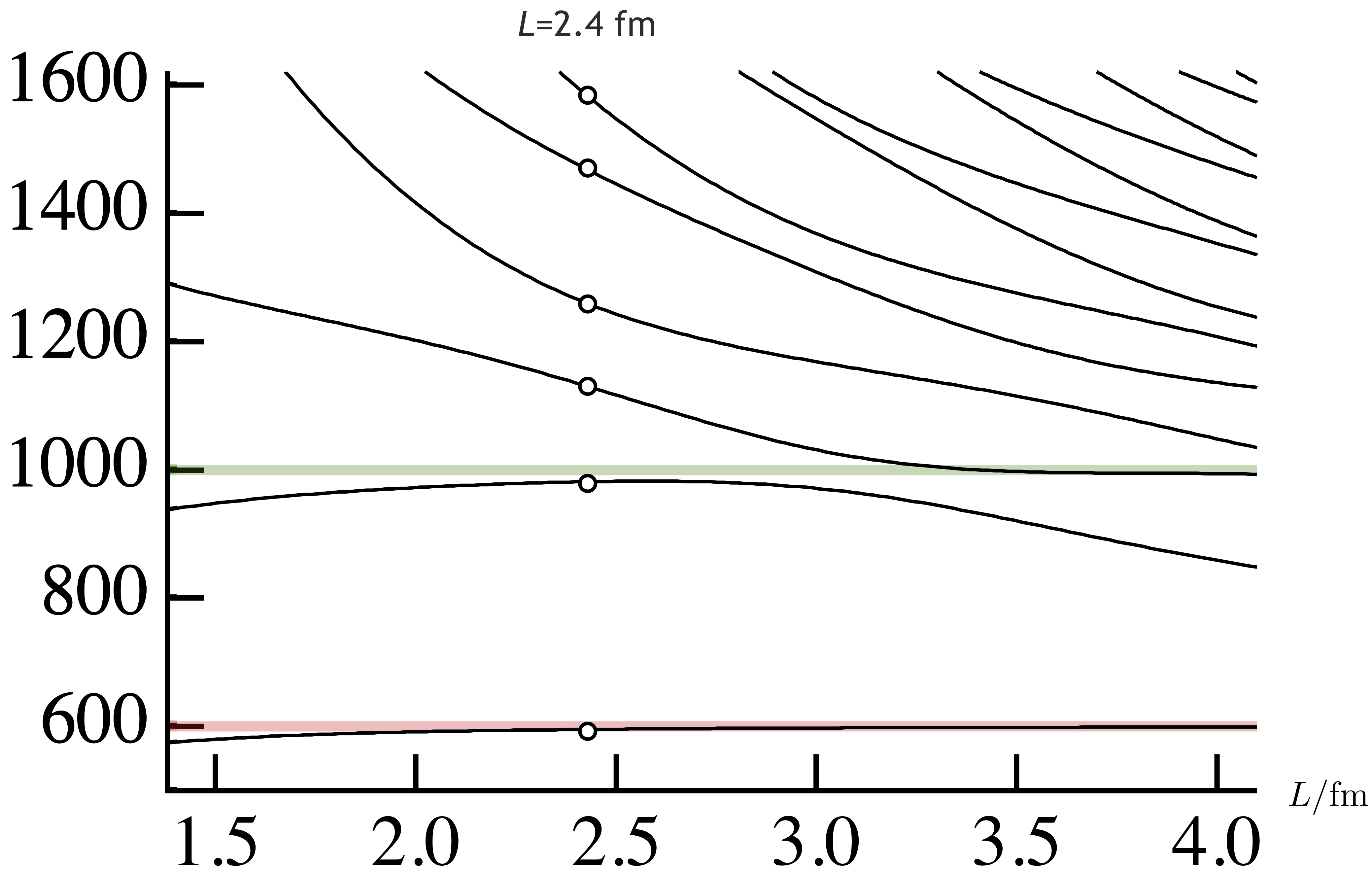

finite-volume spectrum

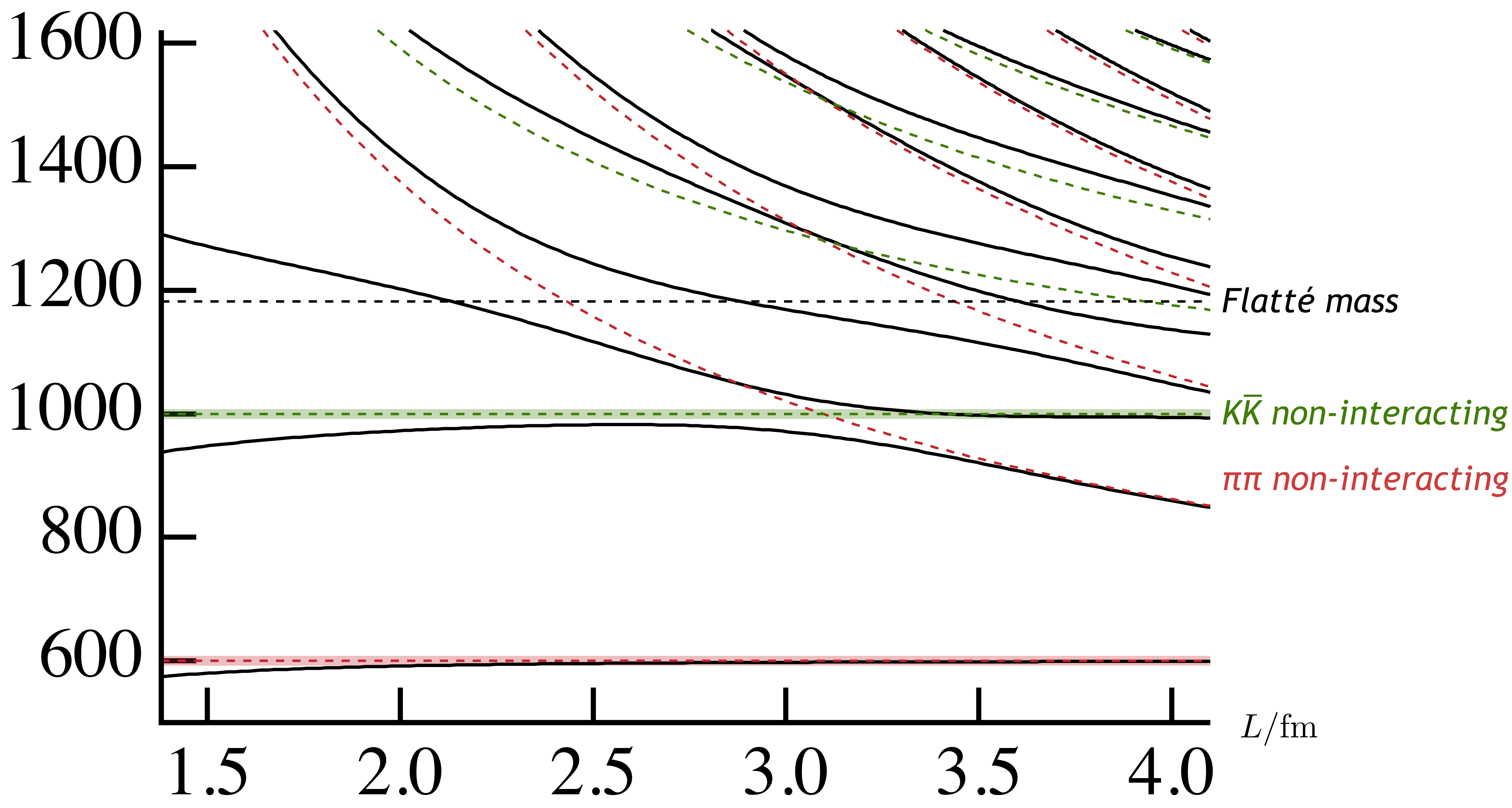

$$\boxed{0 = \det\left[\mathbf{1} + i\boldsymbol{\rho}\cdot\mathbf{t}\cdot\left(\mathbf{1}+i\boldsymbol{\mathcal{M}}\right)\right]}$$

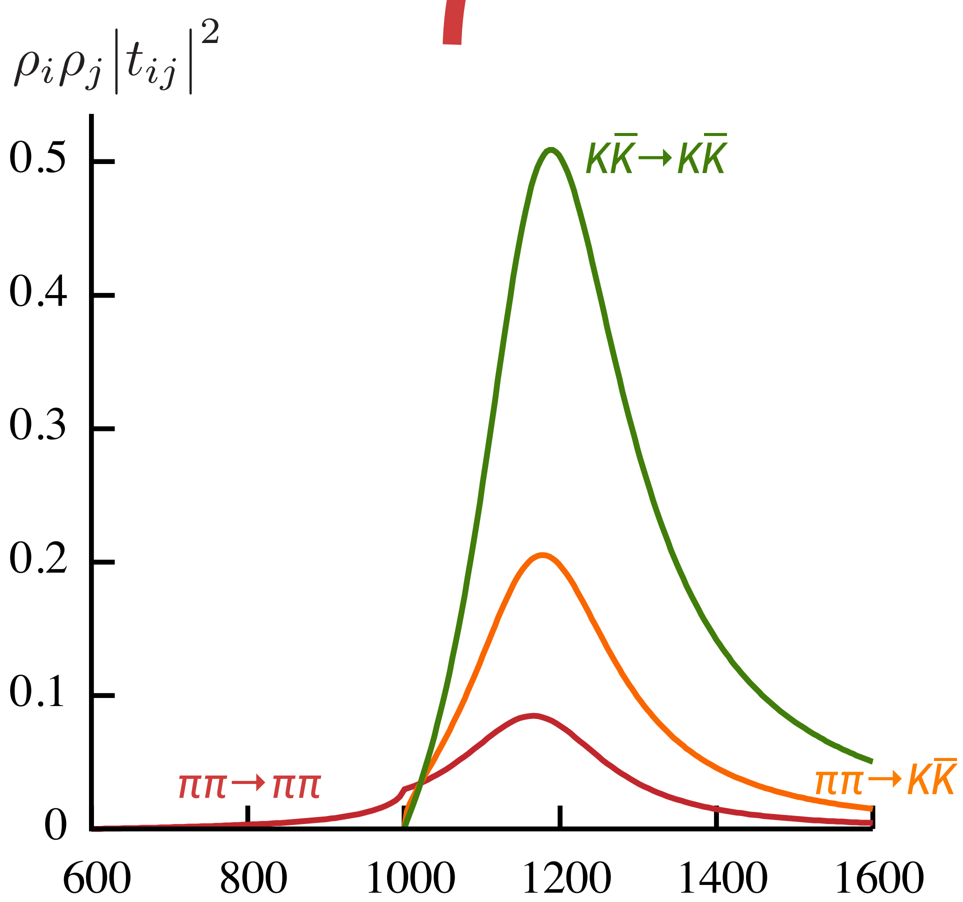

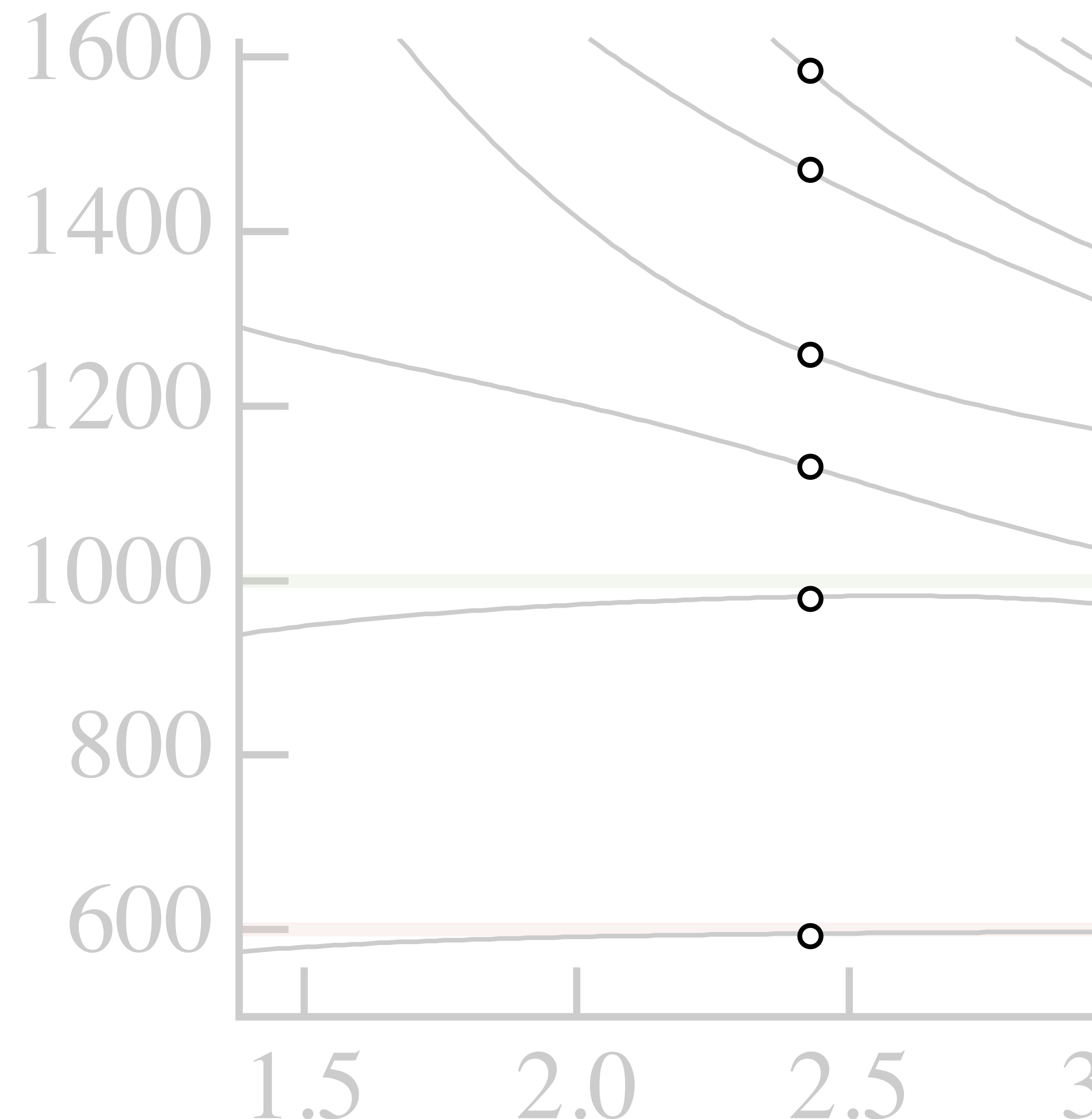

finite-volume approach

$$0 = \det\left[\mathbf{1} + i\boldsymbol{\rho}\cdot\mathbf{t}\cdot\left(\mathbf{1} + i\boldsymbol{\mathcal{M}}\right)\right]$$

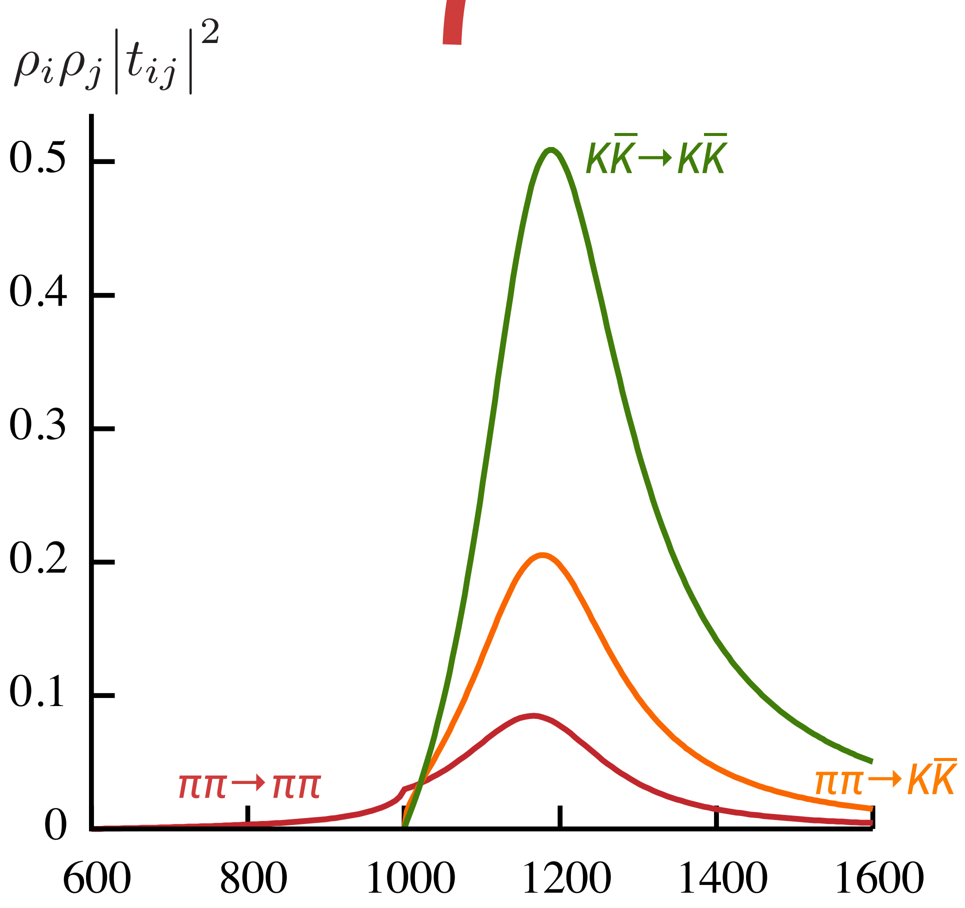

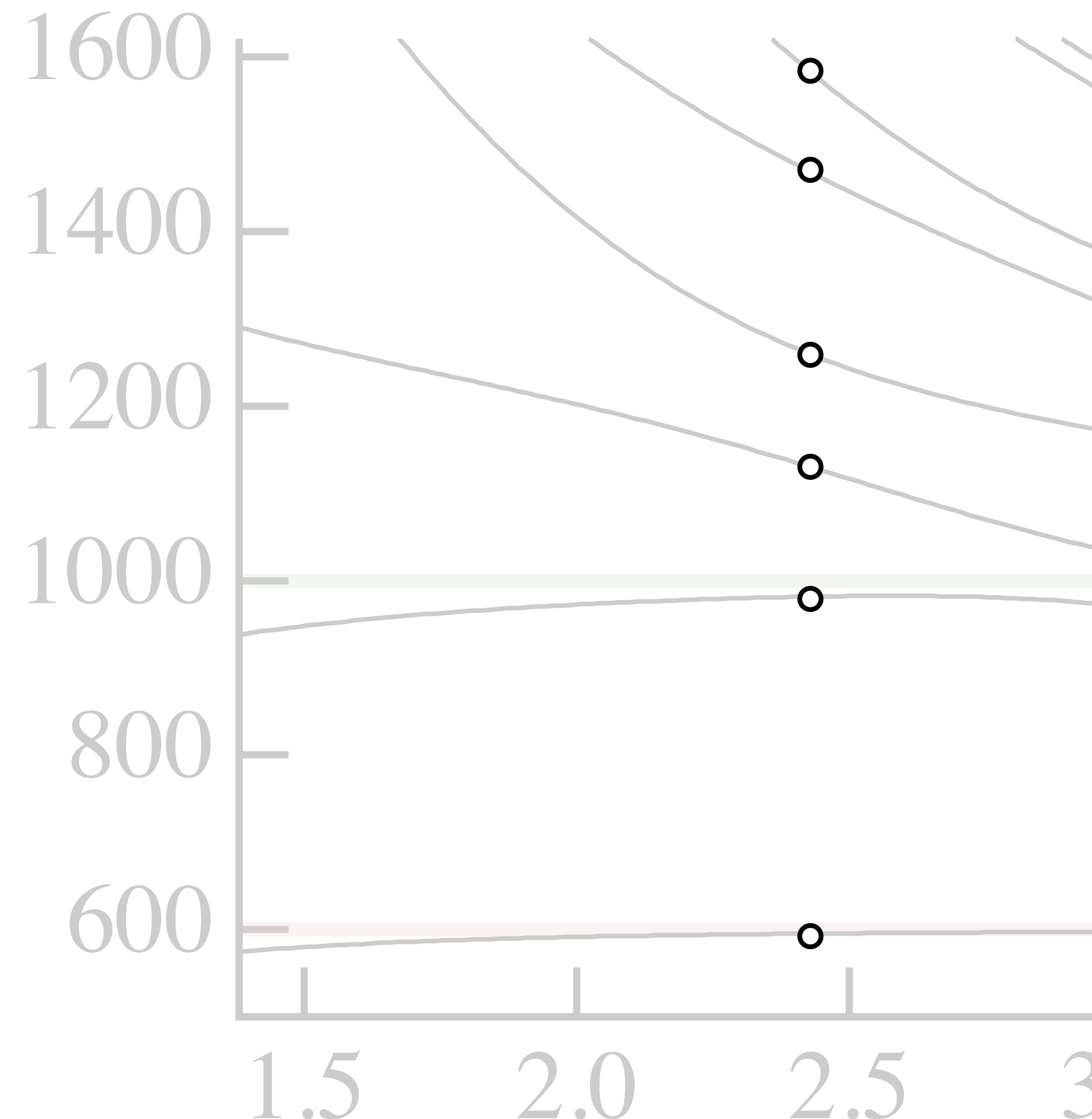

but in a lattice QCD calculation
we have the inverse problem …

?

position of each energy level depends upon all elements of the ***t***-matrix

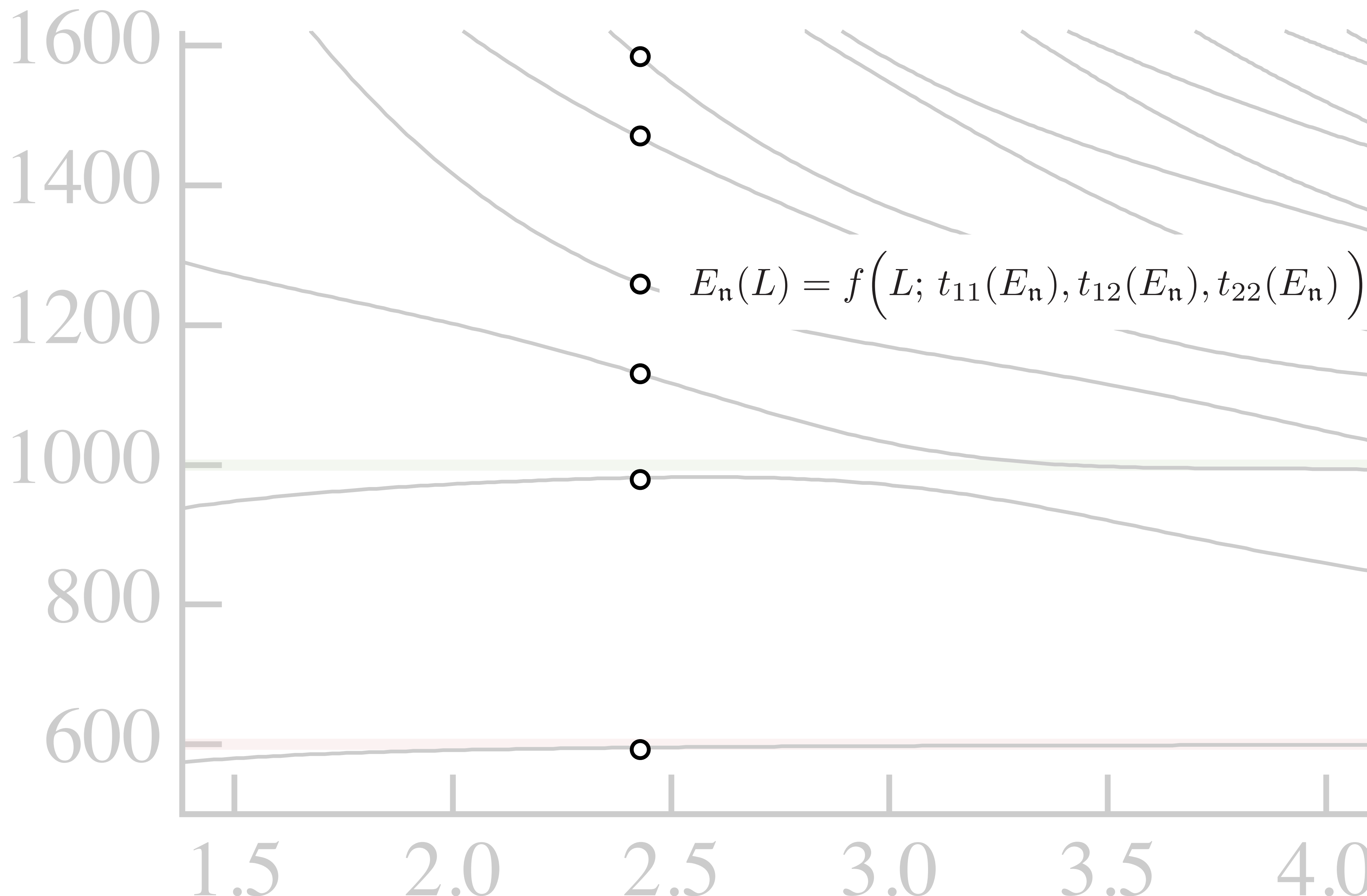

$$\boxed{0 = \det\big[\mathbf{1} + i\boldsymbol{\rho}\cdot\mathbf{t}\cdot\big(\mathbf{1} + i\boldsymbol{\mathcal{M}}\big)\big]}$$

at $E = E_n(L)$
is one equation in three unknowns ...

parameterizing the *t*-matrix

a solution is to propose that different energies are not unrelated – parameterize $\mathbf{t}\big(E;\{a_i\}\big)$

then can use many energy levels to constrain the parameters by minimising a χ^2

$$\chi^2\big(\{a_i\}\big) = \sum_{\mathfrak{n},\mathfrak{n}'} \Big(E^{\text{lat.}}_{\mathfrak{n}} - E^{\text{par.}}_{\mathfrak{n}}(L;\{a_i\})\Big)\, \mathbb{C}^{-1}_{\mathfrak{n},\mathfrak{n}'}\, \Big(E^{\text{lat.}}_{\mathfrak{n}'} - E^{\text{par.}}_{\mathfrak{n}'}(L;\{a_i\})\Big)$$

inverse data covariance

energy levels solving
$0 = \det\big[\mathbf{1} + i\boldsymbol{\rho}\cdot\mathbf{t}\cdot(\mathbf{1}+i\boldsymbol{\mathcal{M}})\big]$
for $\mathbf{t}\big(E;\{a_i\}\big)$

parameterizing the $\boldsymbol{t}$-matrix

a solution is to propose that different energies are not unrelated – parameterize $\mathbf{t}\big(E;\{a_i\}\big)$

then can use many energy levels to constrain the parameters by minimising a χ^2

$$\chi^2\big(\{a_i\}\big) = \sum_{\mathfrak{n},\mathfrak{n}'} \Big(E^{\text{lat.}}_{\mathfrak{n}} - E^{\text{par.}}_{\mathfrak{n}}(L;\{a_i\})\Big)\, \mathbb{C}^{-1}_{\mathfrak{n},\mathfrak{n}'}\, \Big(E^{\text{lat.}}_{\mathfrak{n}'} - E^{\text{par.}}_{\mathfrak{n}'}(L;\{a_i\})\Big)$$

inverse data covariance

energy levels solving
$0 = \det\big[\mathbf{1} + i\boldsymbol{\rho}\cdot\mathbf{t}\cdot(\mathbf{1} + i\boldsymbol{\mathcal{M}})\big]$
for $\mathbf{t}\big(E;\{a_i\}\big)$

decreasing χ^2

parameterizing the *t*-matrix

a solution is to propose that different energies are not unrelated – parameterize $\mathbf{t}\big(E;\{a_i\}\big)$

need to ensure multi-channel unitarity $\mathrm{Im}\,\big(t^{-1}(E)\big)_{ij} = -\delta_{ij}\,\rho_i(E)\,\Theta(E - E_i^{\mathrm{thr.}})$

– ***K***-matrix approach

$\mathbf{t}^{-1}(E) = \mathbf{K}^{-1}(E) + \mathbf{I}(E)$ with $\mathrm{Im}\,\big(I(E)\big)_{ij} = -\delta_{ij}\,\rho_i(E)$

simplest choice has $\mathrm{Re}\,\mathbf{I}(E) = 0$

a more sophisticated approach =
"Chew-Mandelstam" phase-space

K(*E*) should be a real symmetric matrix

for reasons you'll see later,
better to parameterize in terms of $s = E^2$

e.g. $K_{ij} = \dfrac{g_i\,g_j}{m^2 - s}$ gives the Flatté form

Chew-Mandelstam phase space

(subtracted) dispersion of the phase-space
$$I(s) = I(s_0) - \frac{s-s_0}{\pi}\int_{s_{\rm thr}}^{\infty} ds' \frac{\rho(s')}{(s'-s_0)(s'-s)}$$

in the equal mass case evaluates to

$$I(s) = I(4m^2) - \frac{\rho(s)}{\pi}\log\left[\frac{1-\rho(s)}{1+\rho(s)}\right] - i\rho(s)$$

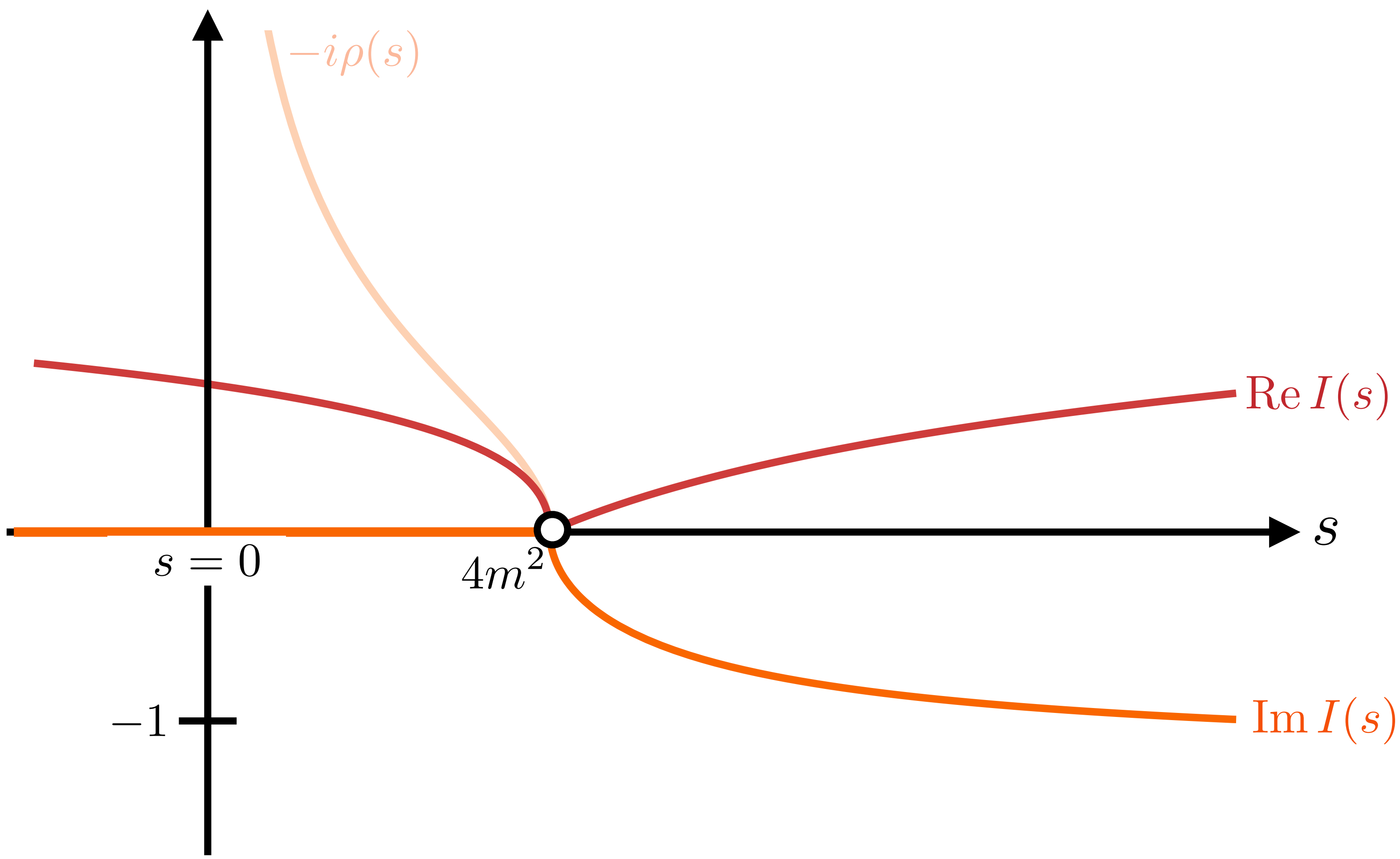

notice the smooth behavior below threshold
& absence of a singularity at *s*=0

equivalent to the scalar loop integral

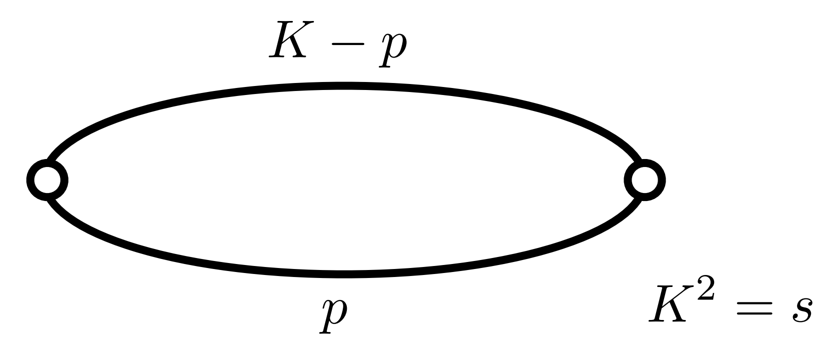

$$16\pi i \int \frac{d^4p}{(2\pi)^4}\frac{1}{p^2-m^2+i\epsilon}\frac{1}{(K-p)^2-m^2+i\epsilon}$$

[regularization → subtraction]

$\pi\pi$, $K\bar{K}$, $\eta\eta$ S-wave scattering

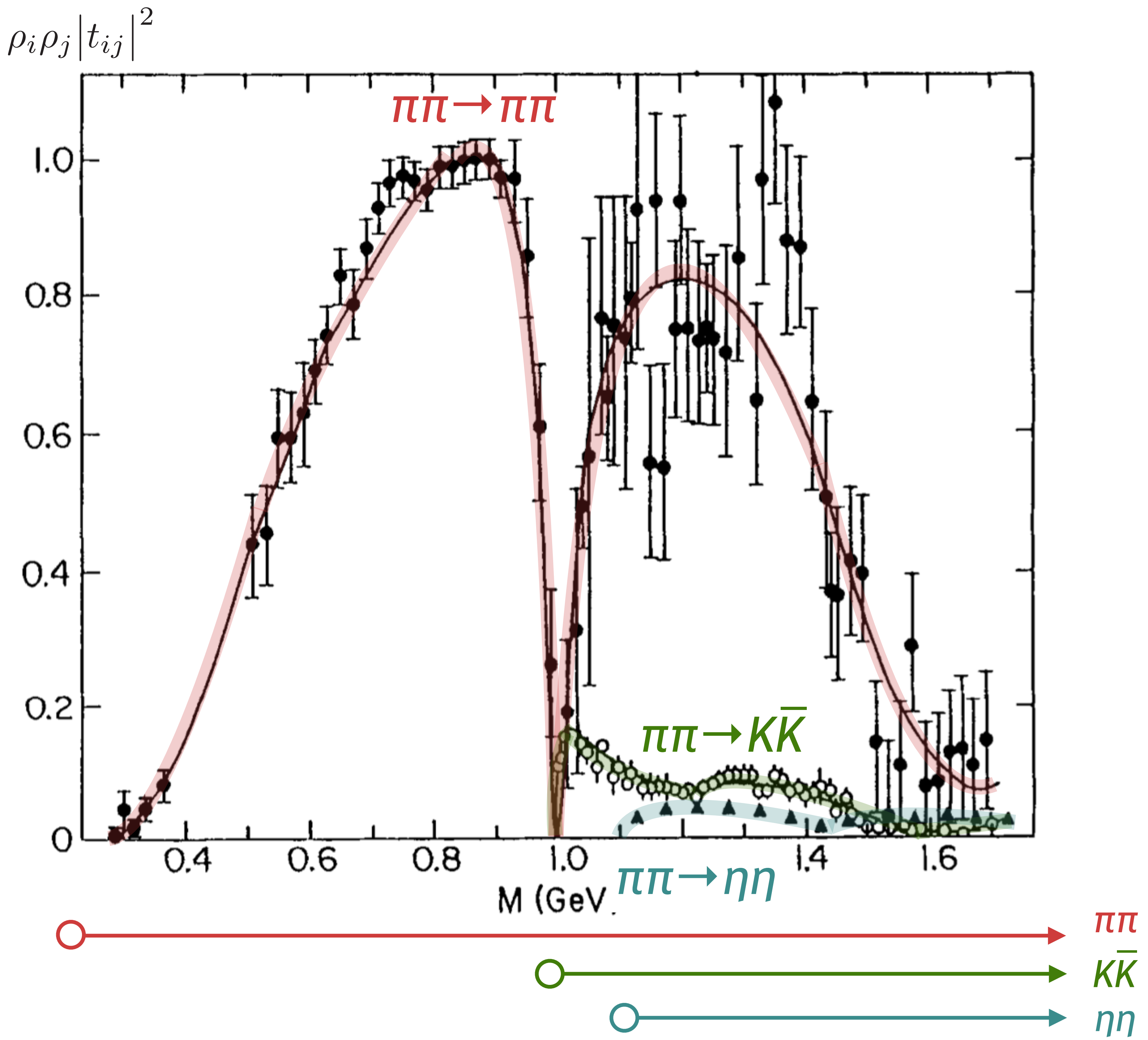

explore this non-trivial system …

… at a higher quark mass …

$\pi\pi$, $K\bar{K}$, $\eta\eta$ scattering with m_π~391 MeV

PRD 97 054513 (2018)

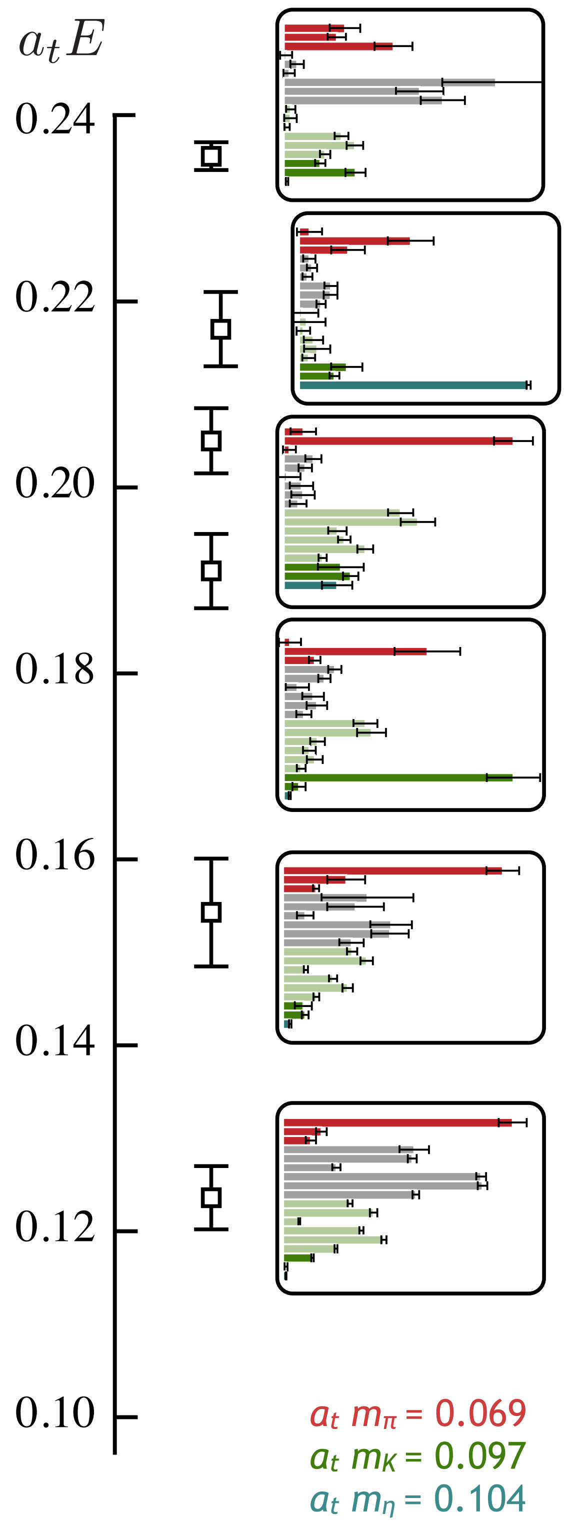

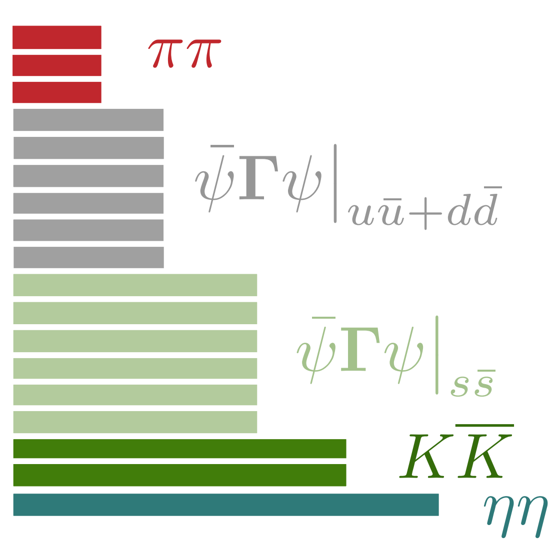

$\pi\pi$, $K\bar{K}$, $\eta\eta$ scattering with m_π~391 MeV

PRD 97 054513 (2018)

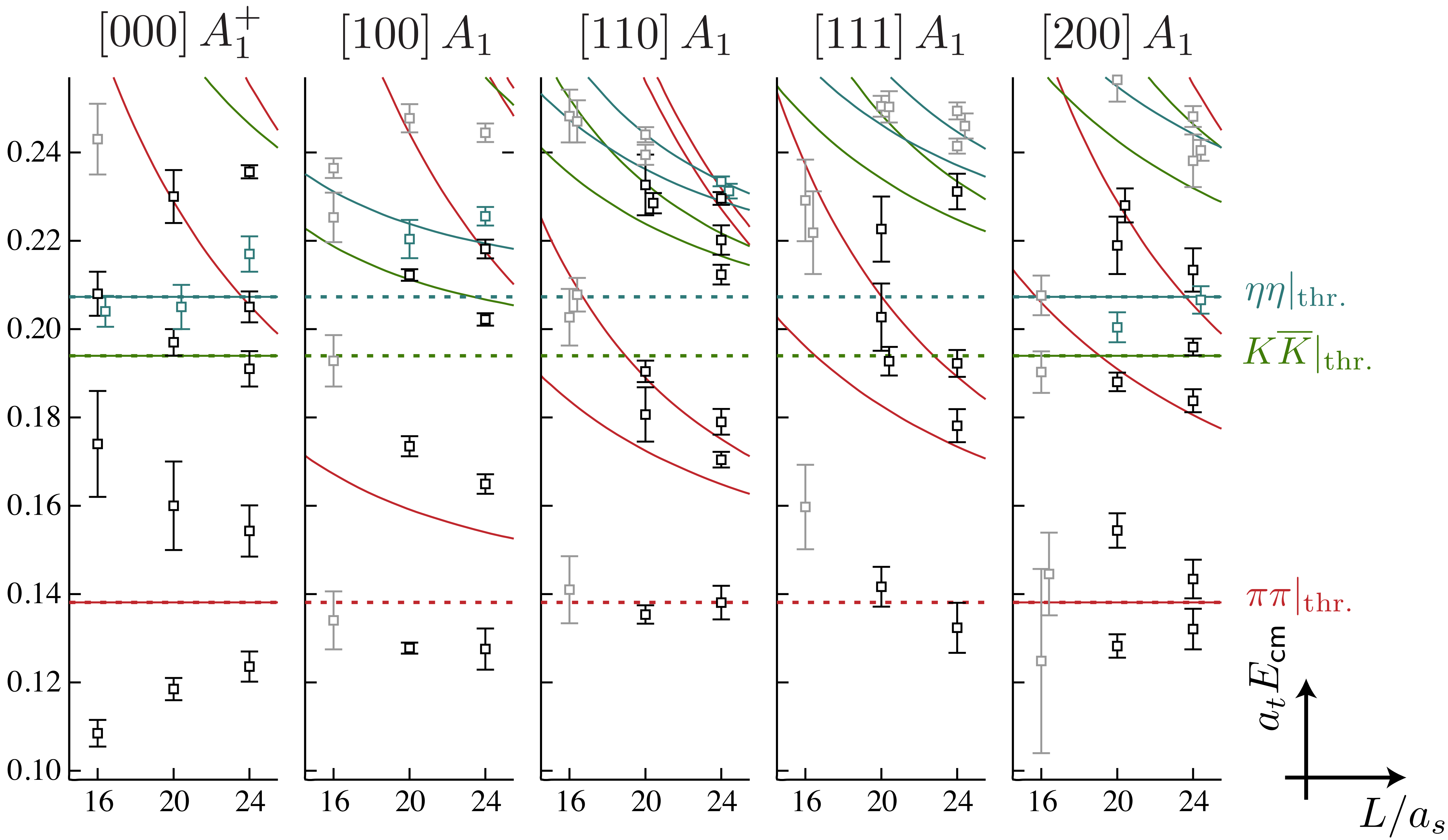

what t-matrix gives these spectra ?

$\pi\pi$, $K\bar{K}$, $\eta\eta$ scattering with m_π~391 MeV

PRD 97 054513 (2018)

not obvious what amplitude parameterization likely to describe the spectra well — try many ...

e.g. $$\mathbf{K}^{-1}(s) = \begin{pmatrix} a + b\,s & c + d\,s & e \\ c + d\,s & f & g \\ e & g & h \end{pmatrix}$$

{ a … h } are free parameters

best fit to lattice spectra

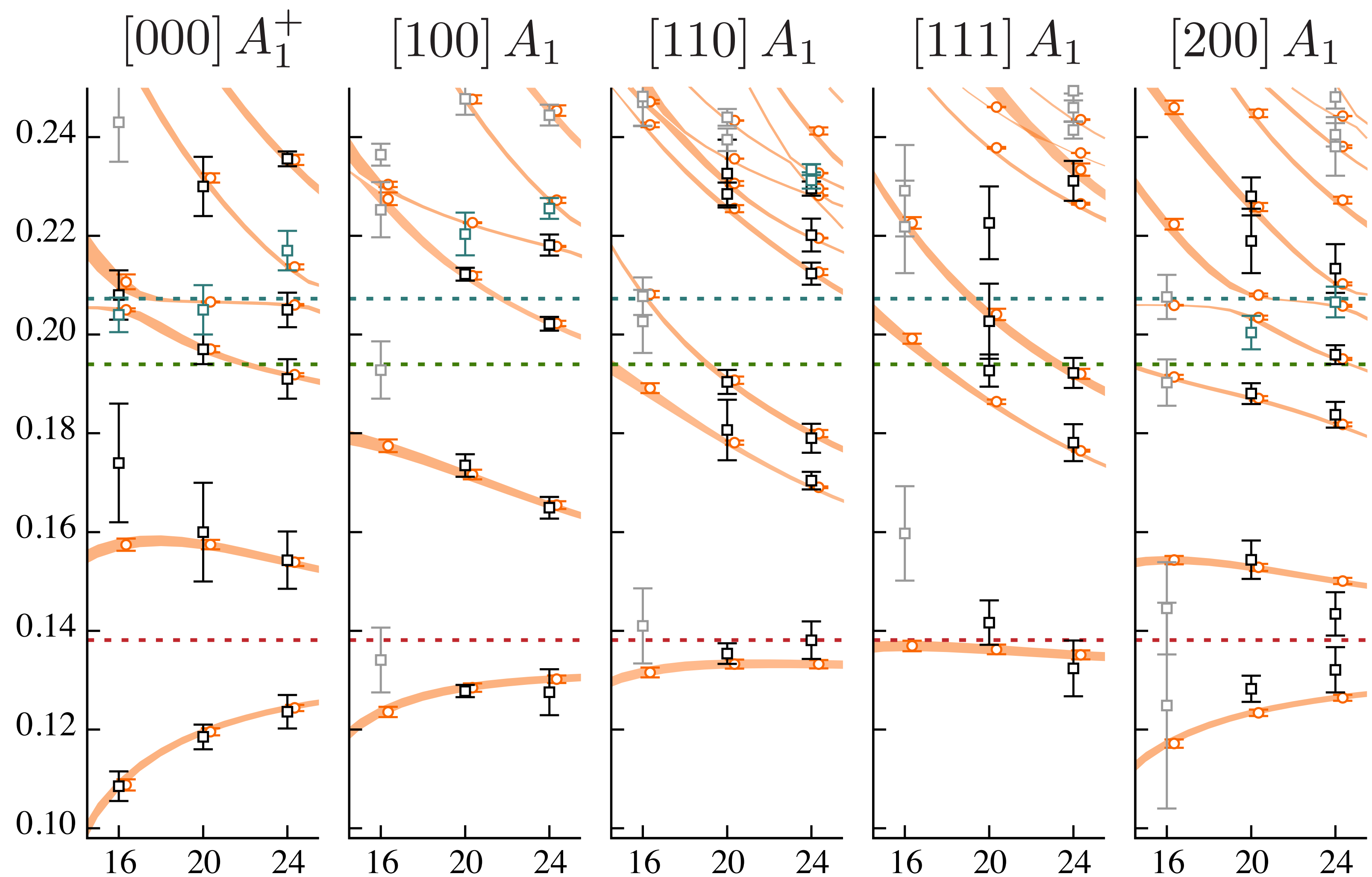

$$\frac{\chi^2}{N_{\mathrm{dof}}} = \frac{44.0}{57-8} = 0.90$$

with Chew-Mandelstam phase-space

$$I(s) = -\frac{\rho(s)}{\pi}\log\left[\frac{\rho(s)-1}{\rho(s)+1}\right]$$

$\pi\pi$, $K\bar{K}$, $\eta\eta$ scattering with m_π~391 MeV

e.g. $$\mathbf{K}^{-1}(s) = \begin{pmatrix} a + b\,s & c + d\,s & e \\ c + d\,s & f & g \\ e & g & h \end{pmatrix}$$

{ *a* … *h* } are free parameters

S-wave amplitudes

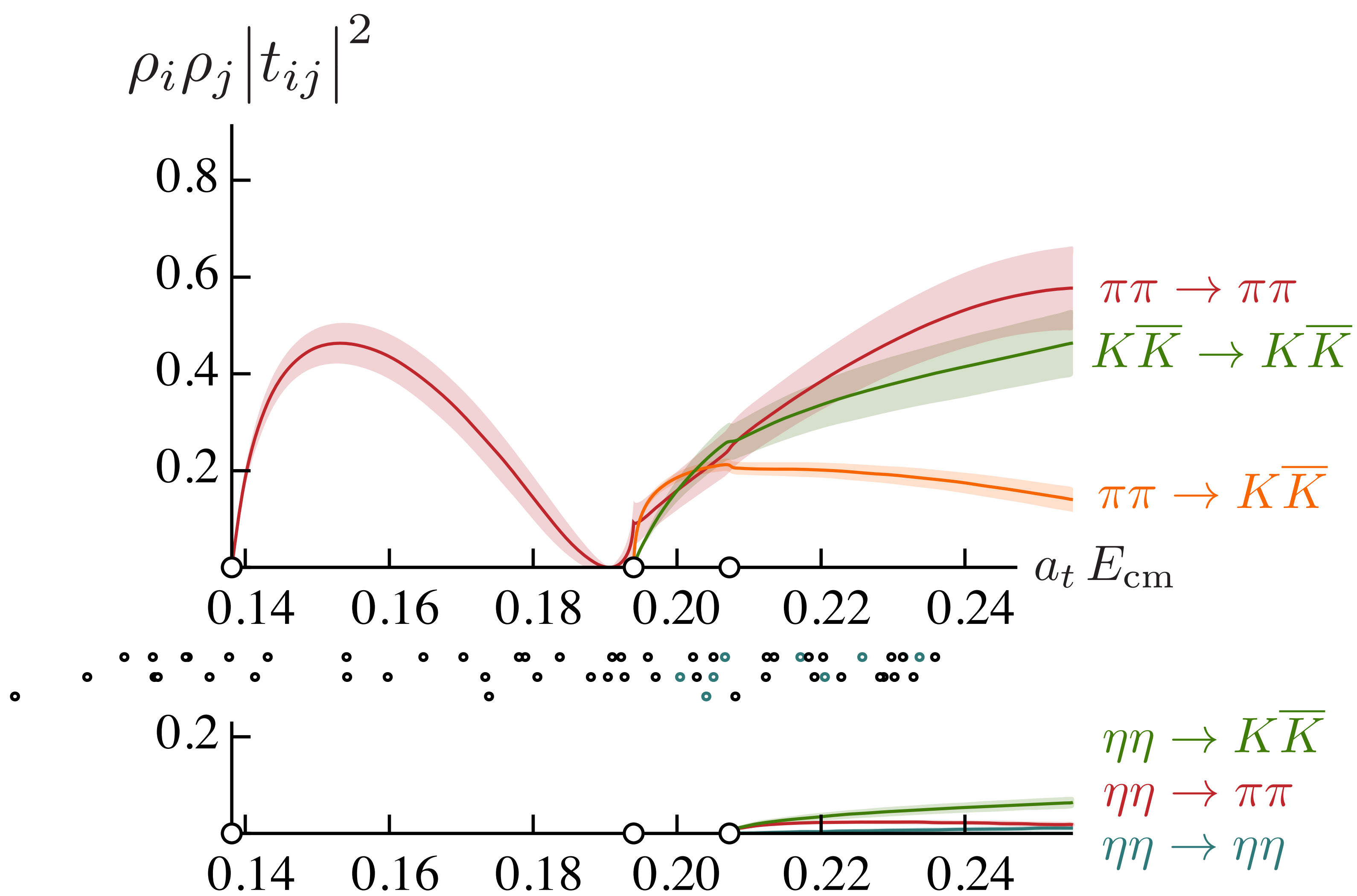

$\pi\pi$, $K\bar{K}$, $\eta\eta$ scattering with m_π~391 MeV

PRD 97 054513 (2018)

not obvious what amplitude parameterization likely to describe the spectra well — **try many ...**

K^{-1} as matrix of polynomials,
K as matrix of polynomials,
K as pole plus matrix of polynomials,
simple versus Chew-Mandelstam phase-space ...

keep choices that can describe spectra with good χ^2

variation with parameterization

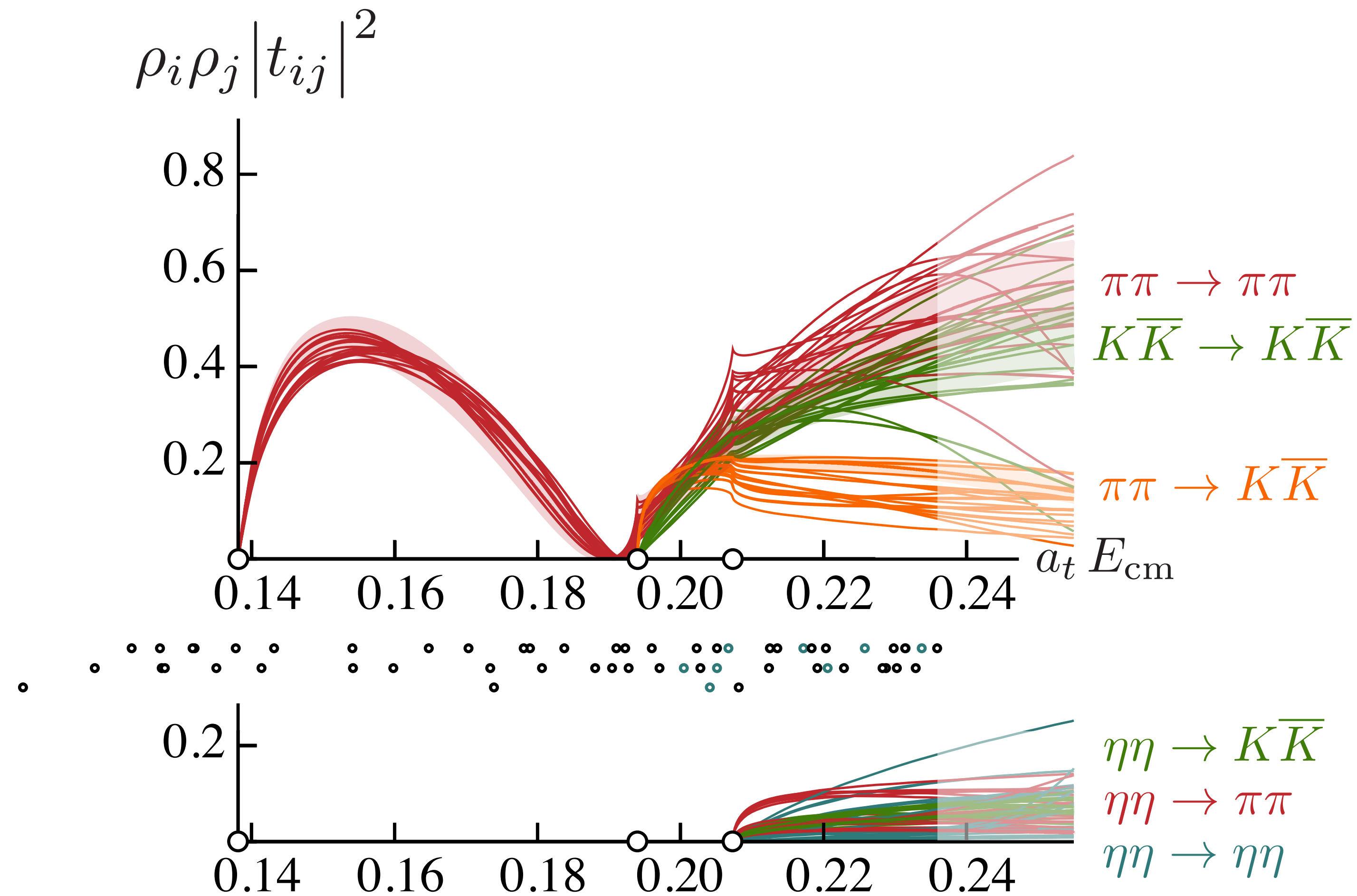

$\pi\pi$, $K\bar{K}$, $\eta\eta$ scattering with m_π~391 MeV

PRD 97 054513 (2018)

scattering amplitude 'prediction'

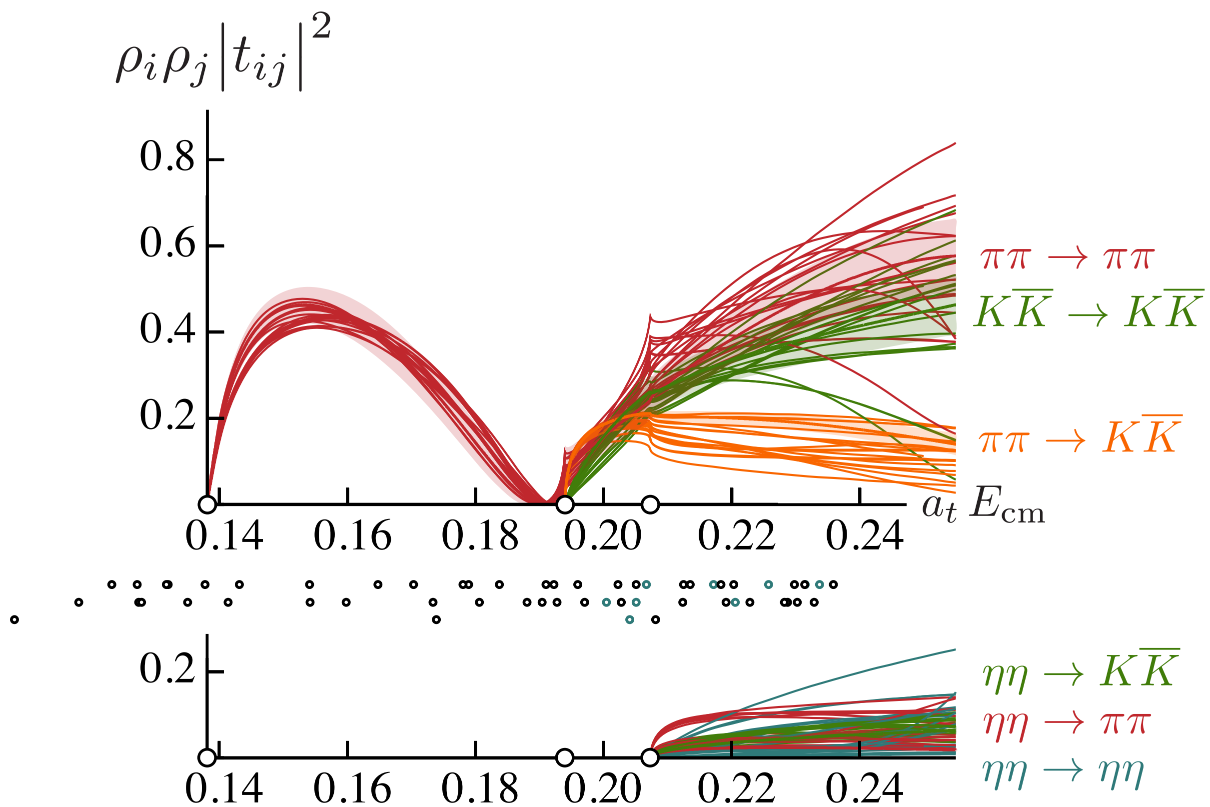

'analogous' experimental data

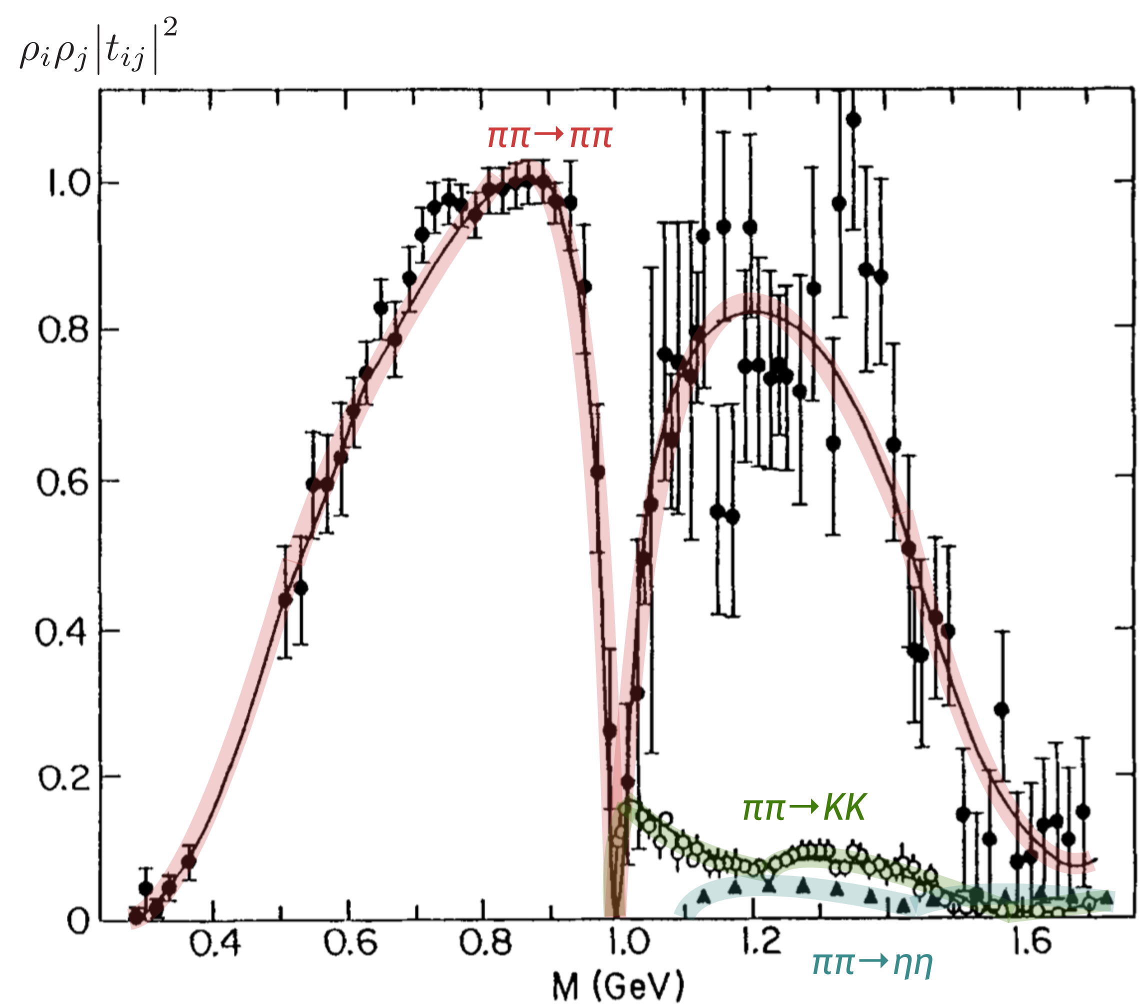

... but what do we do with this ?

... is this strange energy dependence due to resonances ?

$\pi\pi$, $K\bar{K}$, $\eta\eta$ scattering with m_π~391 MeV

also computed spectra for irreps with lowest subduced spin ***J*=2**

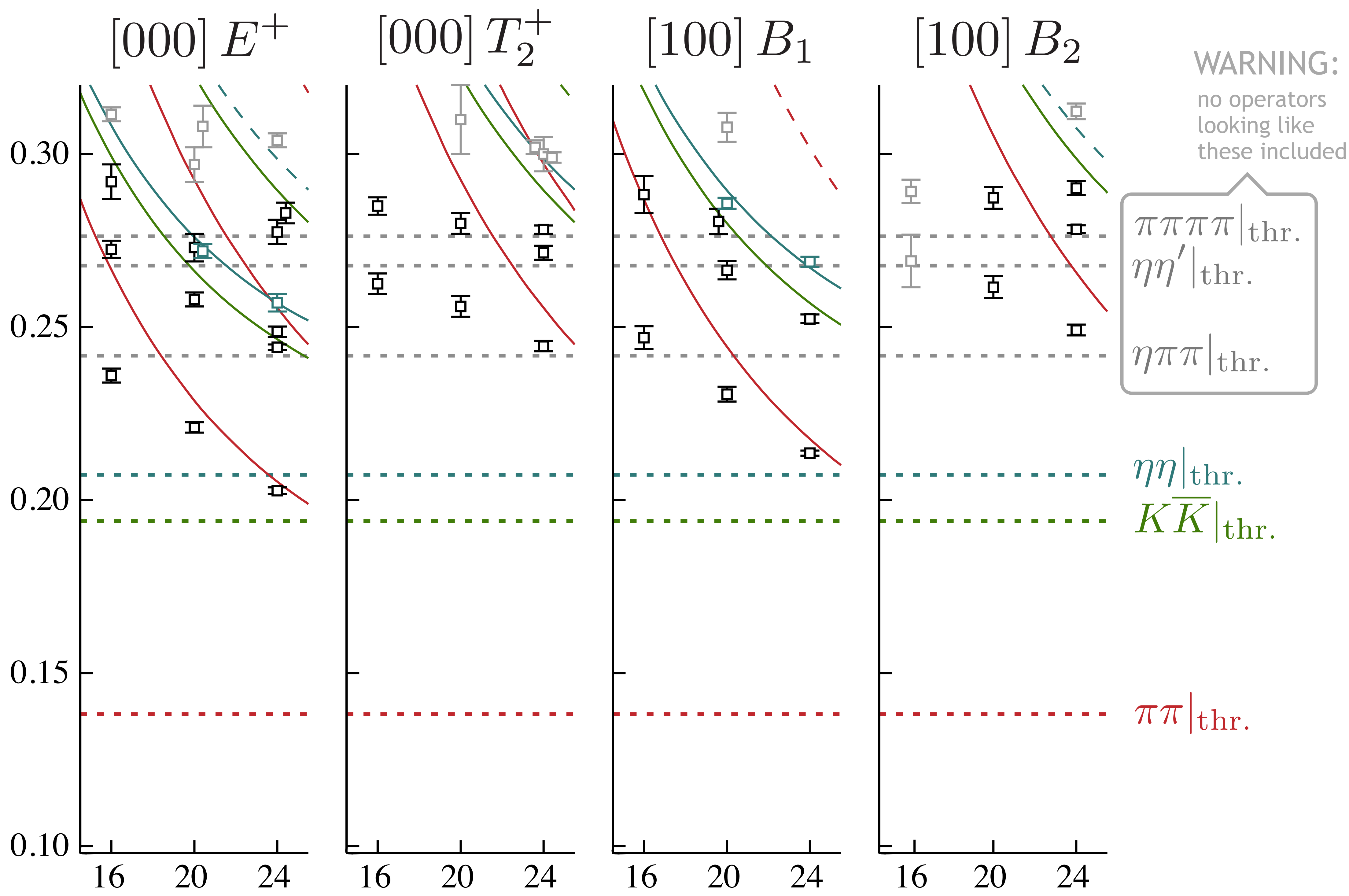

$\pi\pi$, $K\bar{K}$, $\eta\eta$ scattering with m_π~391 MeV

also computed spectra for irreps with lowest subduced spin ***J*=2**

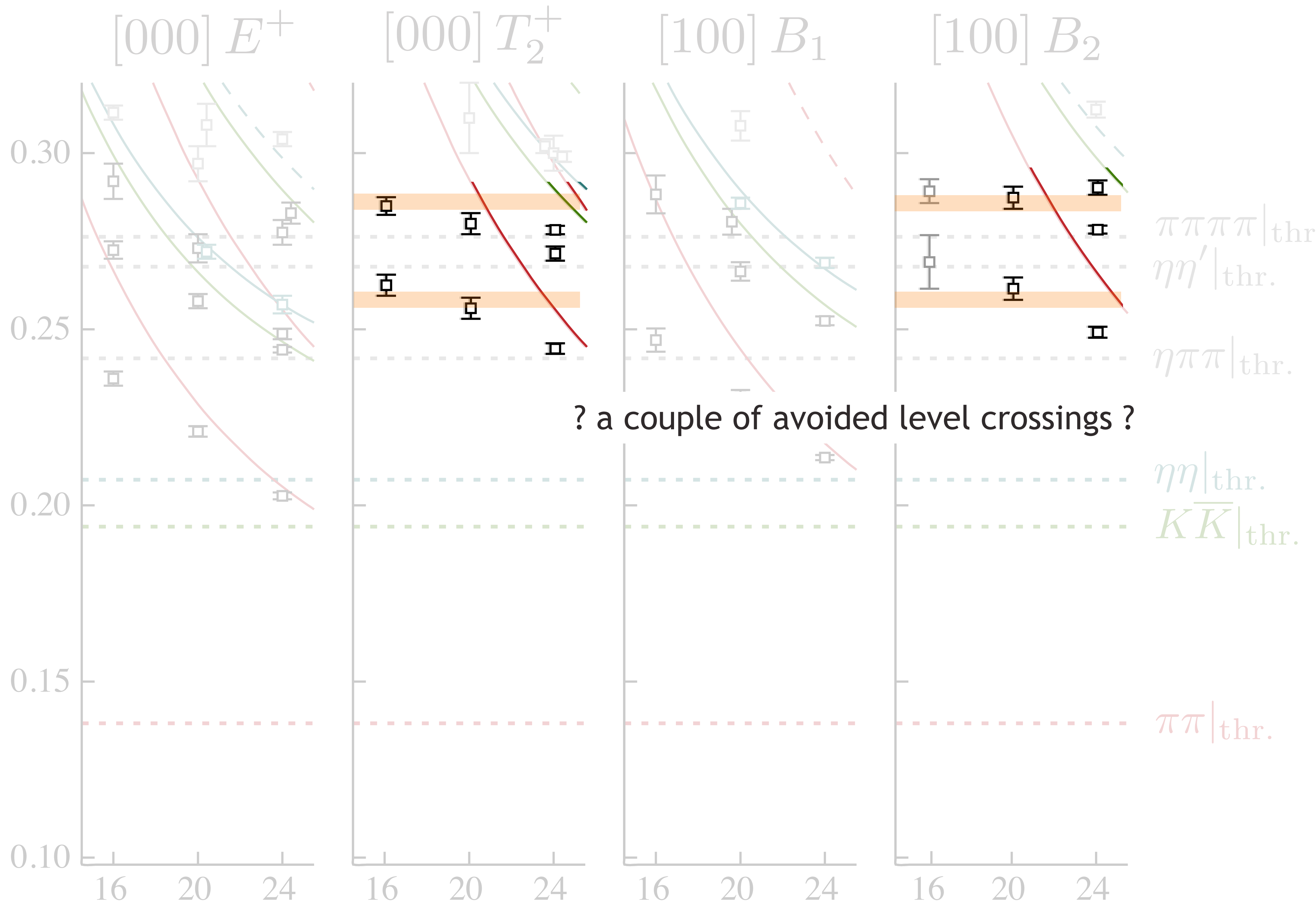

? a couple of avoided level crossings ?

$\pi\pi$, $K\bar{K}$, $\eta\eta$ scattering with m_π~391 MeV

PRD 97 054513 (2018)

e.g. parameterize coupled *D*-wave ***t***-matrix with
$$K_{ij}(s) = \frac{g_i^{(1)} g_j^{(1)}}{m_1^2 - s} + \frac{g_i^{(2)} g_j^{(2)}}{m_2^2 - s} + \gamma_{ij} \qquad \boldsymbol{\gamma} = \begin{pmatrix} 0 & 0 & 0 \\ 0 & 0 & 0 \\ 0 & 0 & \gamma_{\eta\eta,\eta\eta} \end{pmatrix}$$

and the simple phase-space

best fit to lattice spectra

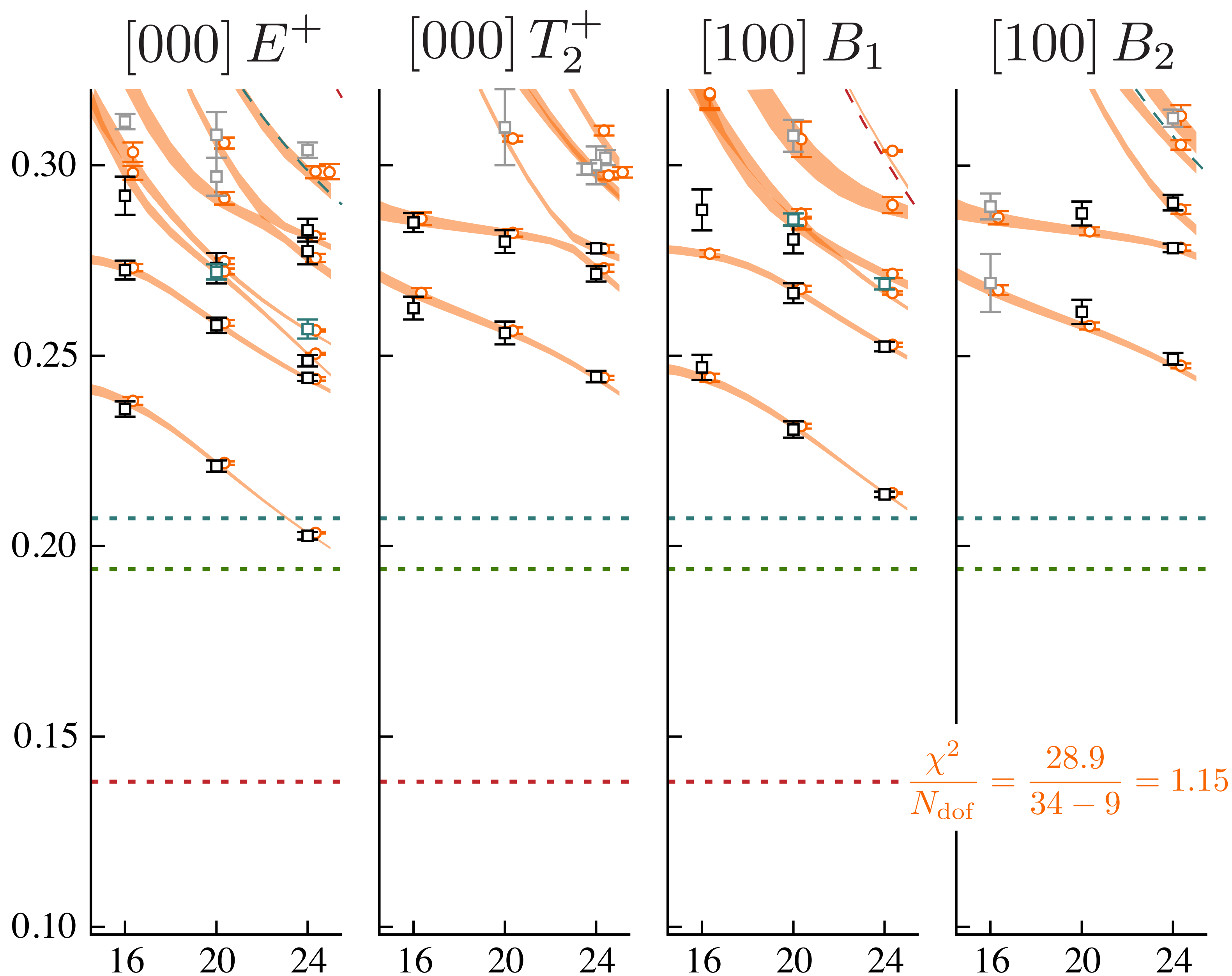

$\pi\pi$, $K\bar{K}$, $\eta\eta$ scattering with m_π~391 MeV

PRD 97 054513 (2018)

e.g. parameterize coupled *D*-wave ***t***-matrix with

$$K_{ij}(s) = \frac{g_i^{(1)} g_j^{(1)}}{m_1^2 - s} + \frac{g_i^{(2)} g_j^{(2)}}{m_2^2 - s} + \gamma_{ij} \qquad \gamma = \begin{pmatrix} 0 & 0 & 0 \\ 0 & 0 & 0 \\ 0 & 0 & \gamma_{\eta\eta,\eta\eta} \end{pmatrix}$$

and the simple phase-space

D-wave amplitudes

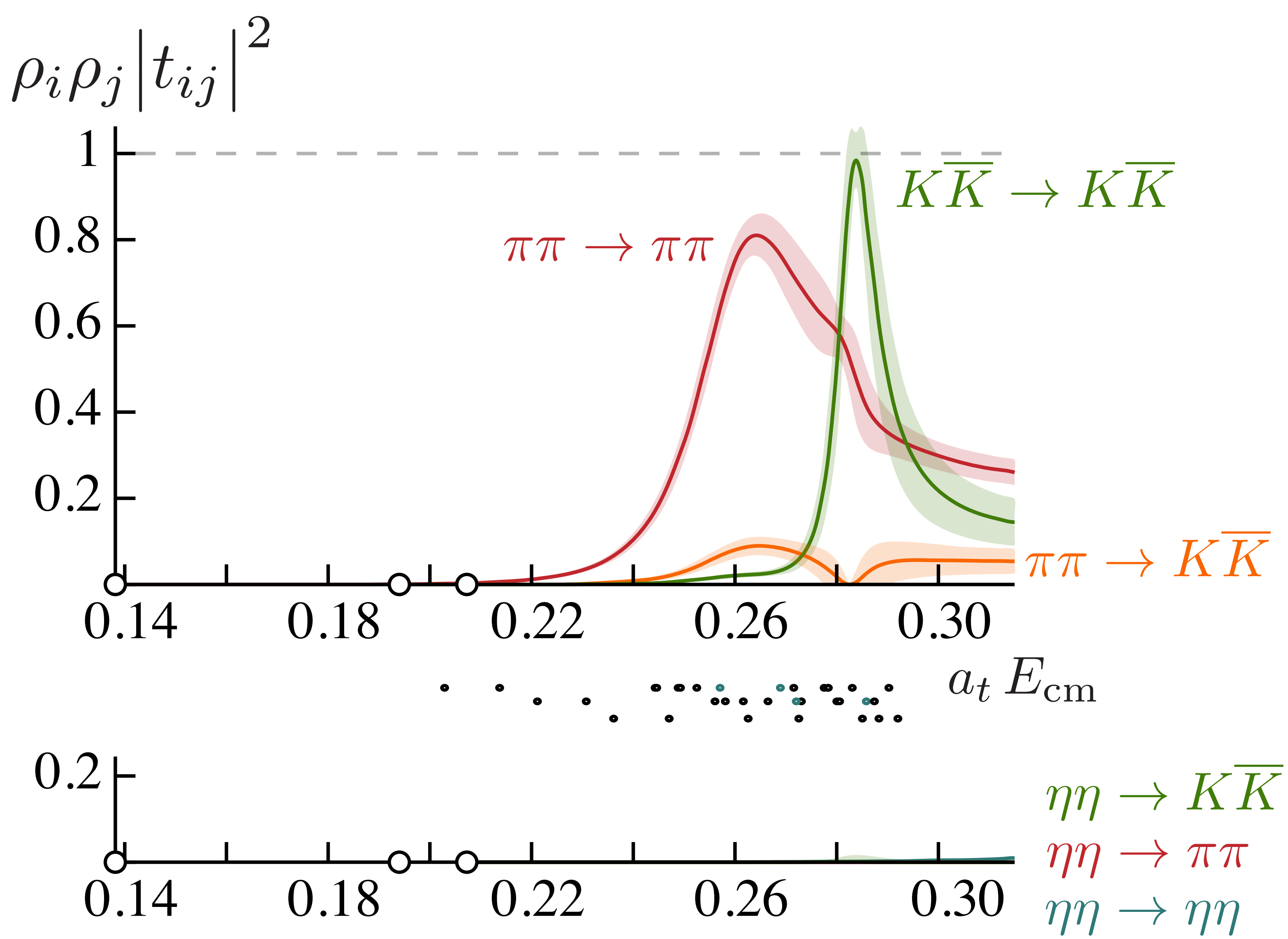

$\pi\pi$, $K\bar{K}$, $\eta\eta$ scattering with m_π~391 MeV

PRD 97 054513 (2018)

… and varying the particular choice of parameterization …

D-wave amplitudes

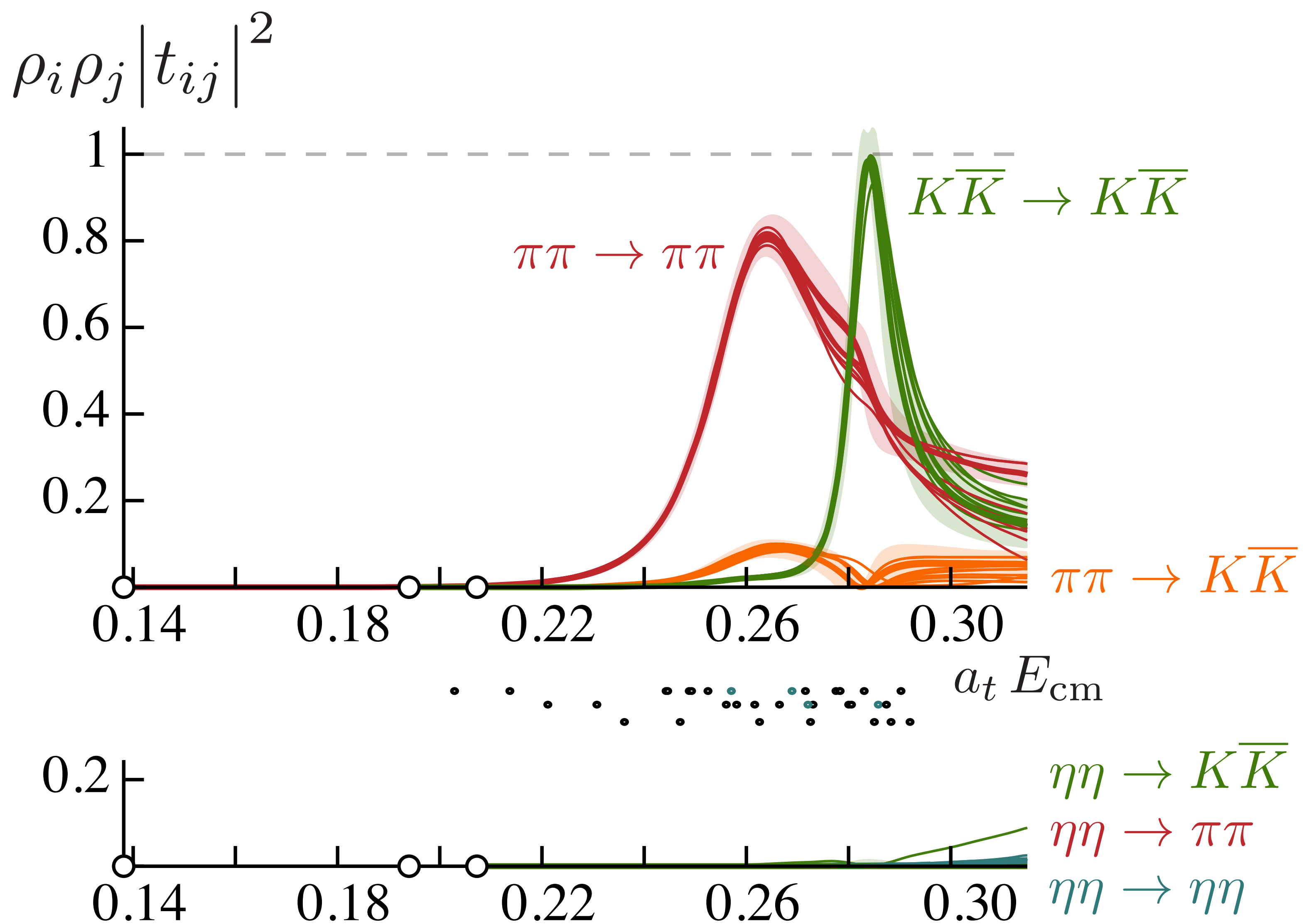

$\pi\pi$, $K\bar{K}$, $\eta\eta$ scattering with m_π~391 MeV

D-wave amplitudes

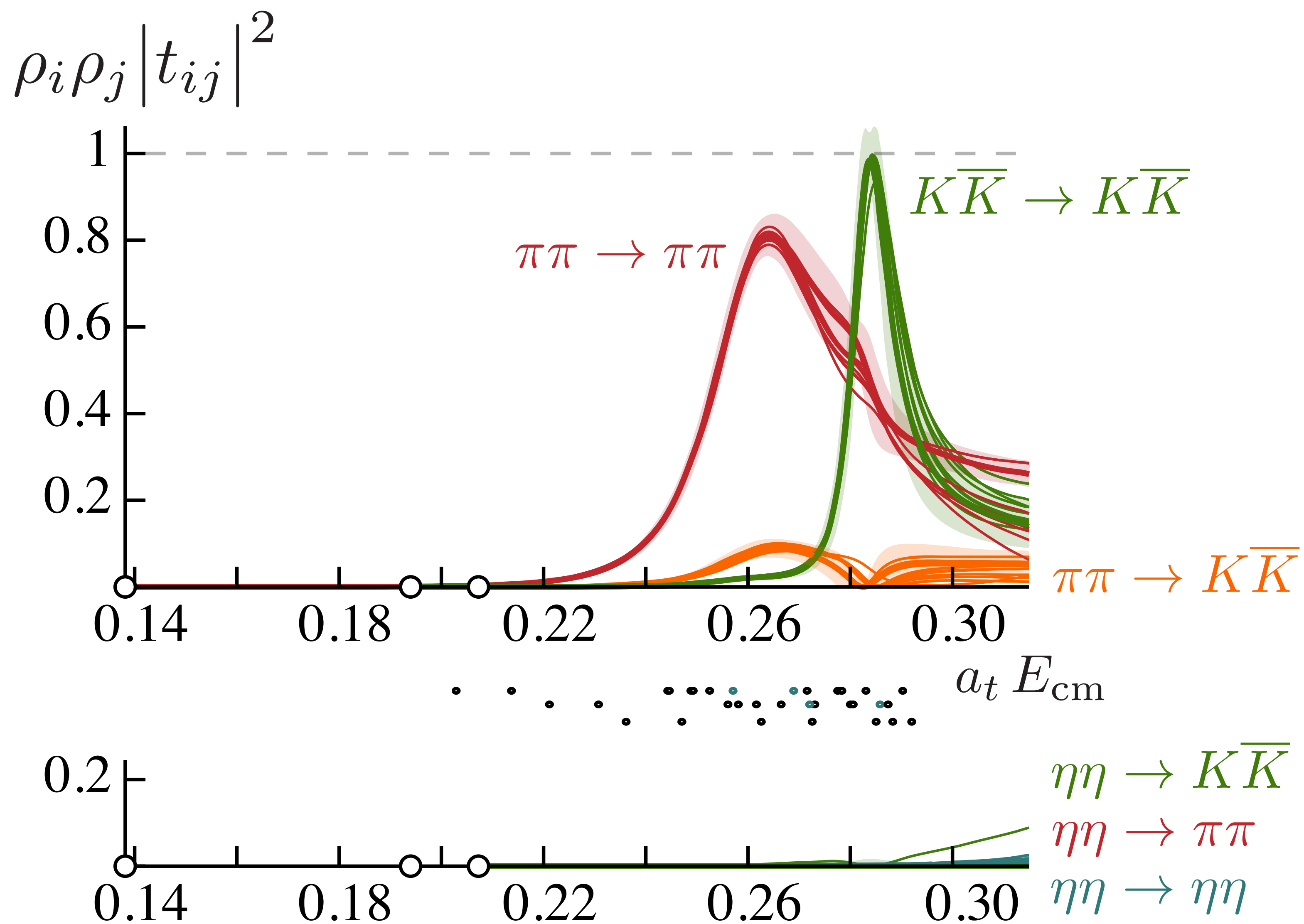

'looks like' two resonances

— lighter one has larger width, big coupling to $\pi\pi$

— heavier one has smaller width, big coupling to $K\bar{K}$

… there must be a more rigorous way to know the resonance content ?

contents

scattering amplitudes are measured for real energies above threshold

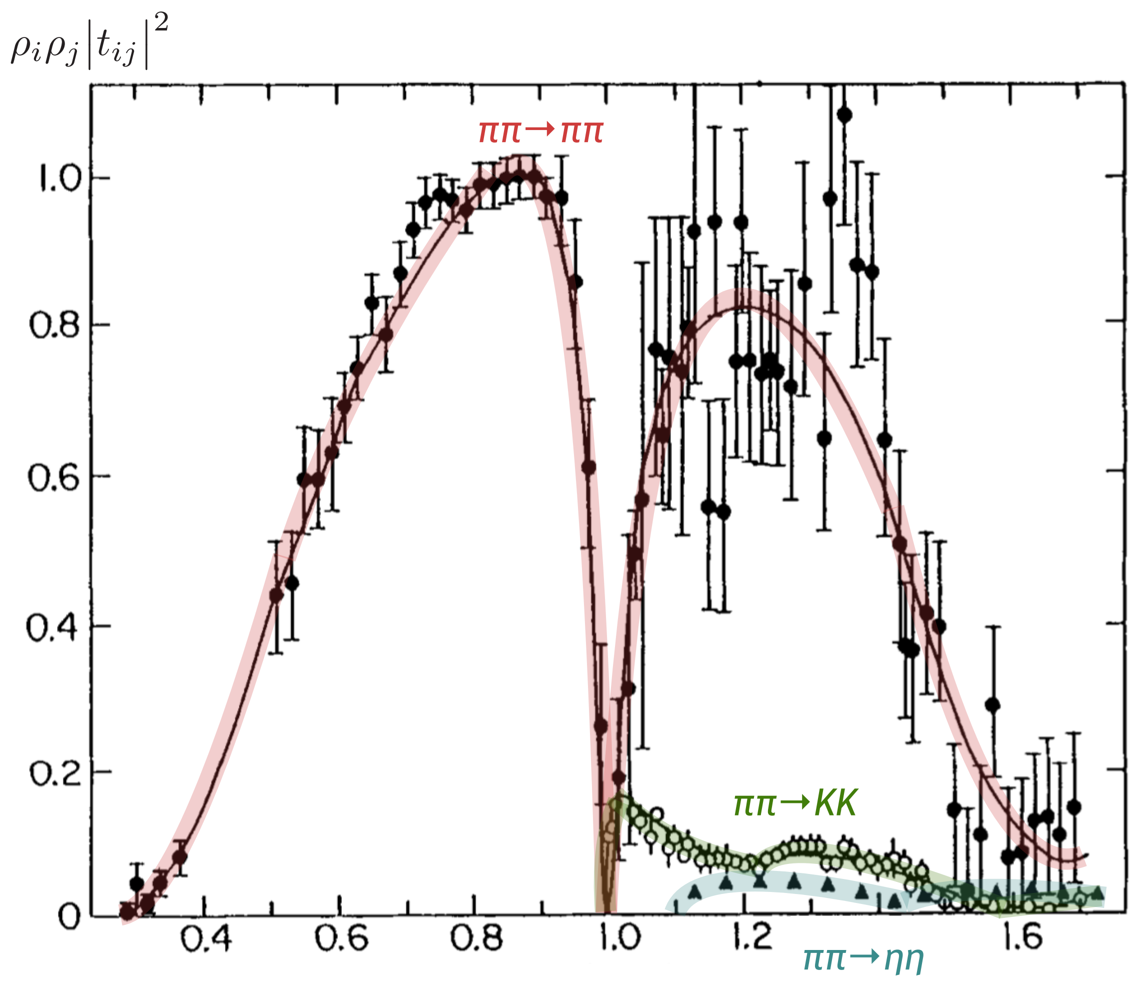

and we've seen that lattice calculations can lead to something similar

singularities in the complex energy plane

does it make sense to consider how the amplitude behaves 'elsewhere'
— below threshold ?
— for complex values of E ?

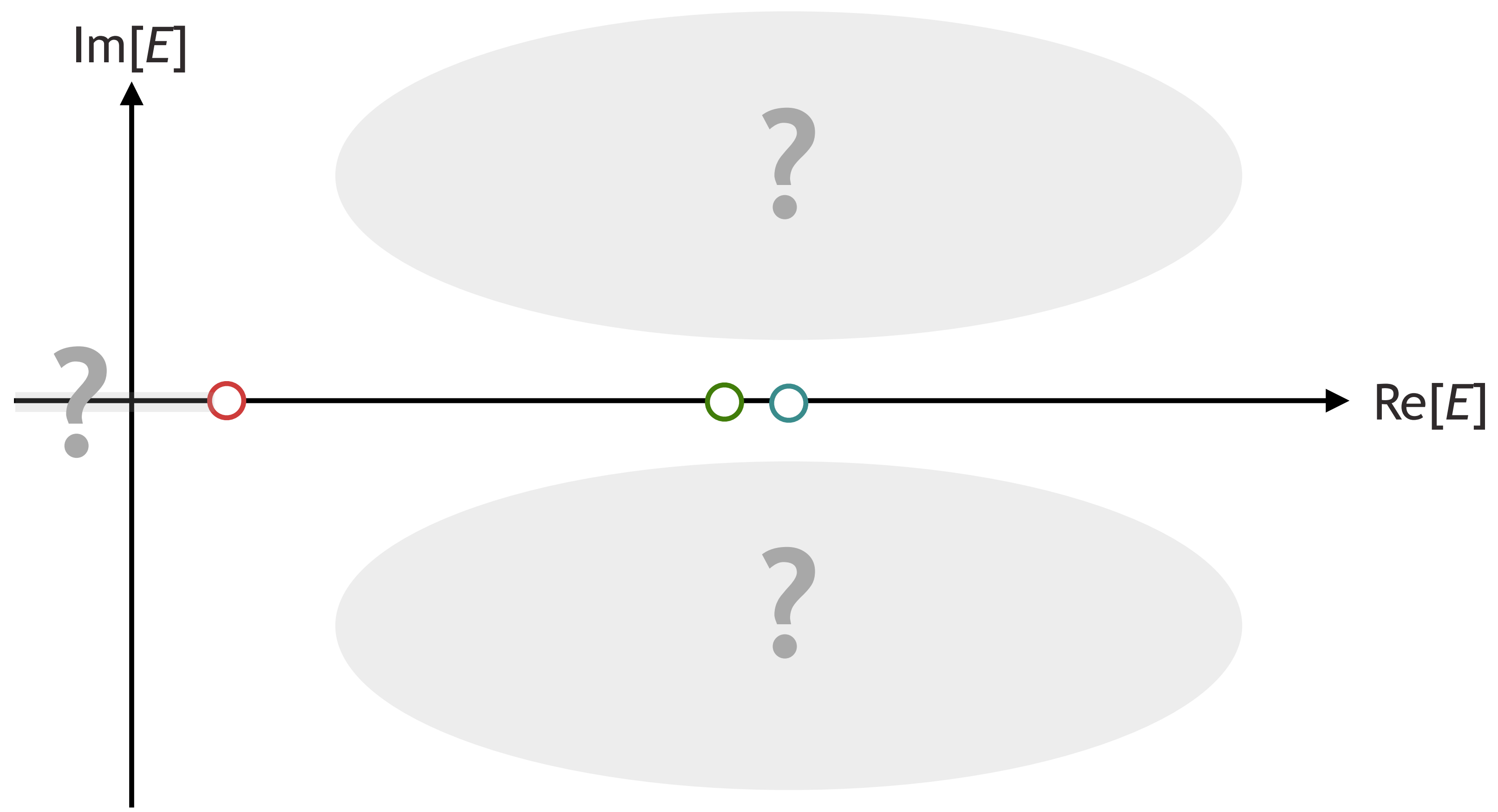

complex variable theory tells us that
singularities (poles, cuts)
'control' the behaviour of functions

— what singularities can our amplitudes have ?

there’s a rather nice (old) book that gives a gentle introduction to this topic

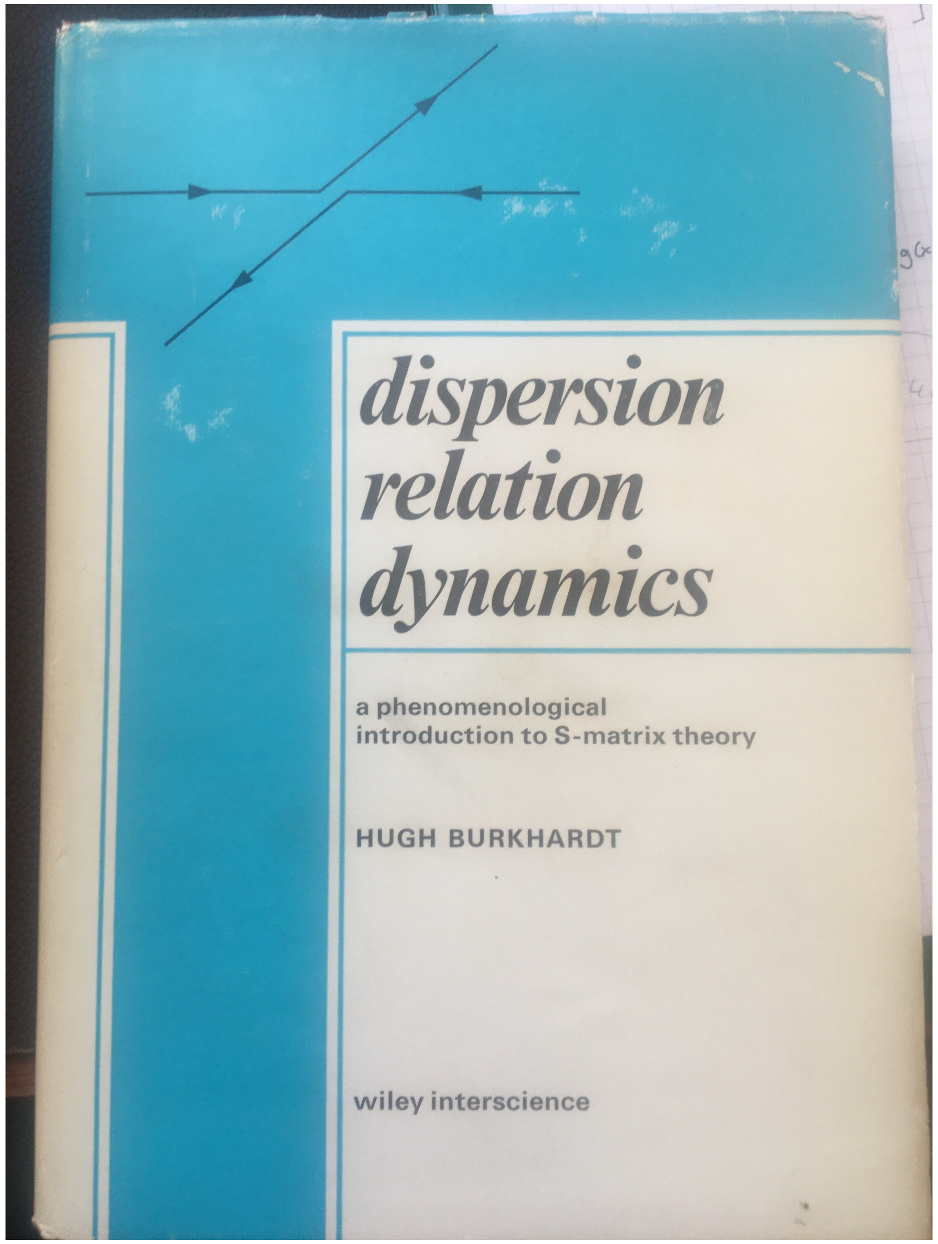

This book is a lowbrow exposition of S-matrix theory, which is the approach to the dynamics of the strong interactions of elementary particles that uses dispersion relations and unitarity as its main tools. This inductive approach has the important advantage that the calculations can be made accessible to experimenters and others who would not wish to follow the more sophisticated derivations. A good deal of attention has been paid to explaining the grammar of the language of analytic functions.

The reasons for choosing an inductive approach lie in the present state of the theory. S-matrix dynamics has proved reasonably successful as a model for correlating and predicting experimental results, but it is still far from being a complete predictive theory. It is important that those methods which are fairly well established and useful in calculations should be widely understood.

the unitarity cut

unitarity gives us one guaranteed singularity — **a branch cut starting at threshold**

e.g. elastic partial-wave case: $\mathrm{Im}\, t_\ell(s) = \rho(s) \big| t_\ell(s) \big|^2 \, \Theta(s - 4m^2)$

the unitarity cut

unitarity gives us one guaranteed singularity — **a branch cut starting at threshold**

e.g. elastic partial-wave case: $\mathrm{Im}\, t_\ell(s) = \rho(s) \left| t_\ell(s) \right|^2 \Theta(s - 4m^2)$

$$\rho(s) = \frac{2k(s)}{\sqrt{s}} = \frac{\boxed{\sqrt{s - 4m^2}}}{\sqrt{s}}$$

square root branch cut

the unitarity cut

unitarity gives us one guaranteed singularity — **a branch cut starting at threshold**

e.g. elastic partial-wave case: $\mathrm{Im}\, t_\ell(s) = \rho(s) \left| t_\ell(s) \right|^2 \Theta(s - 4m^2)$

$$\rho(s) = \frac{2k(s)}{\sqrt{s}} = \frac{\boxed{\sqrt{s-4m^2}}}{\sqrt{s}}$$

square root branch cut

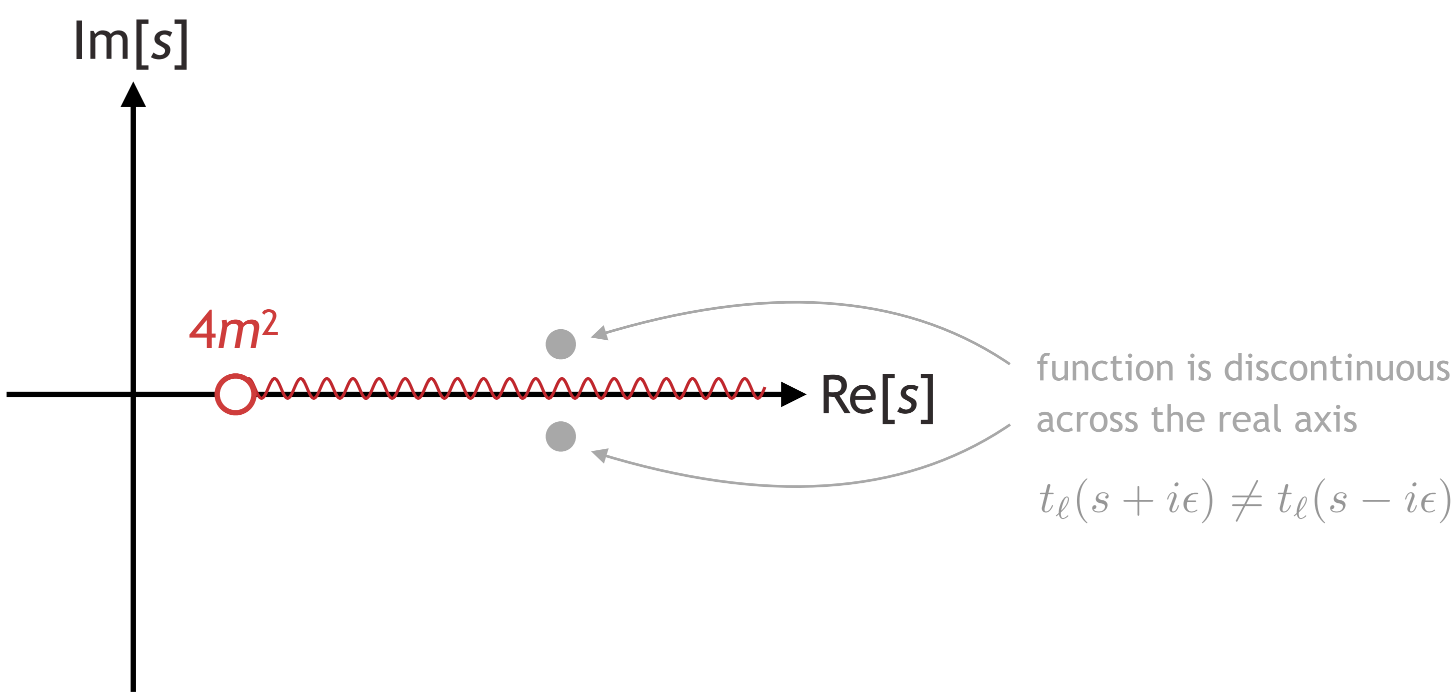

has an immediate consequence
— the complex plane must be **multi-sheeted**

Riemann sheet structure

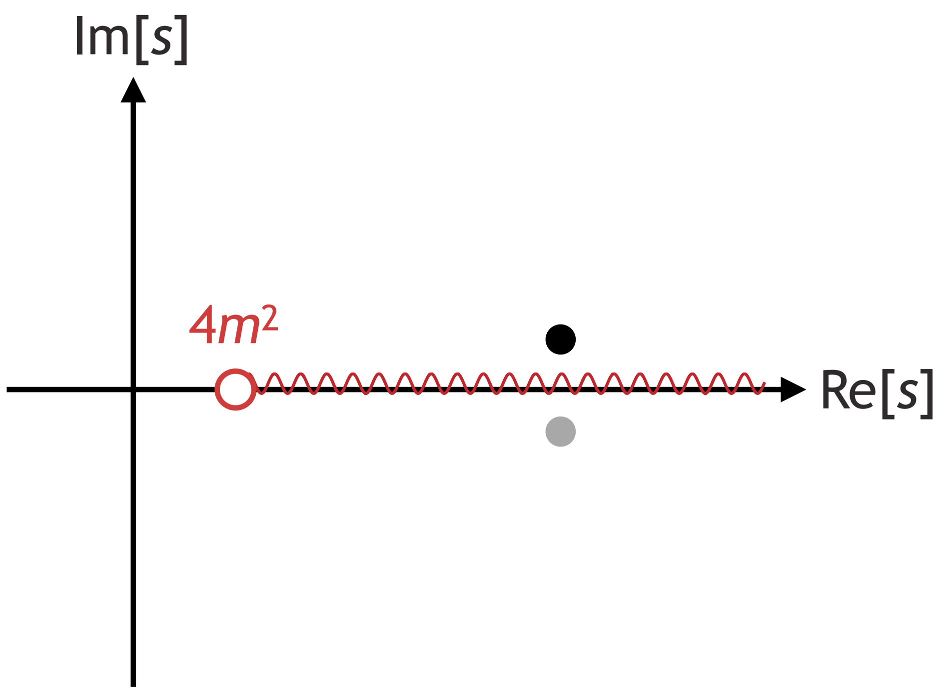

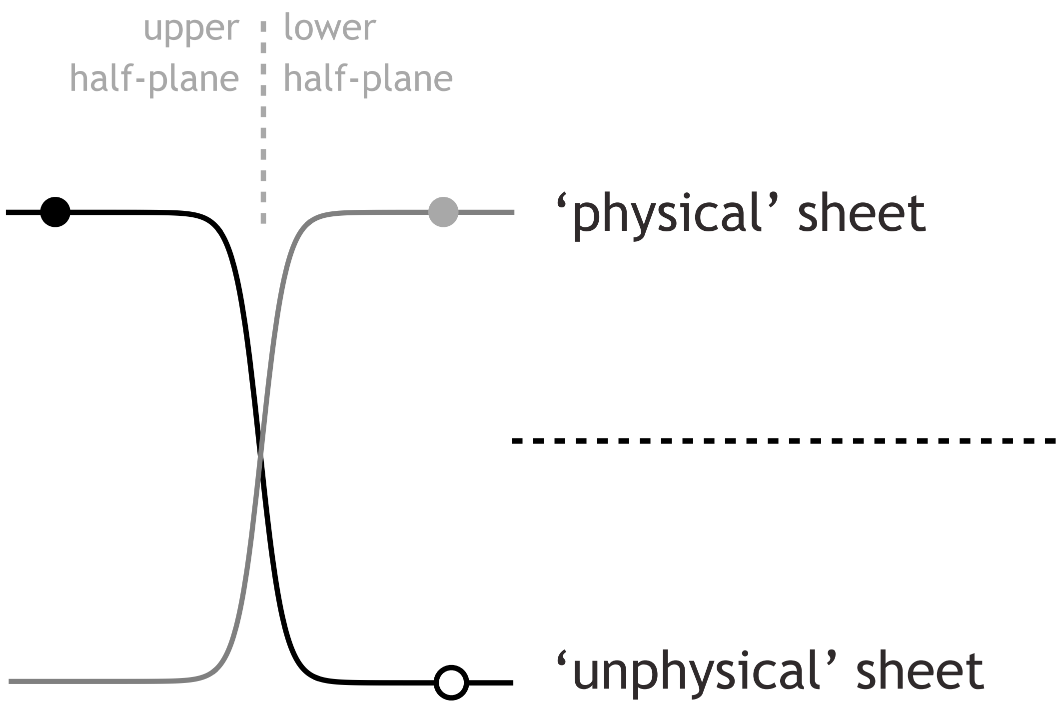

sheets can be characterised by the sign of Im[k]

physical sheet = sheet I = Im[k] > 0

unphysical sheet = sheet II = Im[k] < 0

pole singularities ?

scattering amplitudes can have pole singularities only in certain locations

real energy axis, below threshold on **physical sheet**

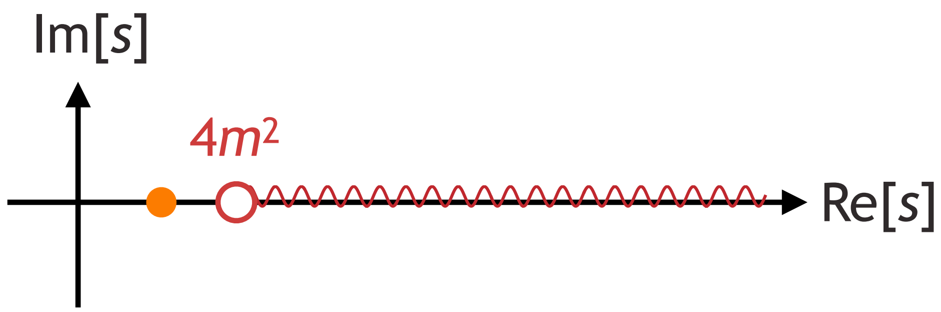

corresponds to a **stable bound-state**

pole singularities ?

scattering amplitudes can have pole singularities only in certain locations

real energy axis, below threshold on **physical sheet**

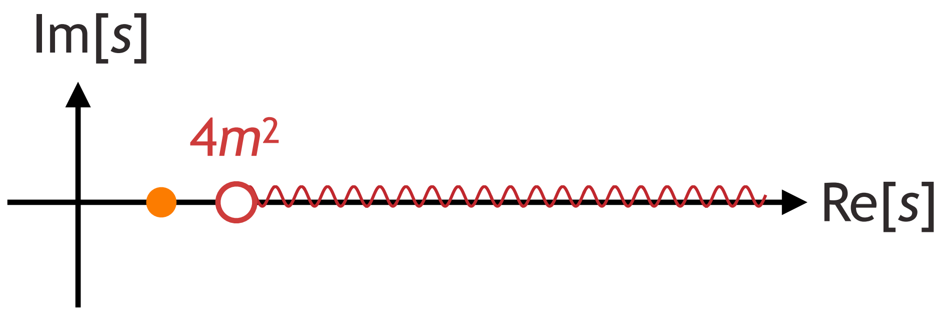

corresponds to a **stable bound-state**

a stable bound-state
will strongly enhance scattering at threshold

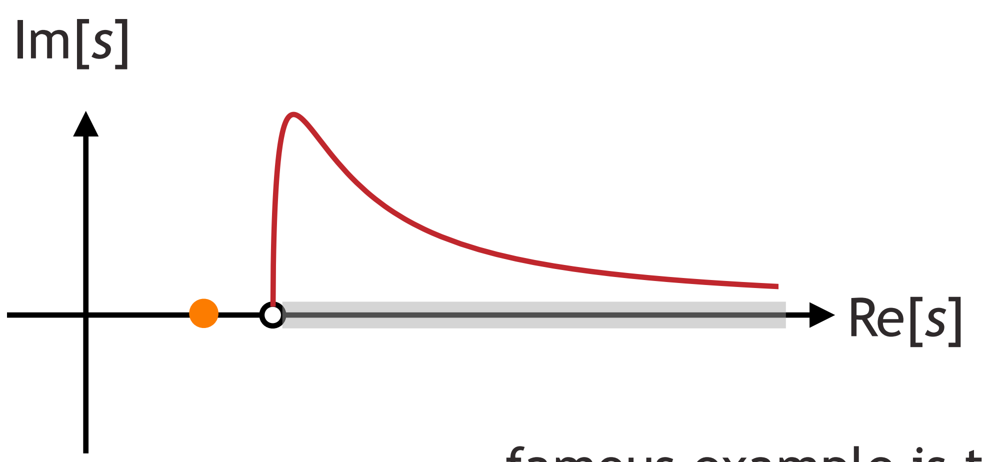

famous example is the
deuteron at NN threshold

pole singularities ?

scattering amplitudes can have pole singularities only in certain locations

real energy axis, below threshold on **physical sheet**

corresponds to a **stable bound-state**

off the real axis, on the **unphysical sheet**

(in complex conjugate pairs)

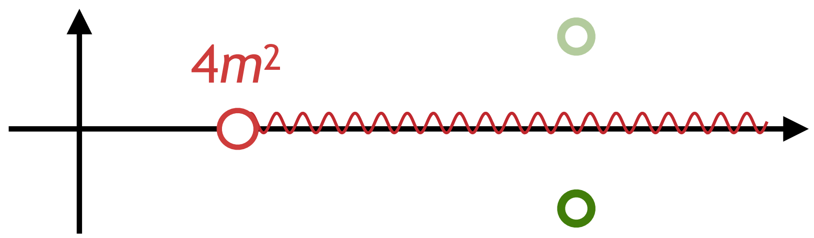

corresponds to a **resonance**

pole on the unphysical sheet

an **isolated** pole on the unphysical sheet will produce a bump on the real axis

– the classic resonance signature

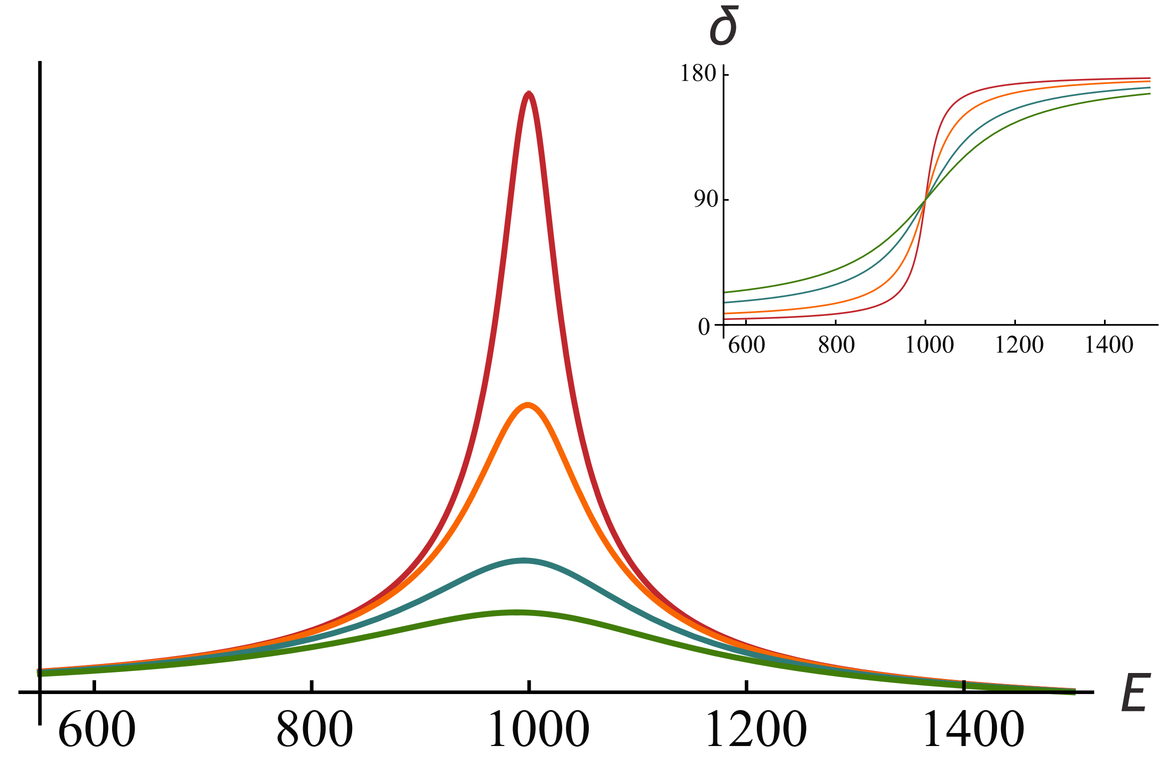

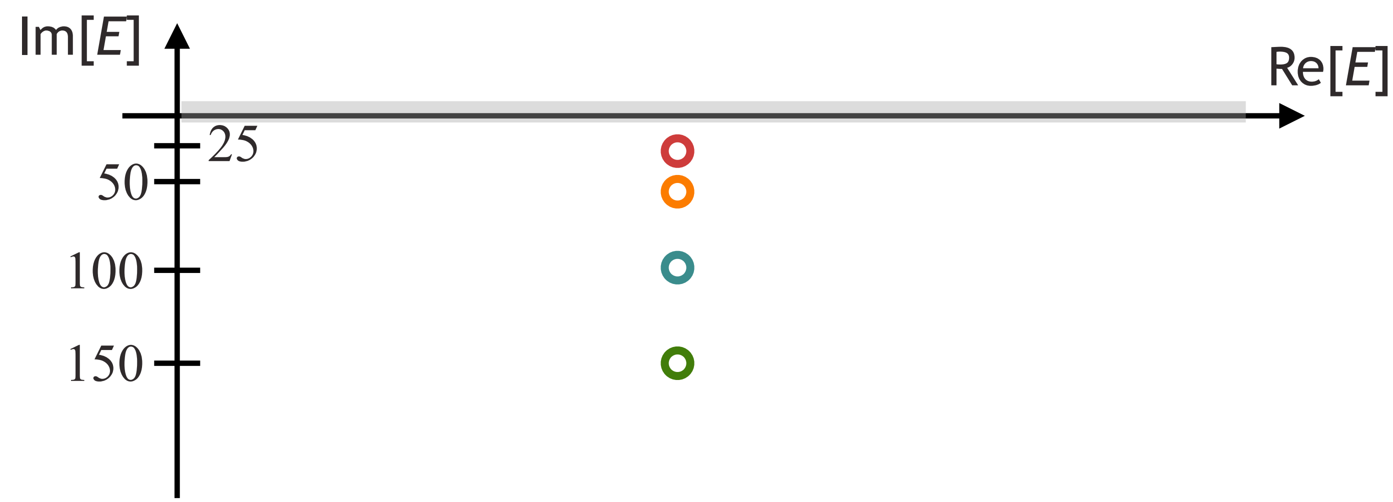

close to the pole

$$t_\ell(s) \sim \frac{1}{s_0 - s}$$

$$s_0 = \left(m - i\tfrac{1}{2}\Gamma\right)^2$$

pole singularities ?

scattering amplitudes can have pole singularities only in certain locations

real energy axis, below threshold on **physical sheet**

corresponds to a **stable bound-state**

off the real axis, on the **unphysical sheet**

(in complex conjugate pairs)

corresponds to a **resonance**

real energy axis, below threshold on **unphysical sheet**

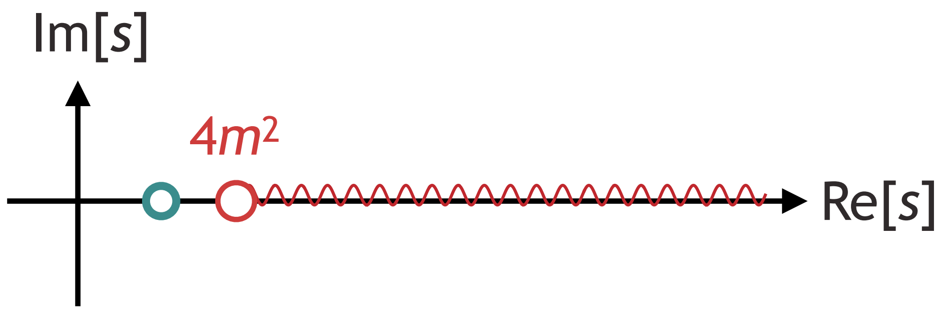

corresponds to a **virtual bound-state**

pole singularities ?

scattering amplitudes can have pole singularities only in certain locations

not allowed: poles off the real axis
on the **physical sheet**

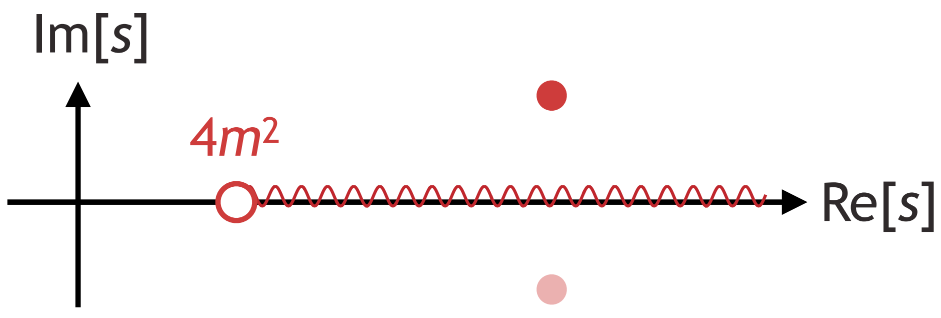

would violate **causality**

singularity structure from lattice calculations — elastic

$\pi\pi$ isospin=2

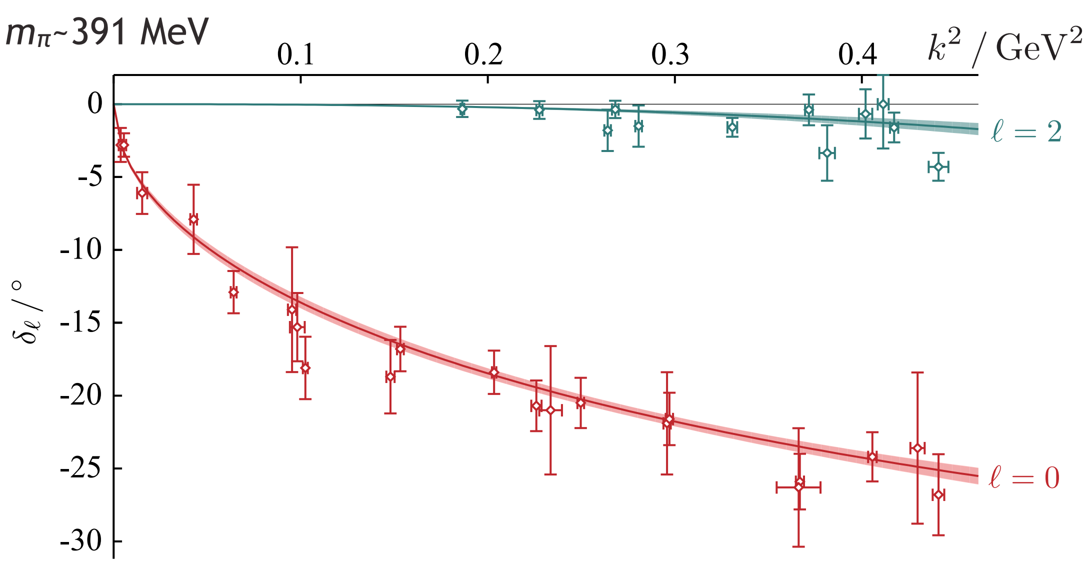

PRD86 034031 (2012)

no nearby poles

weak and repulsive interaction

$$k \cot \delta_0 = \frac{1}{a_0} + \ldots$$

[first term in the 'effective range expansion' $k \cot \delta_0 = \frac{1}{a_0} + \frac{1}{2} r_0 k^2 + \ldots$]

$$m_\pi a_0 = -0.285(6)$$

$$t_{\ell=0} = \frac{\sqrt{s}}{2} \frac{1}{k \cot \delta_0 - ik}$$

$$s_0 \approx -45\, m_\pi^2$$

a pole, but very far away

singularity structure from lattice calculations — elastic

$\pi\pi$ isospin=1

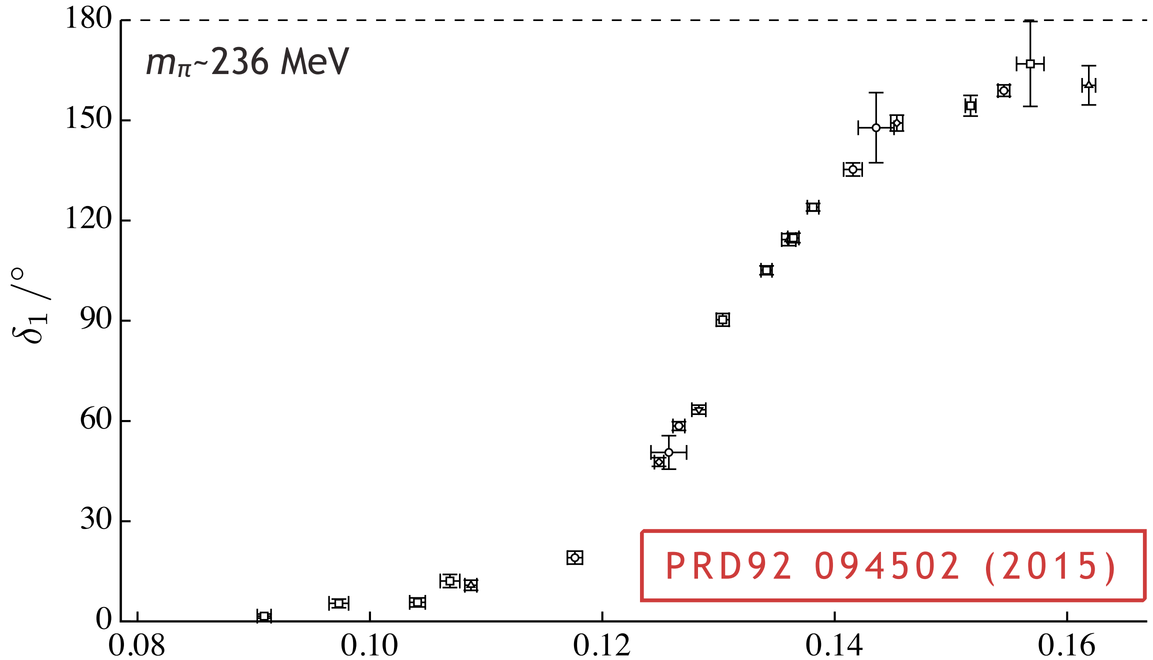

a single isolated pole

a narrow resonance

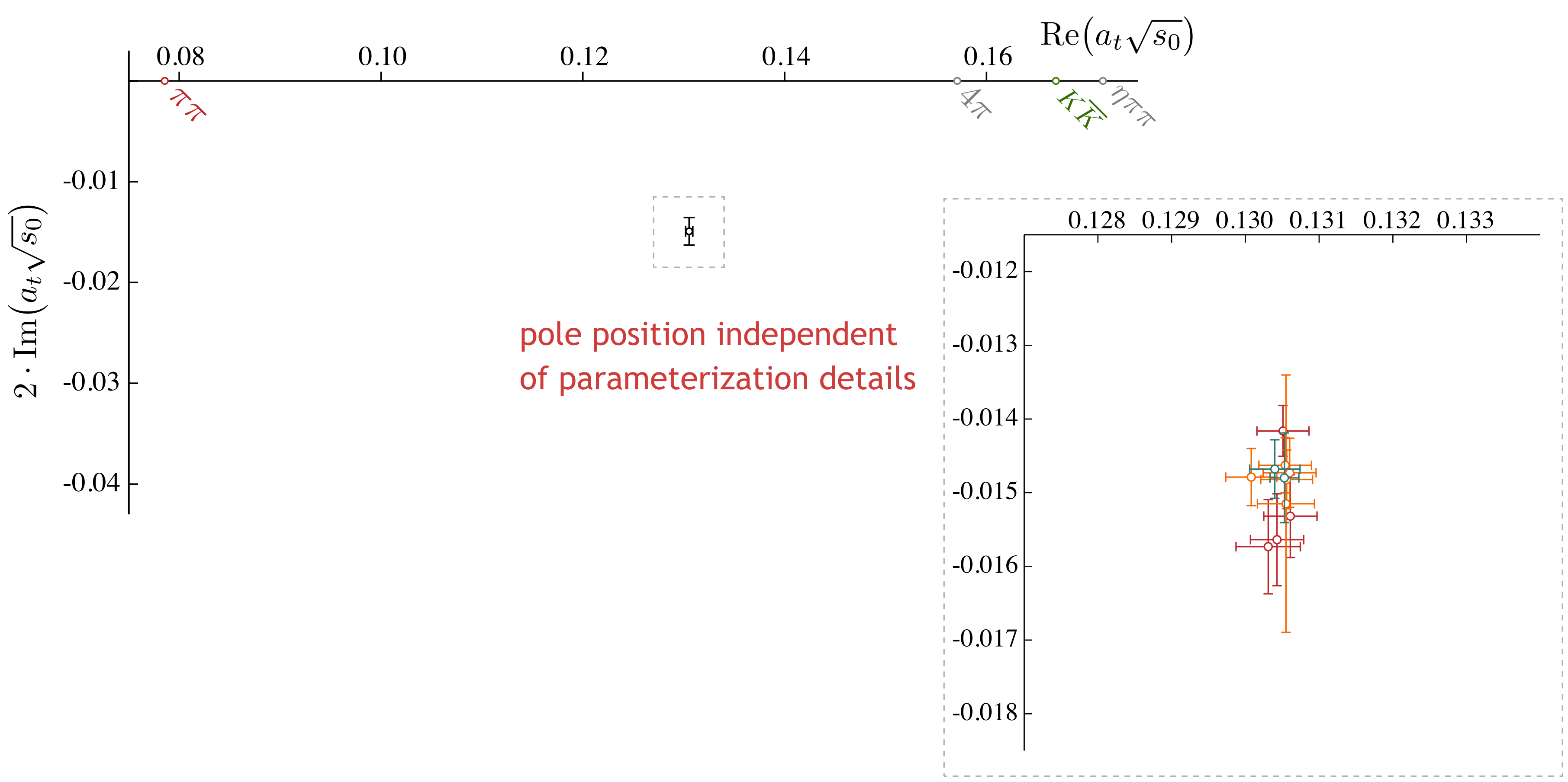

pole position independent of parameterization details

singularity structure from lattice calculations — elastic

$\pi\pi$ isospin=1

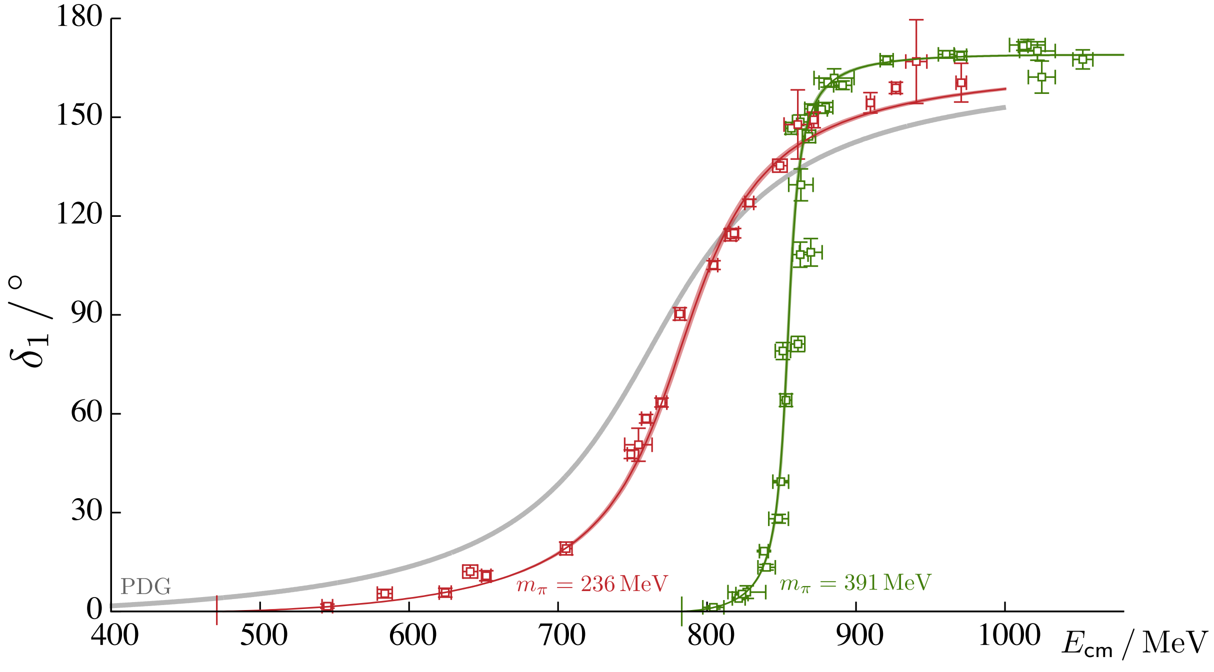

evolution with changing quark mass

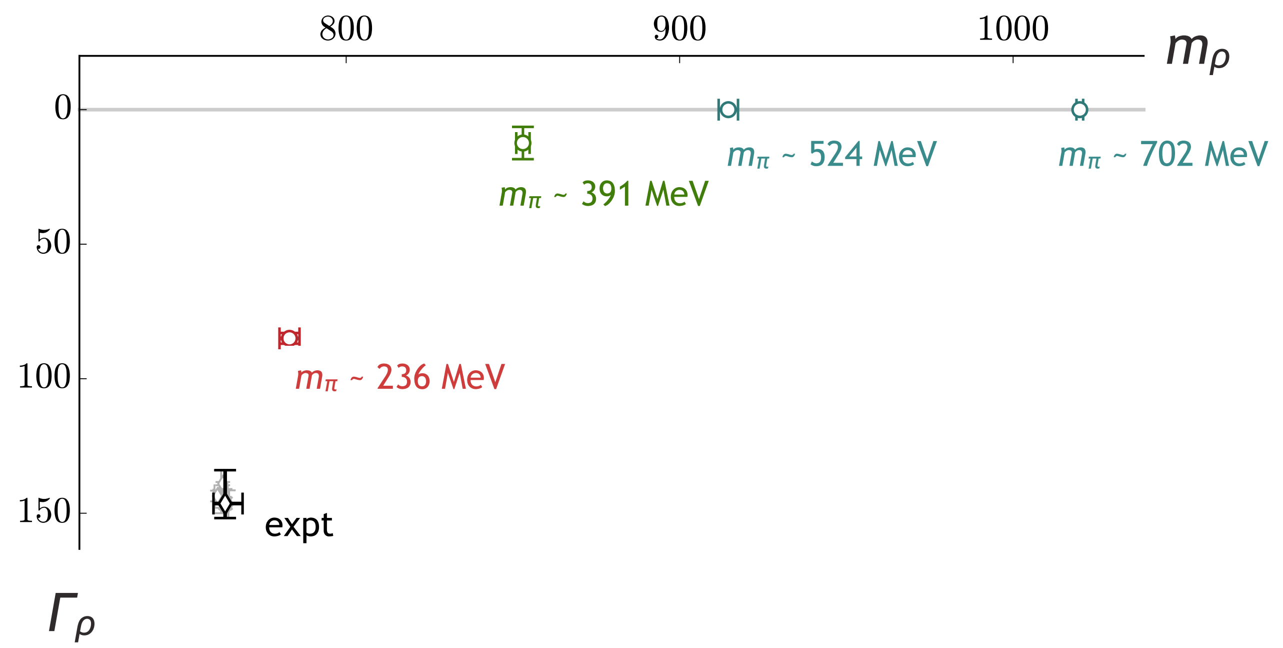

poles don't 'appear' or 'disappear' with changing quark mass — they smoothly move round the complex plane

singularity structure from lattice calculations — elastic

$\pi\pi$ isospin=0

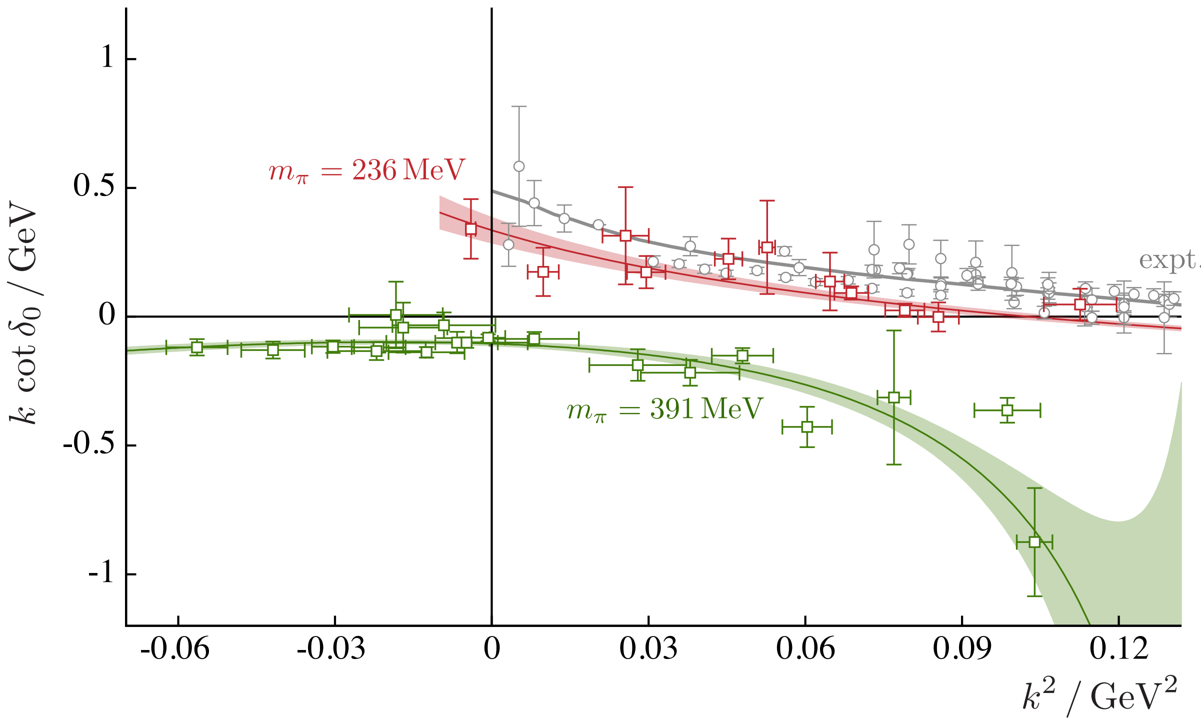

PRL118 022002 (2017)

$$t_{\ell=0} = \frac{\sqrt{s}}{2}\frac{1}{k\cot\delta_0 - ik}$$

m_π~391 MeV — a bound-state pole

m_π~236 MeV — a resonance pole

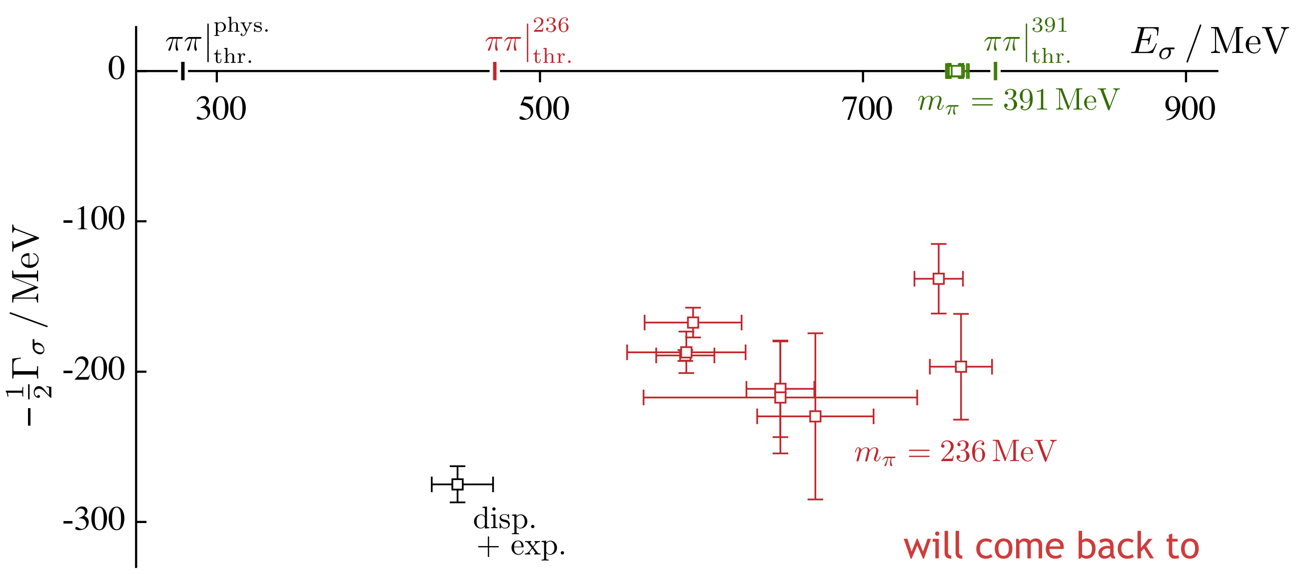

will come back to this scatter later if there's time for each new channel, each sheet splits in two ⇒ 2^N sheets for N channels

e.g. two channels ($\pi\pi$, $K\bar{K}$)

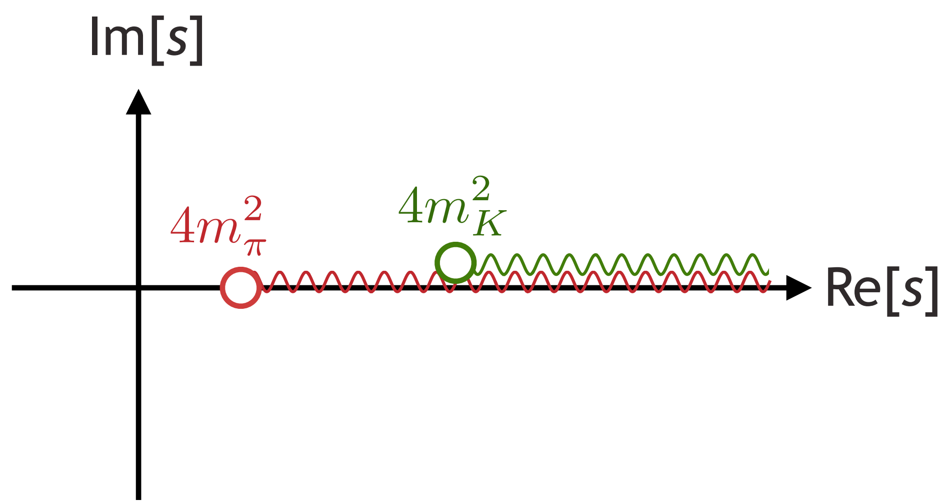

coupled-channels

for each new channel, each sheet splits in two ⇒ 2^N sheets for N channels

e.g. two channels ($\pi\pi$, $K\bar{K}$)

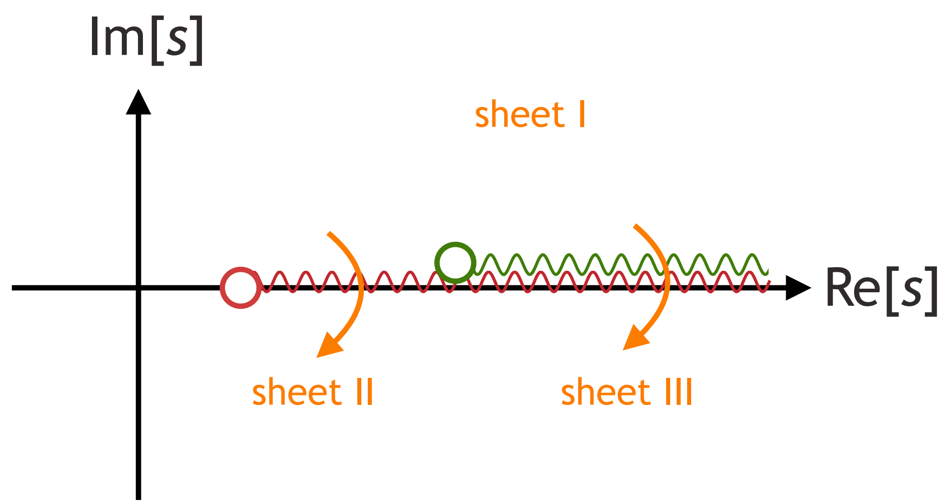

	Im[$k_{\pi\pi}$]	Im[k_{KK}]
sheet I	+	+
sheet II	−	+
sheet III	−	−
sheet IV	+	−

coupled-channels

for each new channel, each sheet splits in two ⇒ 2^N sheets for N channels

e.g. two channels ($\pi\pi$, $K\bar{K}$)

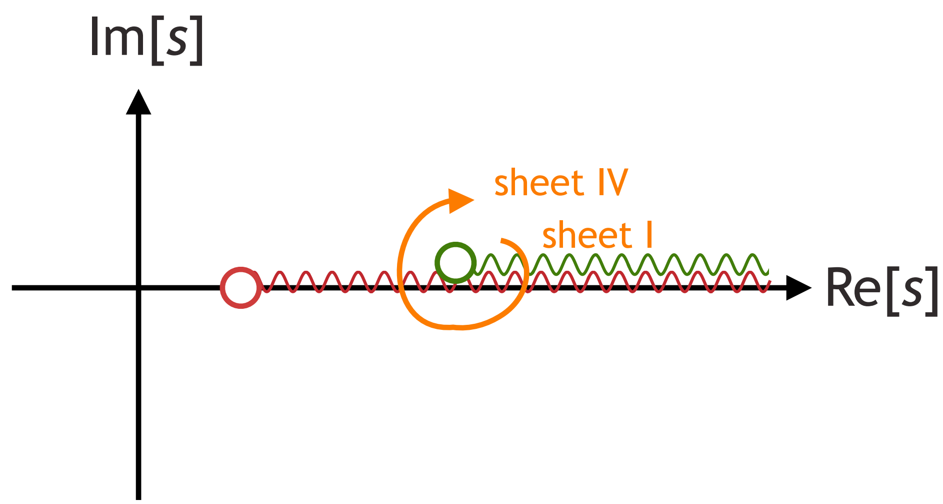

	Im[$k_{\pi\pi}$]	Im[k_{KK}]
sheet I	+	+
sheet II	−	+
sheet III	−	−
sheet IV	+	−

coupled-channels

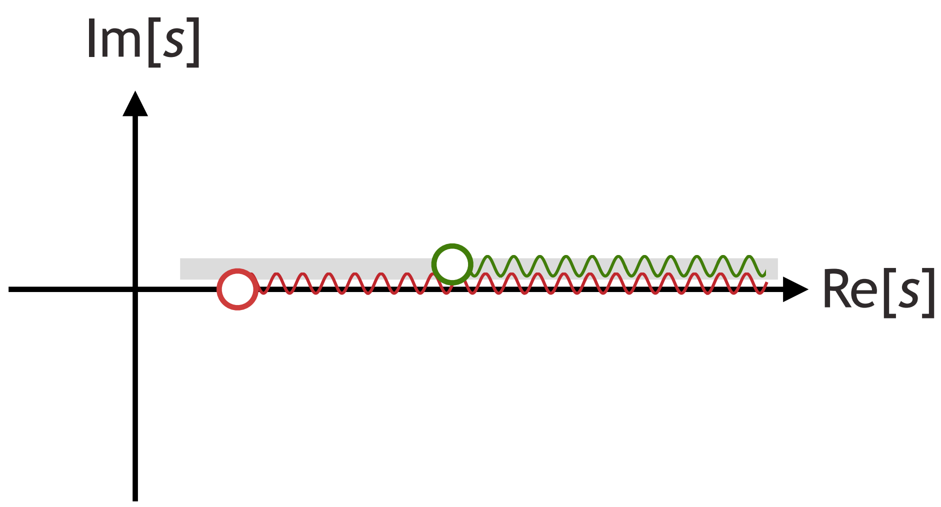

	Im[$k_{\pi\pi}$]	Im[k_{KK}]
sheet I	+	+
sheet II	−	+
sheet III	−	−
sheet IV	+	−

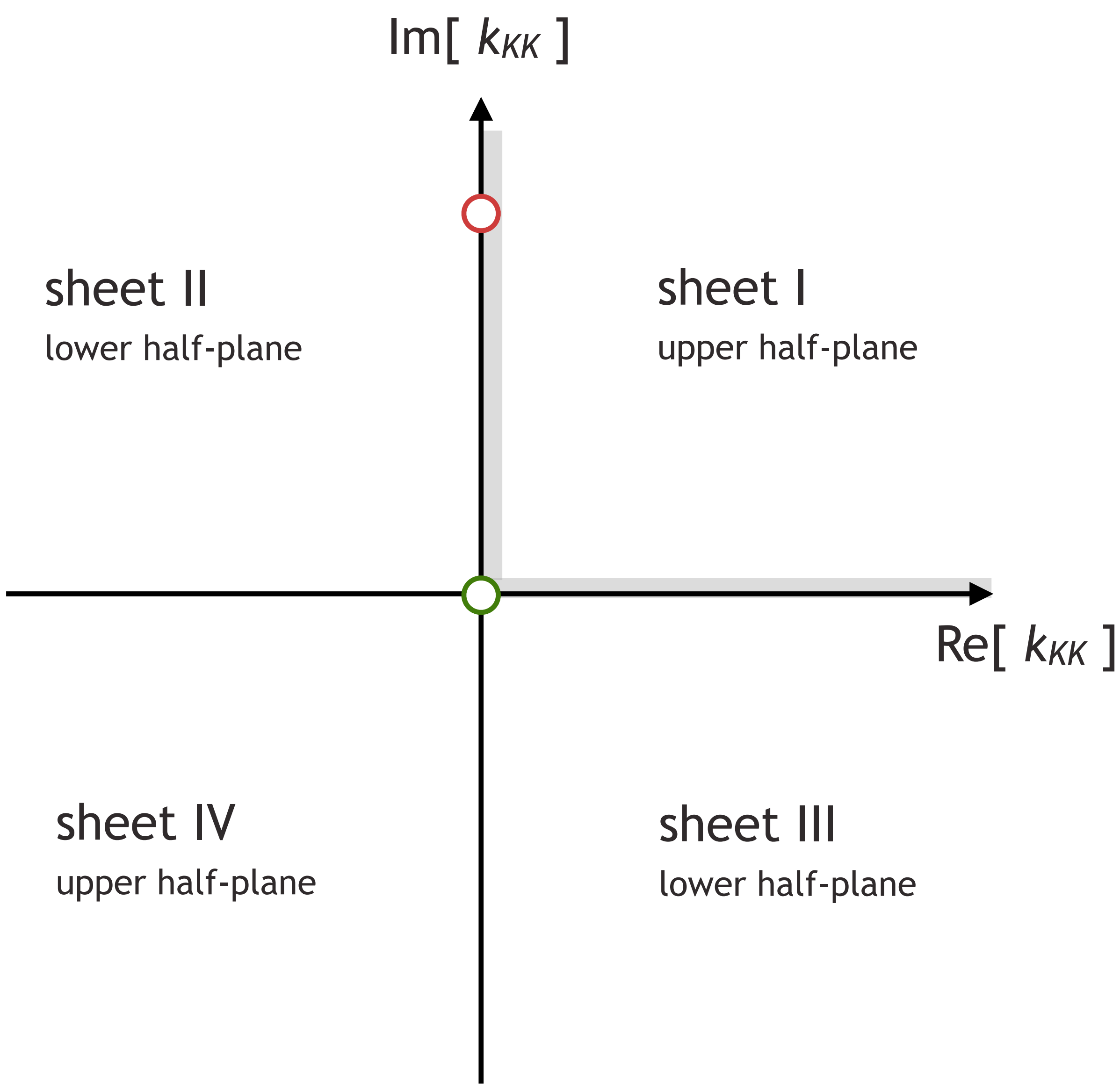

coupled-channels — between thresholds

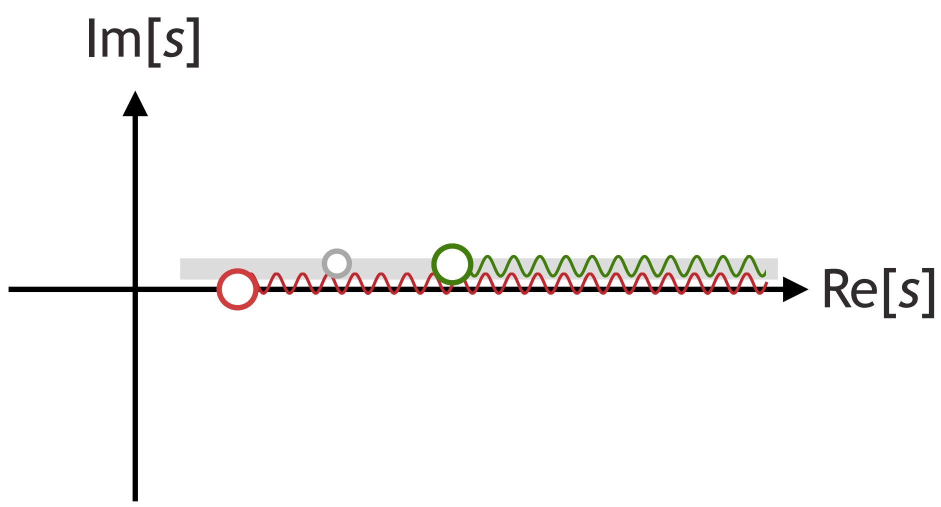

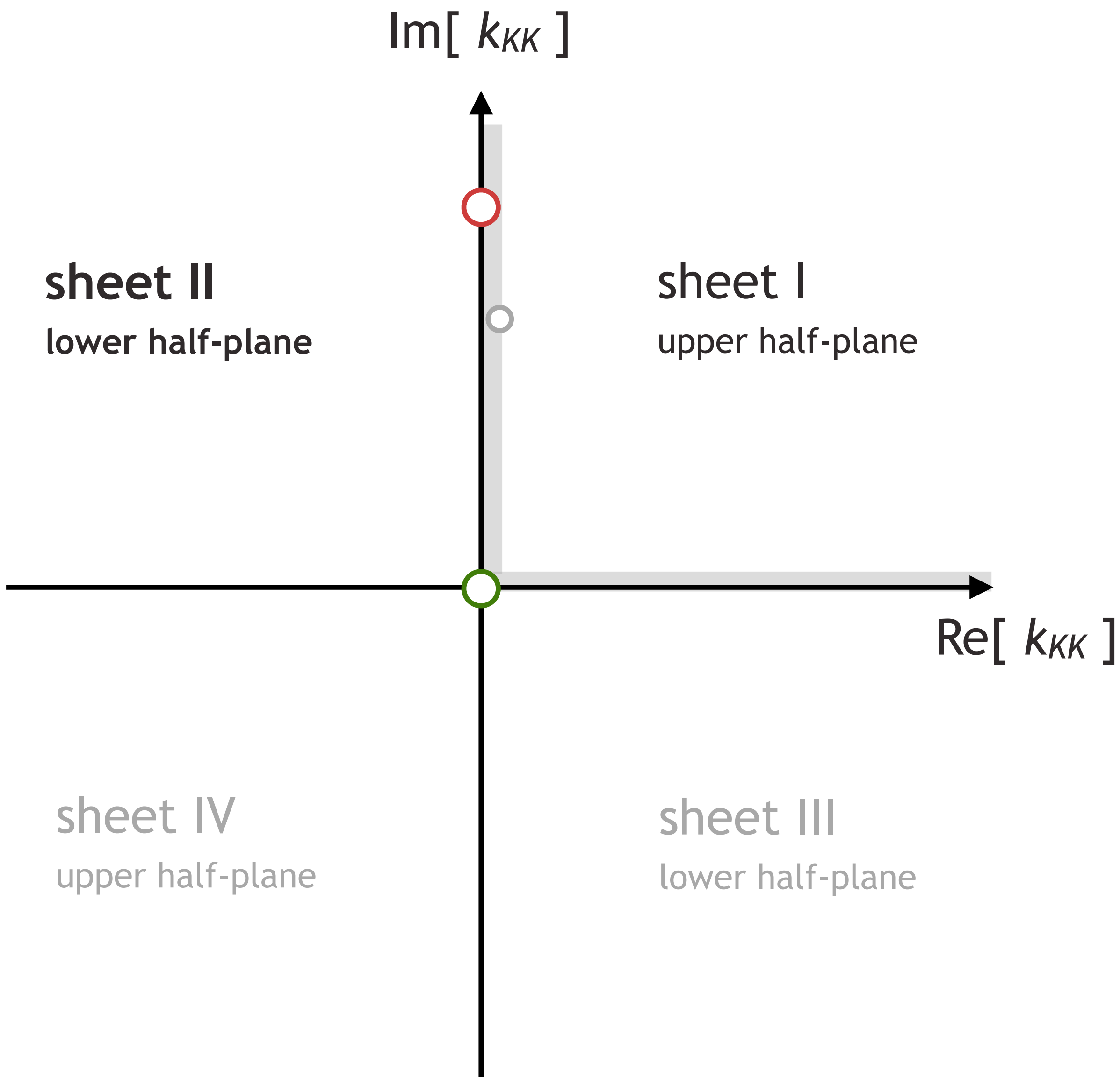

coupled-channels — near second threshold

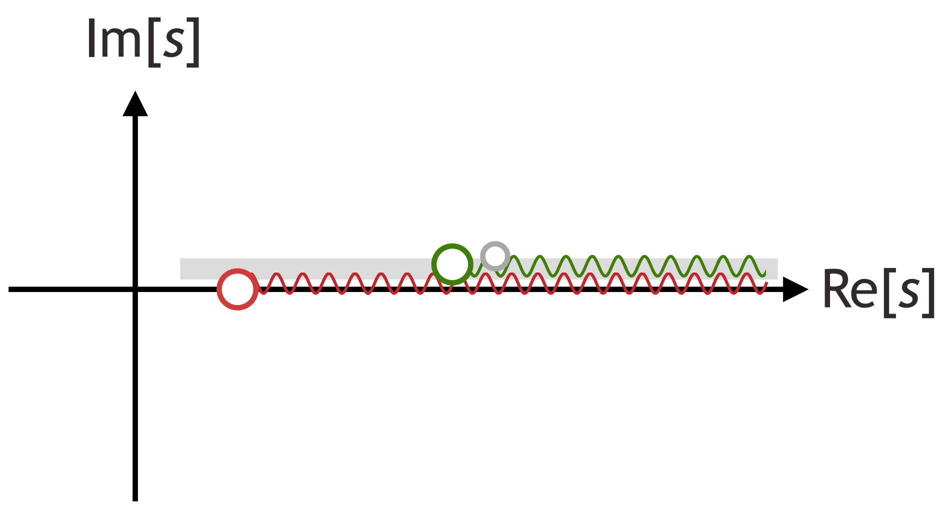

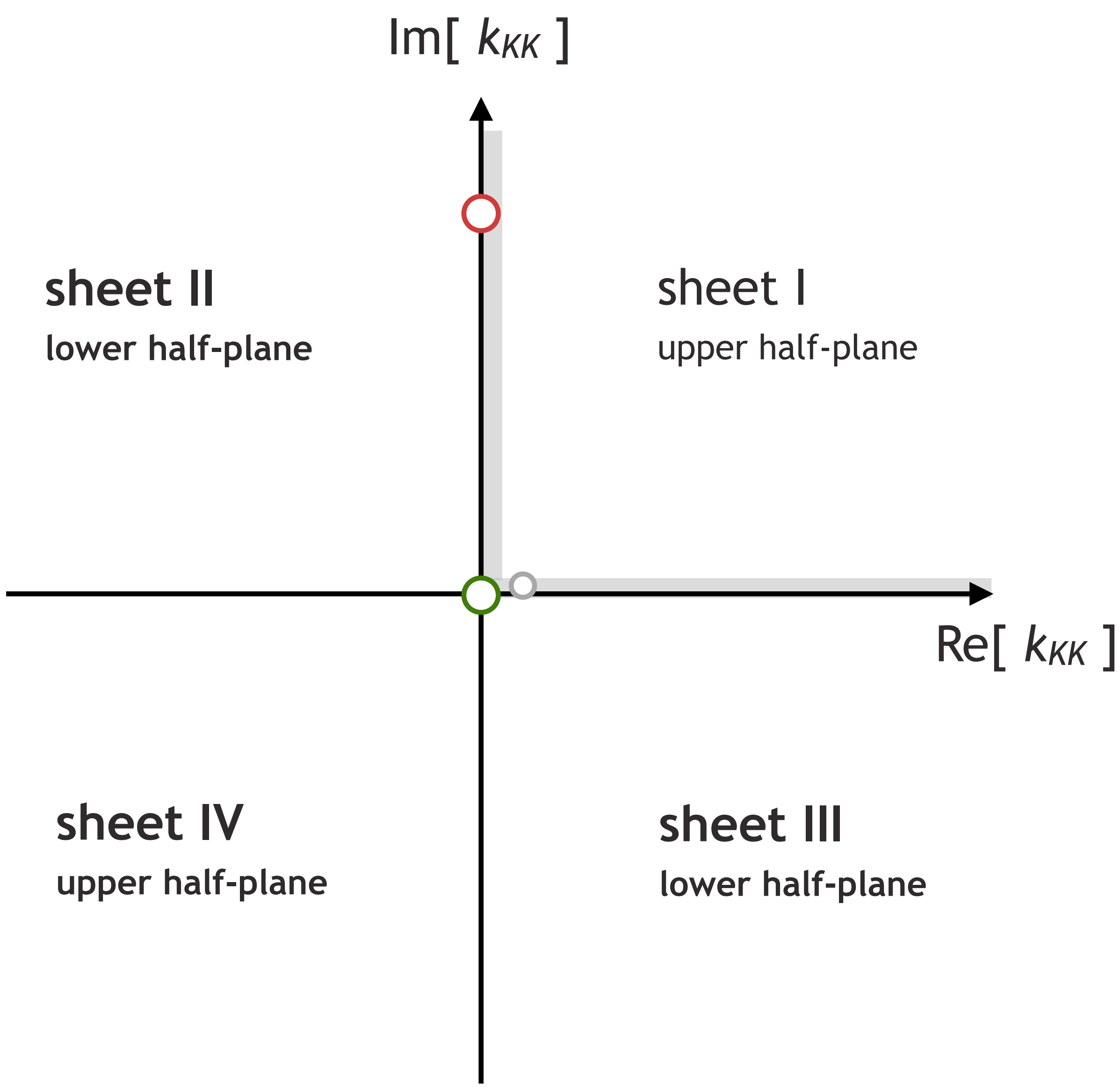

coupled-channels — well above both thresholds

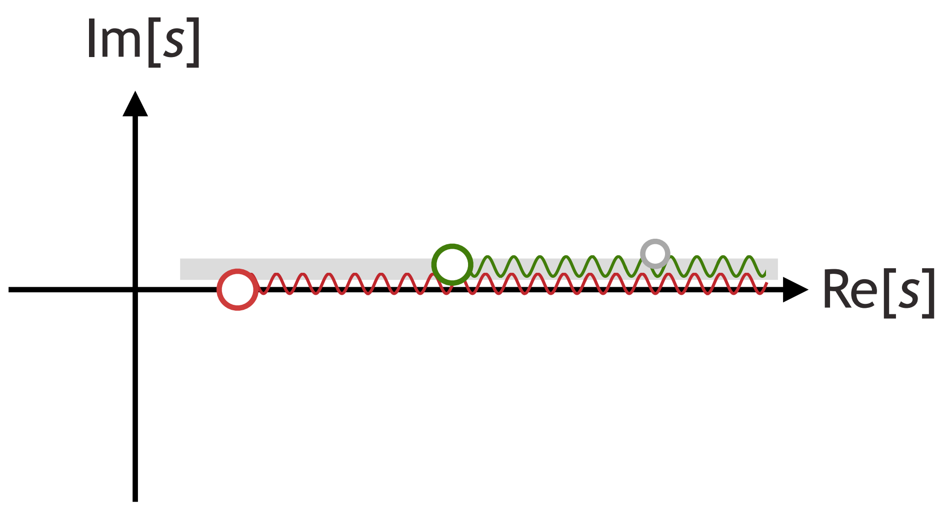

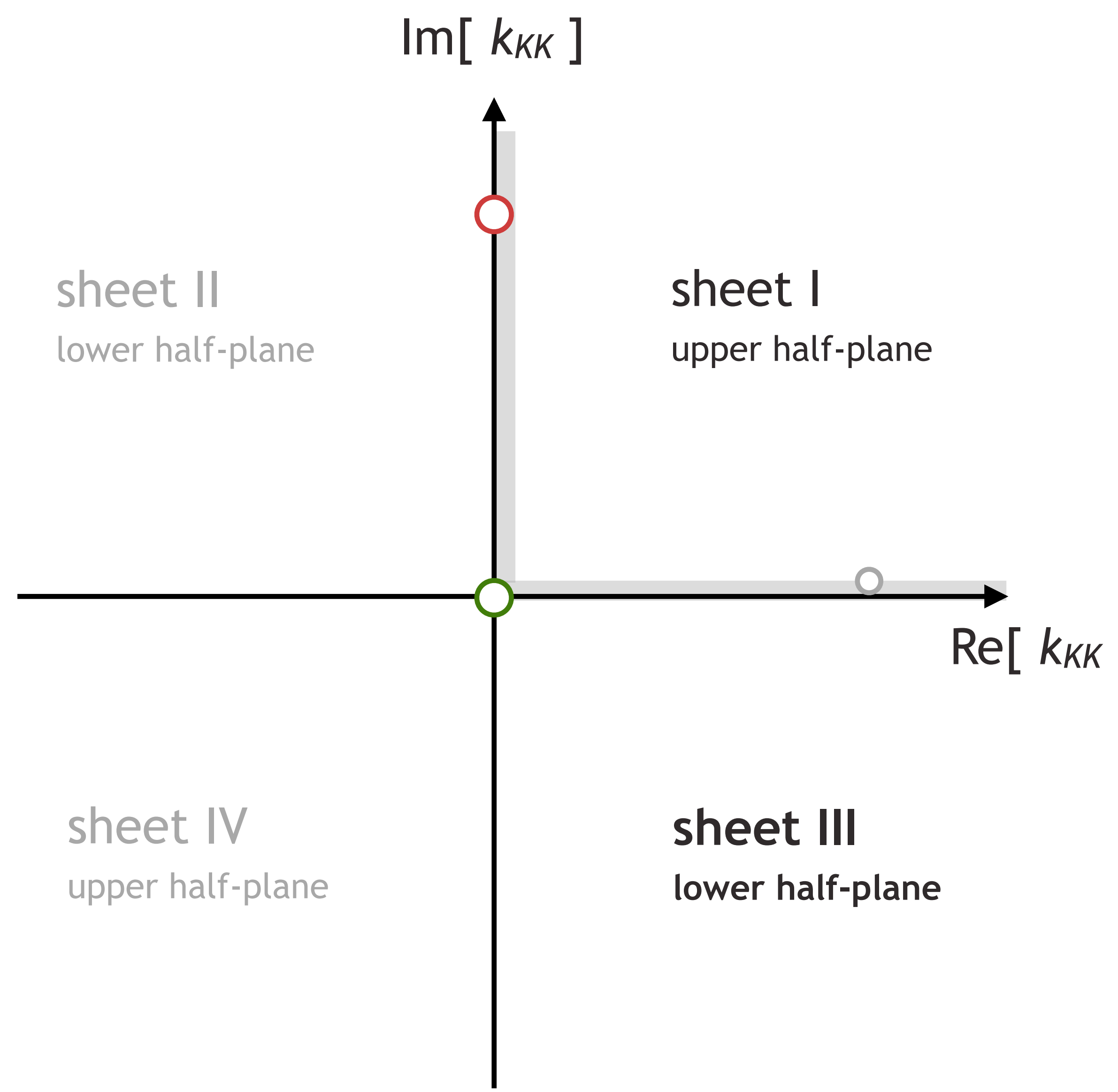

two-channel Flatté amplitude

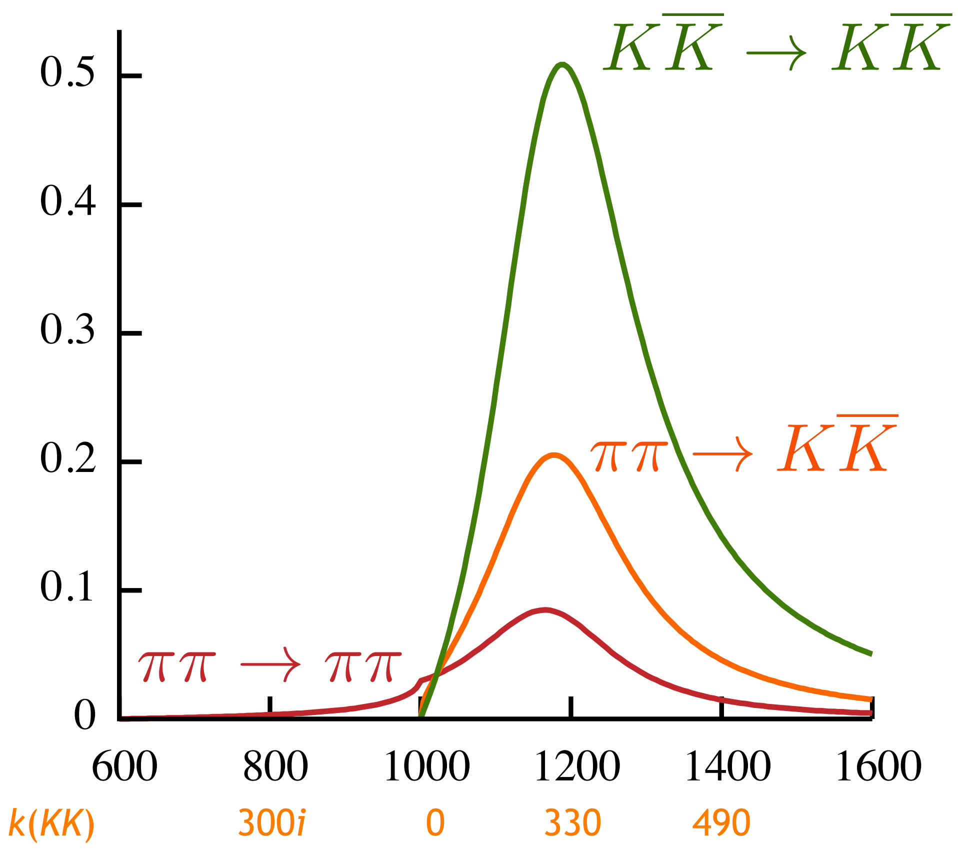

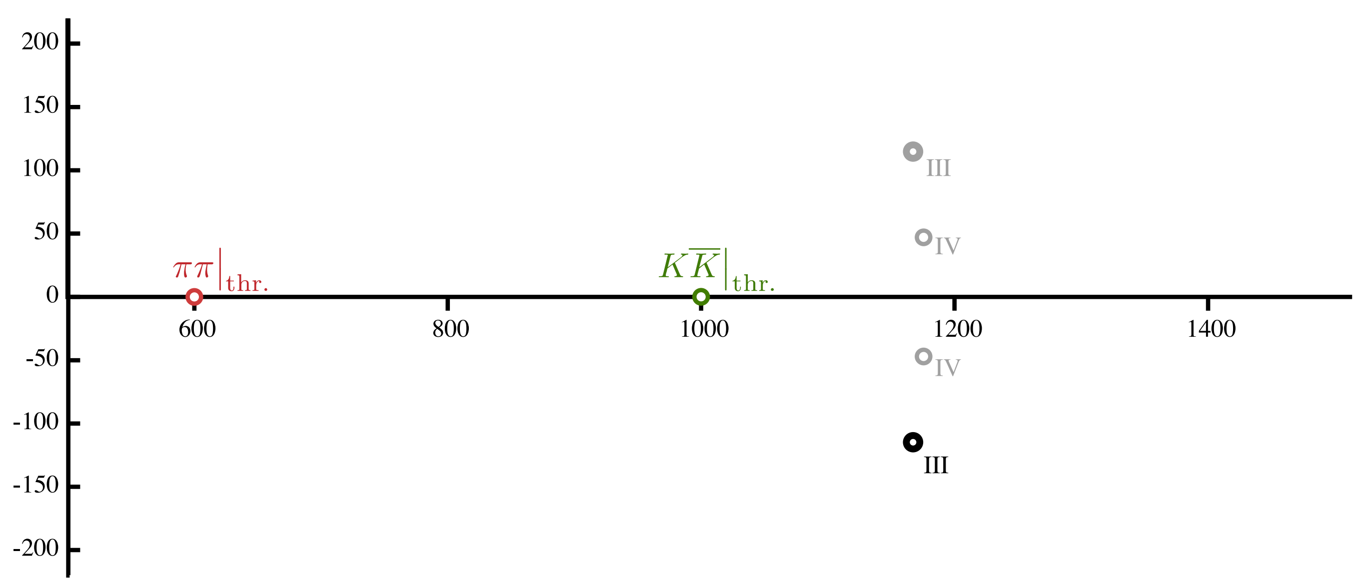

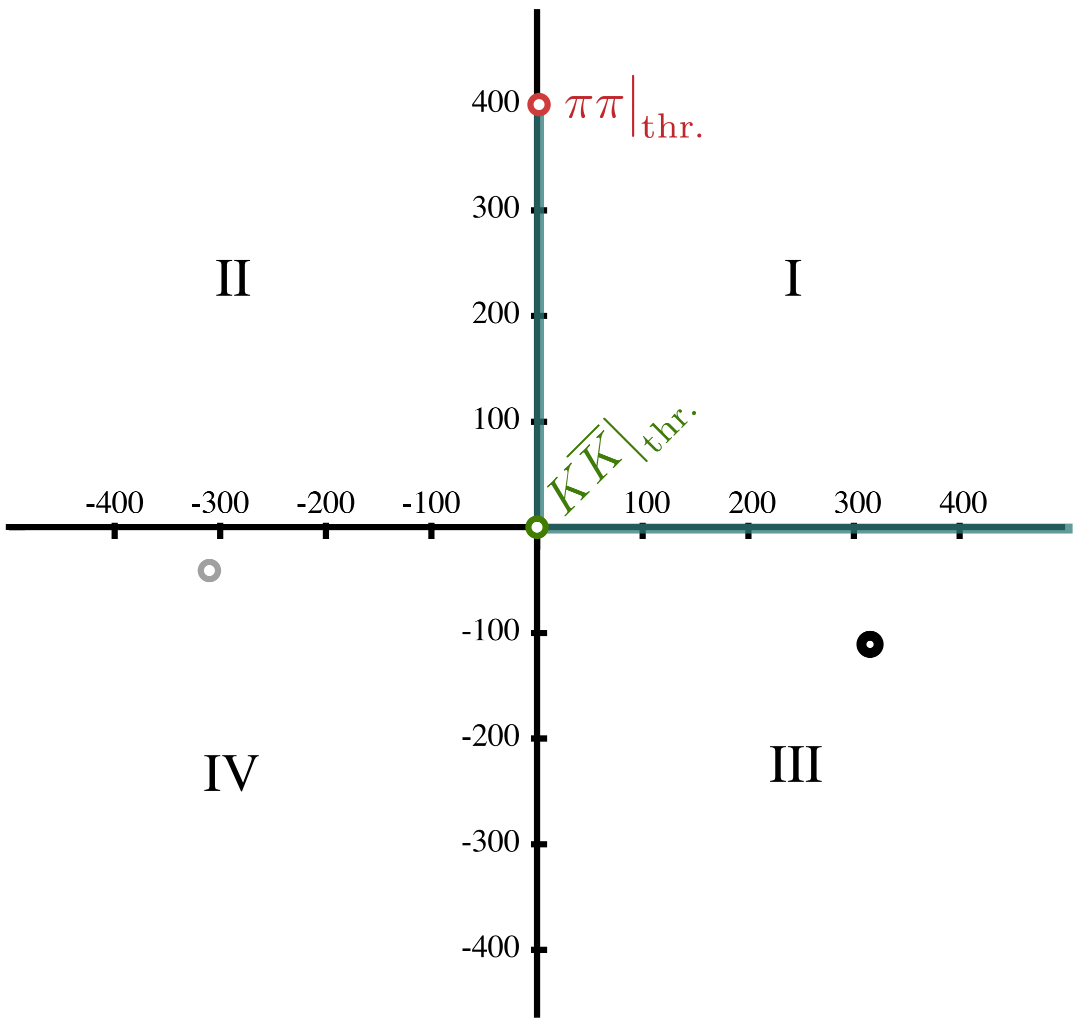

a less obviously resonant amplitude

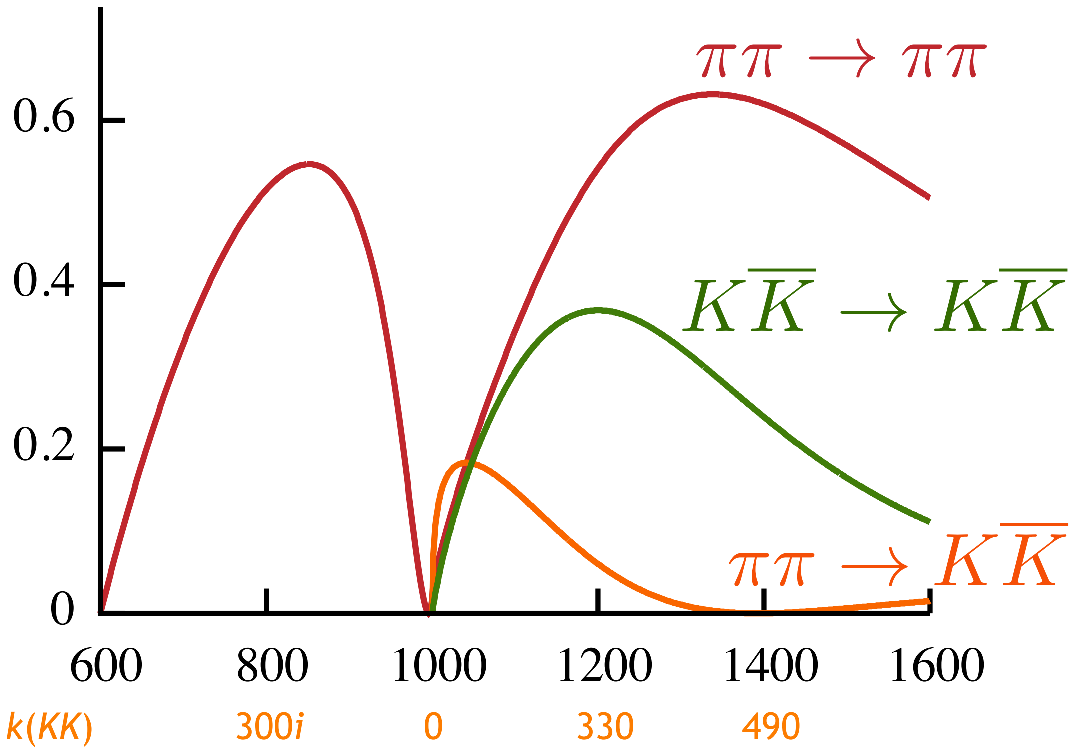

$$\mathbf{K}^{-1}(s) = \begin{pmatrix} a & b + c\,s \\ b + c\,s & d + e\,s \end{pmatrix}$$

with Chew-Mandelstam phase-space

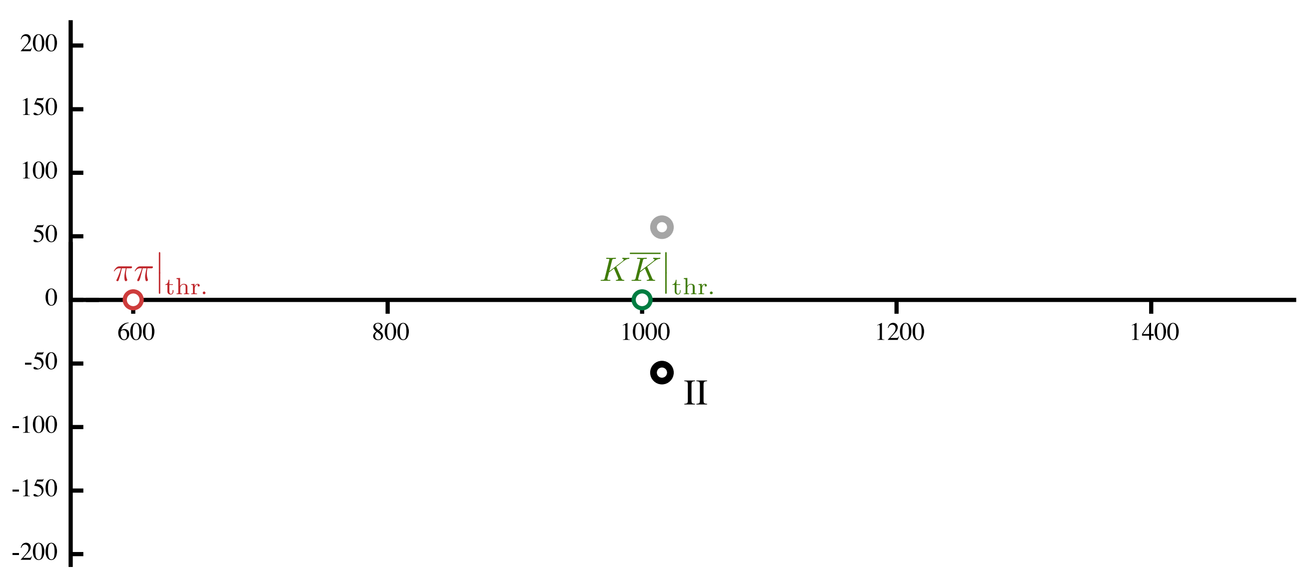

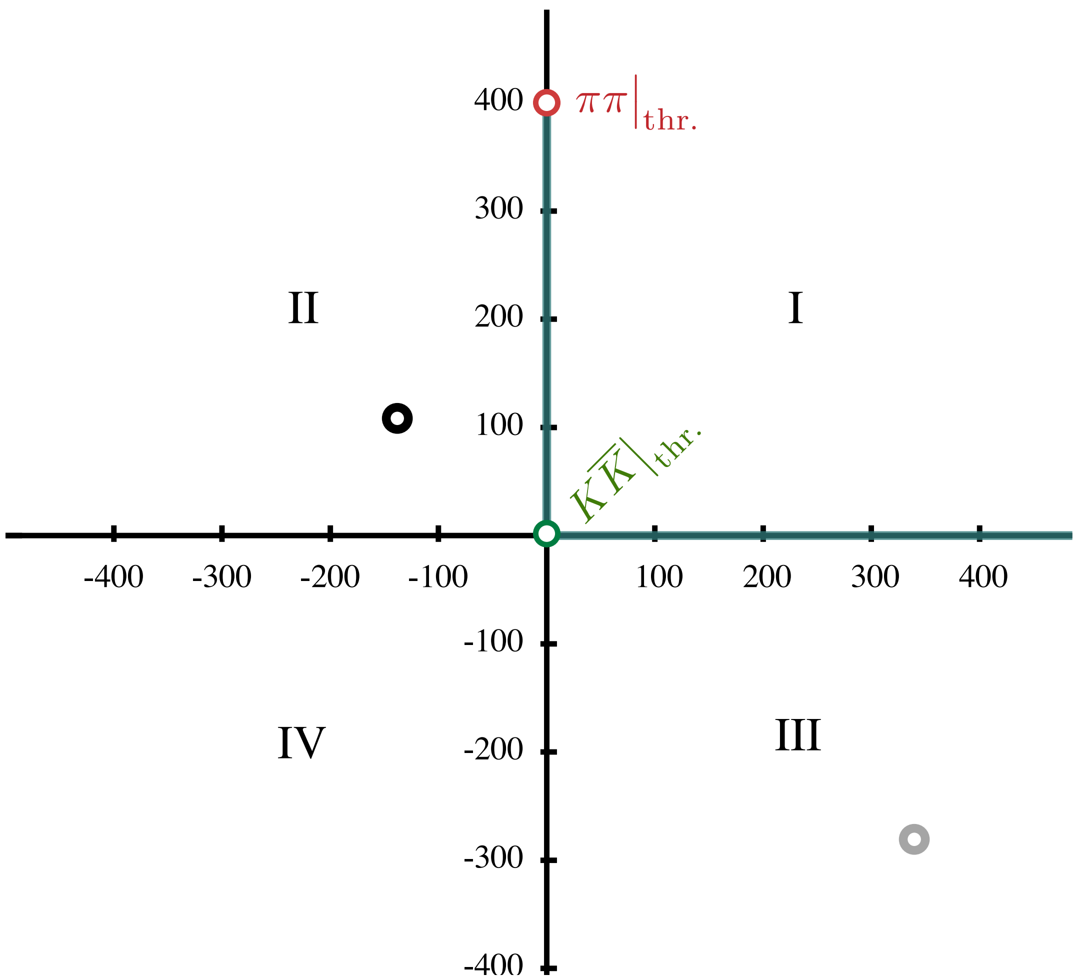

information from the pole

near the complex pole, s_0

$$t_{ij}(s \sim s_0) \sim \frac{c_i\, c_j}{s_0 - s}$$

pole position can be interpreted as **mass** and **width**

$$s_0 = \left(m_R \pm i\tfrac{1}{2}\Gamma_R\right)^2$$

information from the pole

near the complex pole, s_0

$$t_{ij}(s \sim s_0) \sim \frac{c_i\, c_j}{s_0 - s}$$

pole position can be interpreted as mass and width

$$s_0 = \left(m_R \pm i\tfrac{1}{2}\Gamma_R\right)^2$$

pole residue factorizes into a product of resonance **couplings** to the various decay channels

$c_{\pi\pi},\, c_{K\bar{K}},\, \ldots$

information from the pole

near the complex pole, s_0

$$t_{ij}(s \sim s_0) \sim \frac{c_i\, c_j}{s_0 - s}$$

pole position can be interpreted as mass and width

$$s_0 = \left(m_R \pm i\tfrac{1}{2}\Gamma_R\right)^2$$

pole residue factorizes into a product of resonance couplings
to the various decay channels

$$c_{\pi\pi},\, c_{K\bar{K}},\, \dots$$

as we've seen a single resonance can be responsible
for poles on more than one sheet

— often only one is close enough to physical scattering to have a large effect

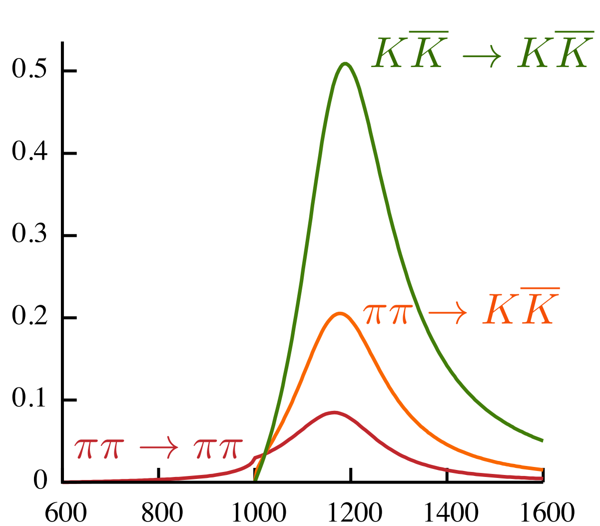

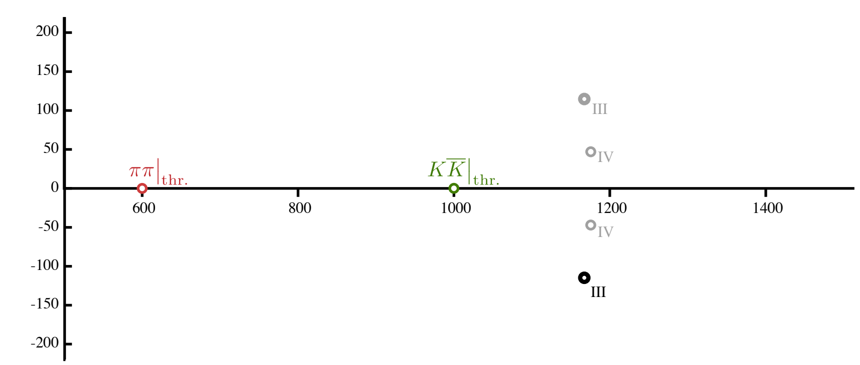

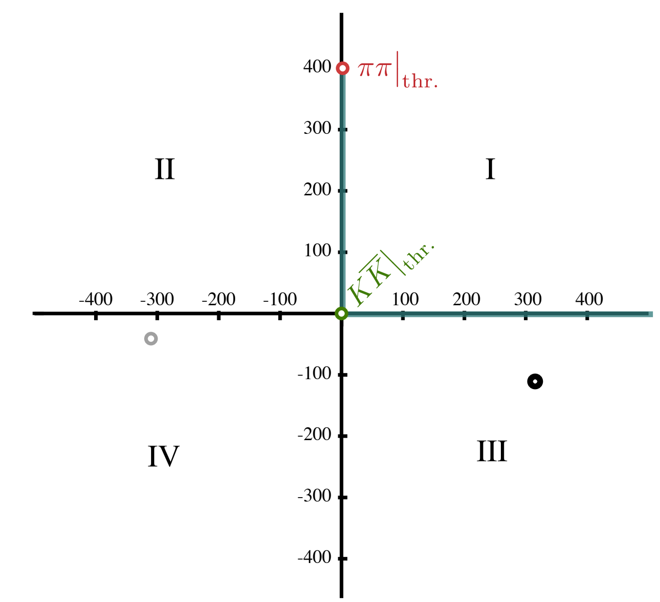

$\pi\pi$, $K\bar{K}$, $\eta\eta$ scattering with m_π~391 MeV

PRD 97 054513 (2018)

S-wave amplitudes

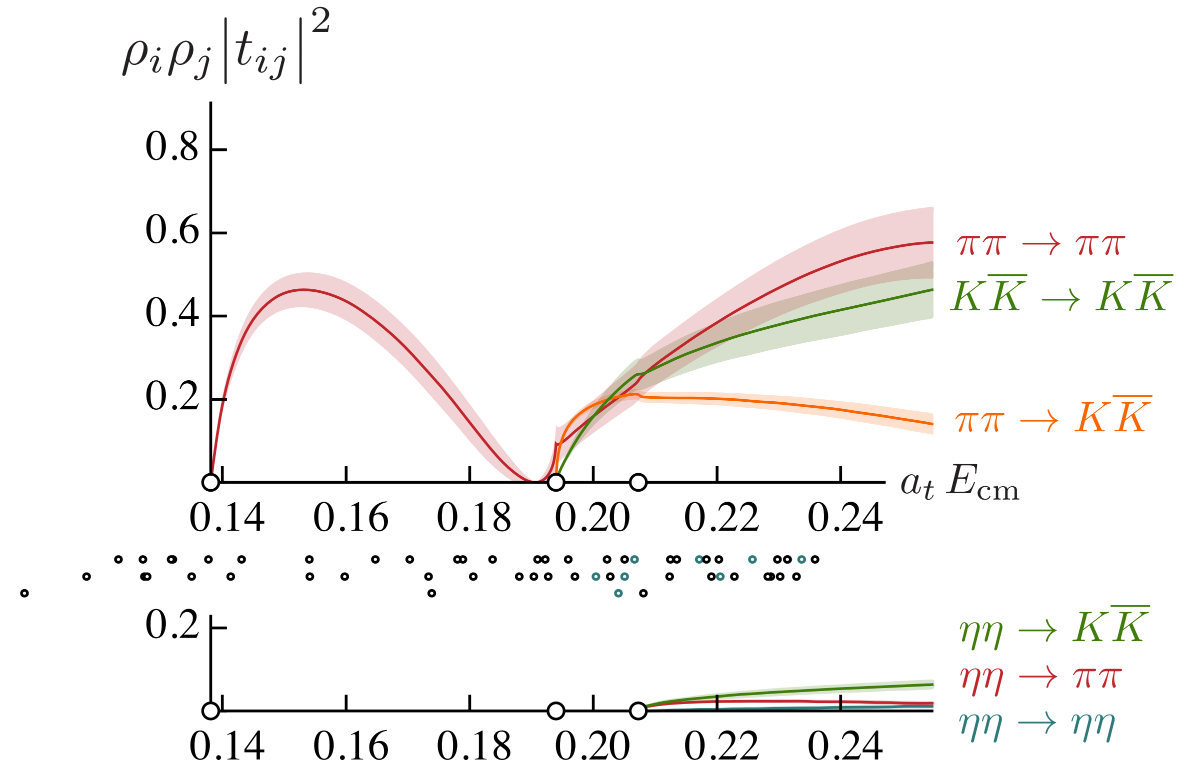

$$\mathbf{K}^{-1}(s) = \begin{pmatrix} a + b\, s & c + d\, s & e \\ c + d\, s & f & g \\ e & g & h \end{pmatrix}$$

with Chew-Mandelstam phase-space

pole singularities

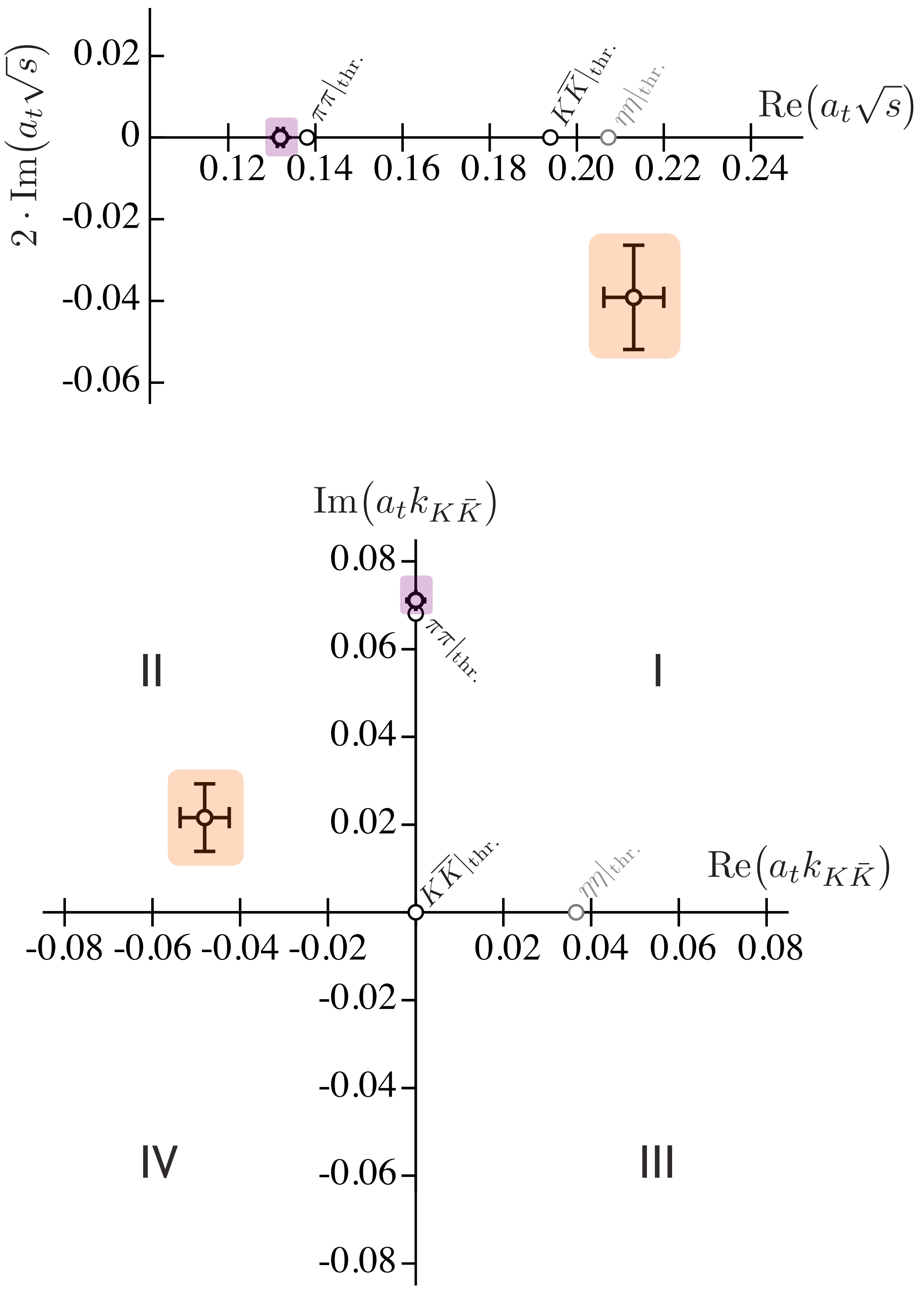

$\pi\pi$, $K\bar{K}$, $\eta\eta$ scattering with m_π~391 MeV

PRD 97 054513 (2018)

S-wave amplitudes

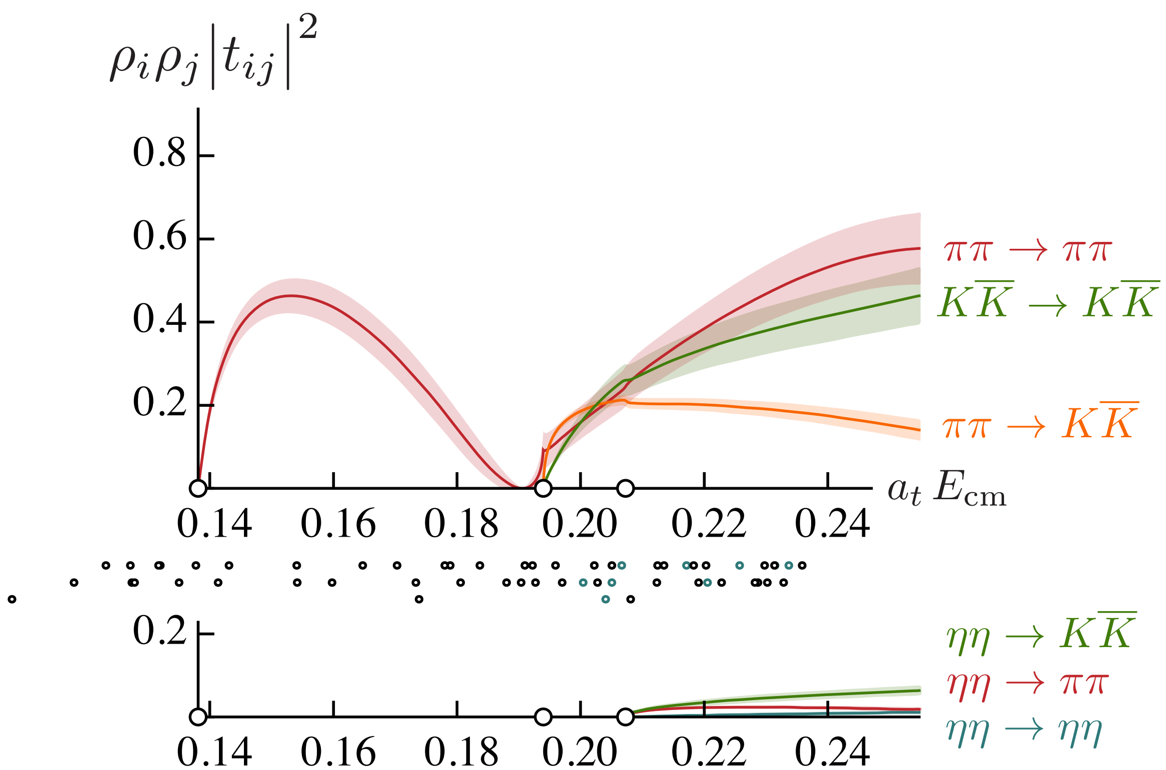

$$\mathbf{K}^{-1}(s) = \begin{pmatrix} a + b\,s & c + d\,s & e \\ c + d\,s & f & g \\ e & g & h \end{pmatrix}$$

with Chew-Mandelstam phase-space

pole singularities

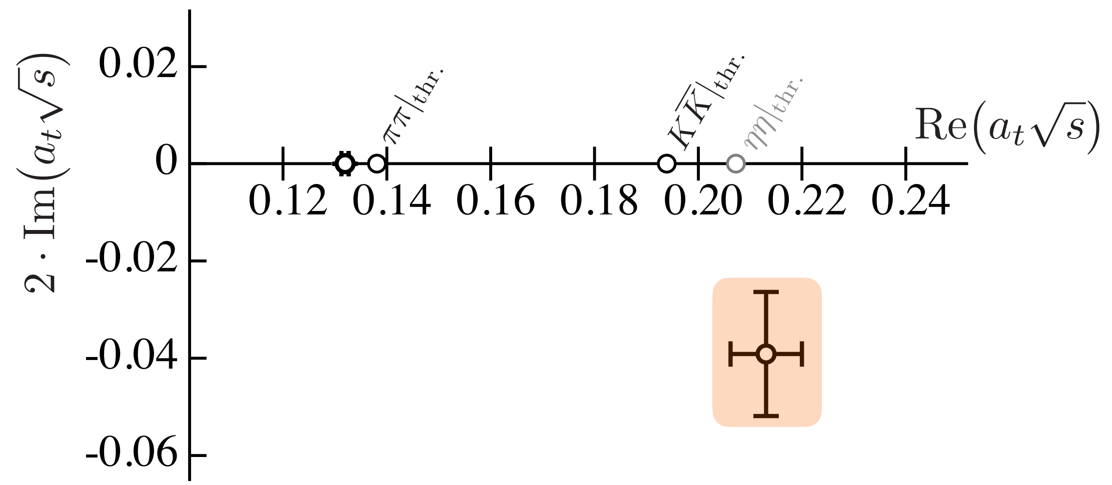

sheet II pole couplings

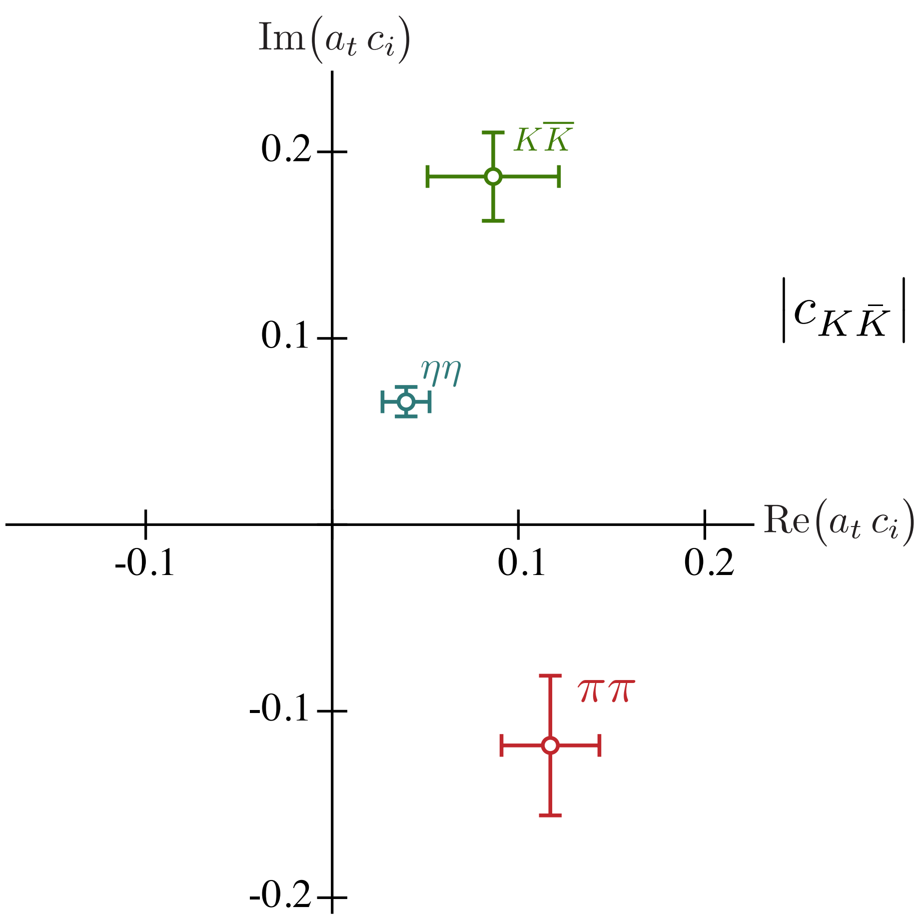

$$|c_{K\bar{K}}| \approx |c_{\pi\pi}|$$

$\pi\pi$, $K\overline{K}$, $\eta\eta$ scattering with m_π~391 MeV

PRD 97 054513 (2018)

S-wave amplitudes

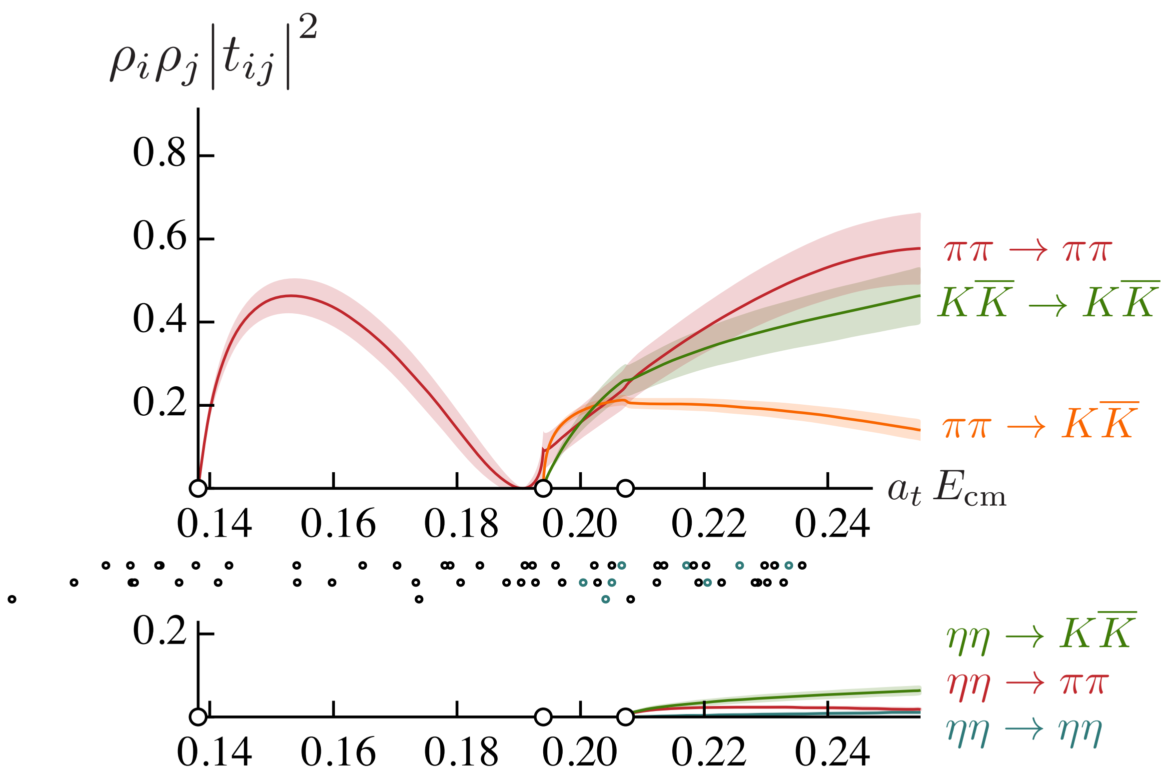

pole singularities

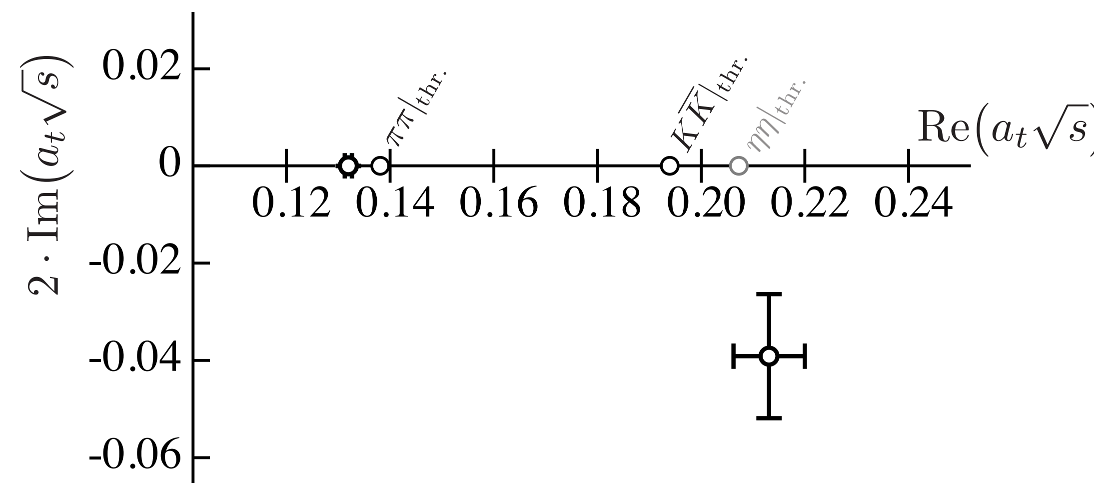

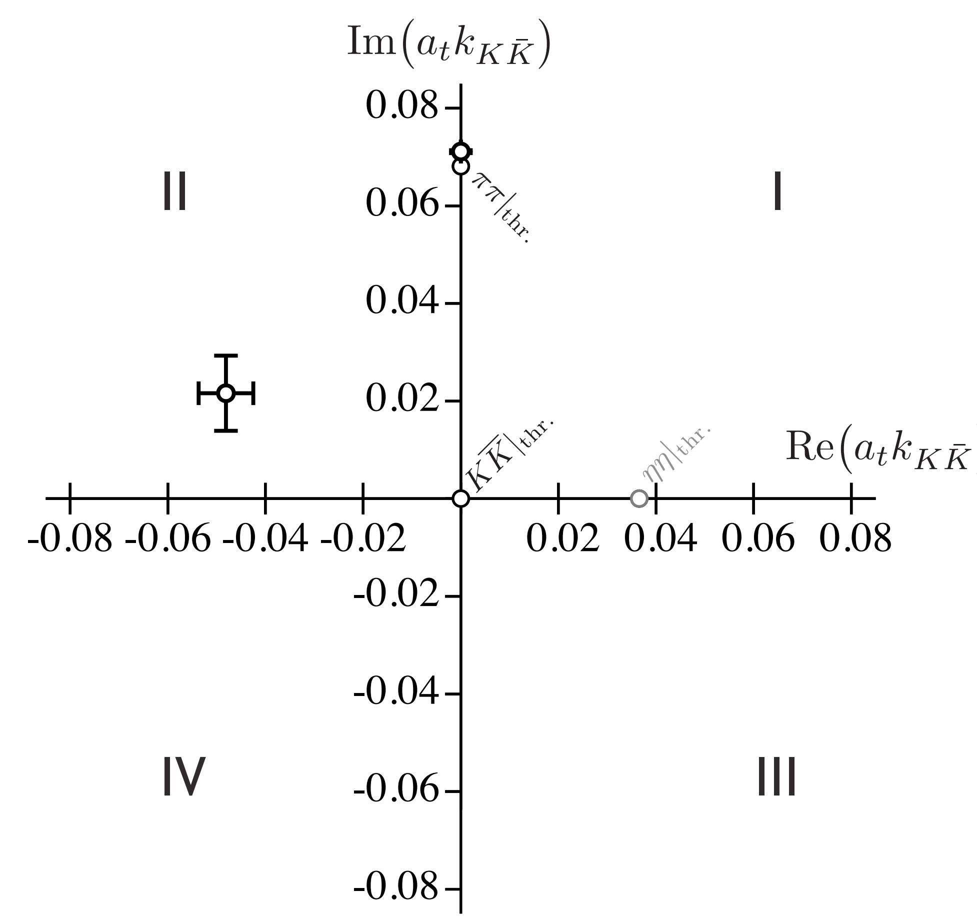

$$\mathbf{K}^{-1}(s) = \begin{pmatrix} a + b\,s & c + d\,s & e \\ c + d\,s & f & g \\ e & g & h \end{pmatrix}$$

with Chew-Mandelstam phase-space

$\pi\pi$, $K\bar{K}$, $\eta\eta$ scattering with m_π~391 MeV

PRD 97 054513 (2018)

S-wave amplitudes

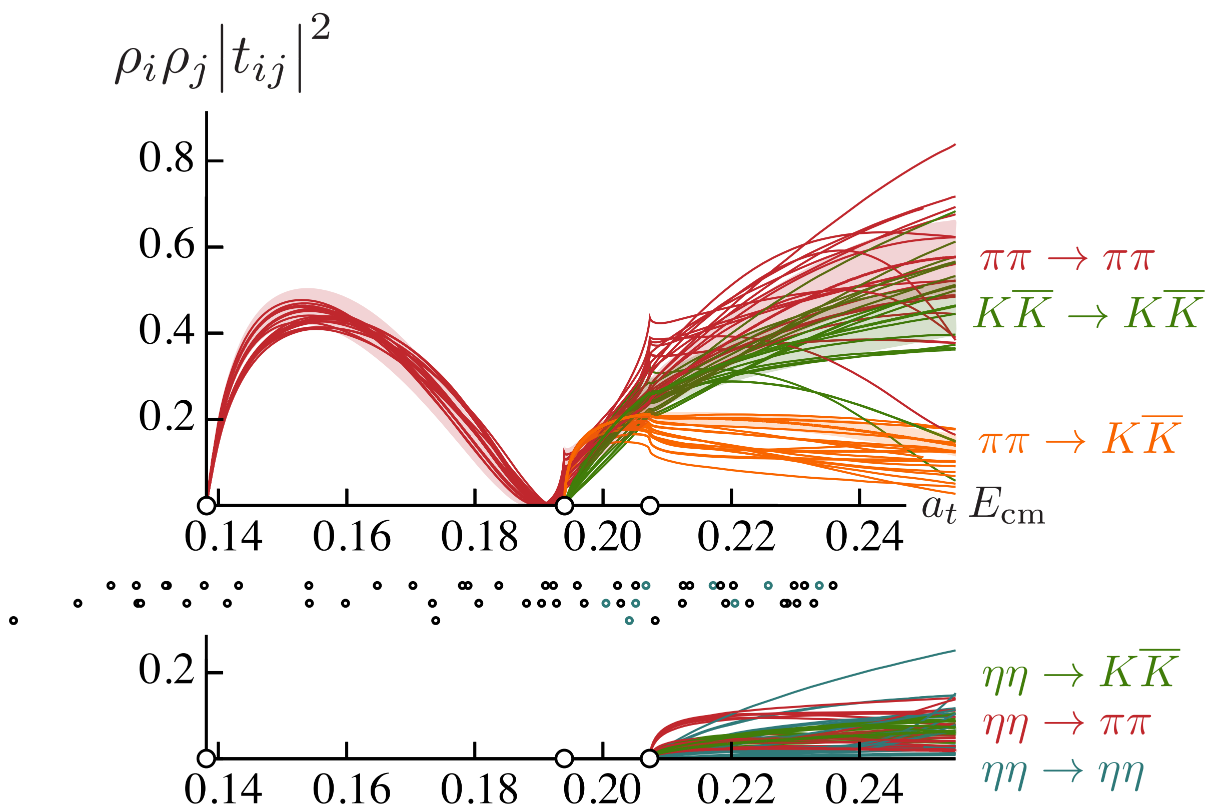

pole singularities

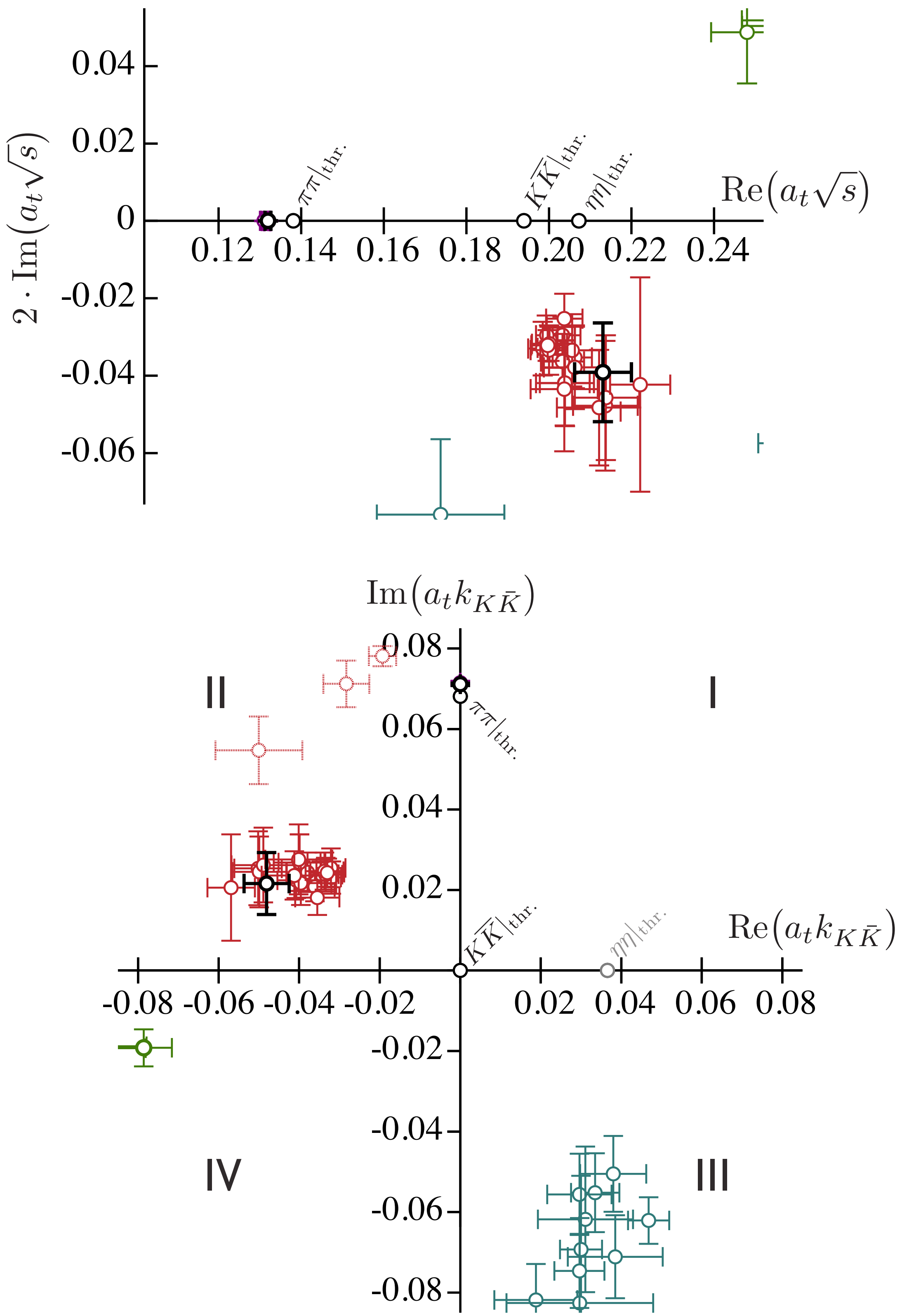

summary, including spread over parameterizations in pole uncertainty

S-wave amplitudes & poles

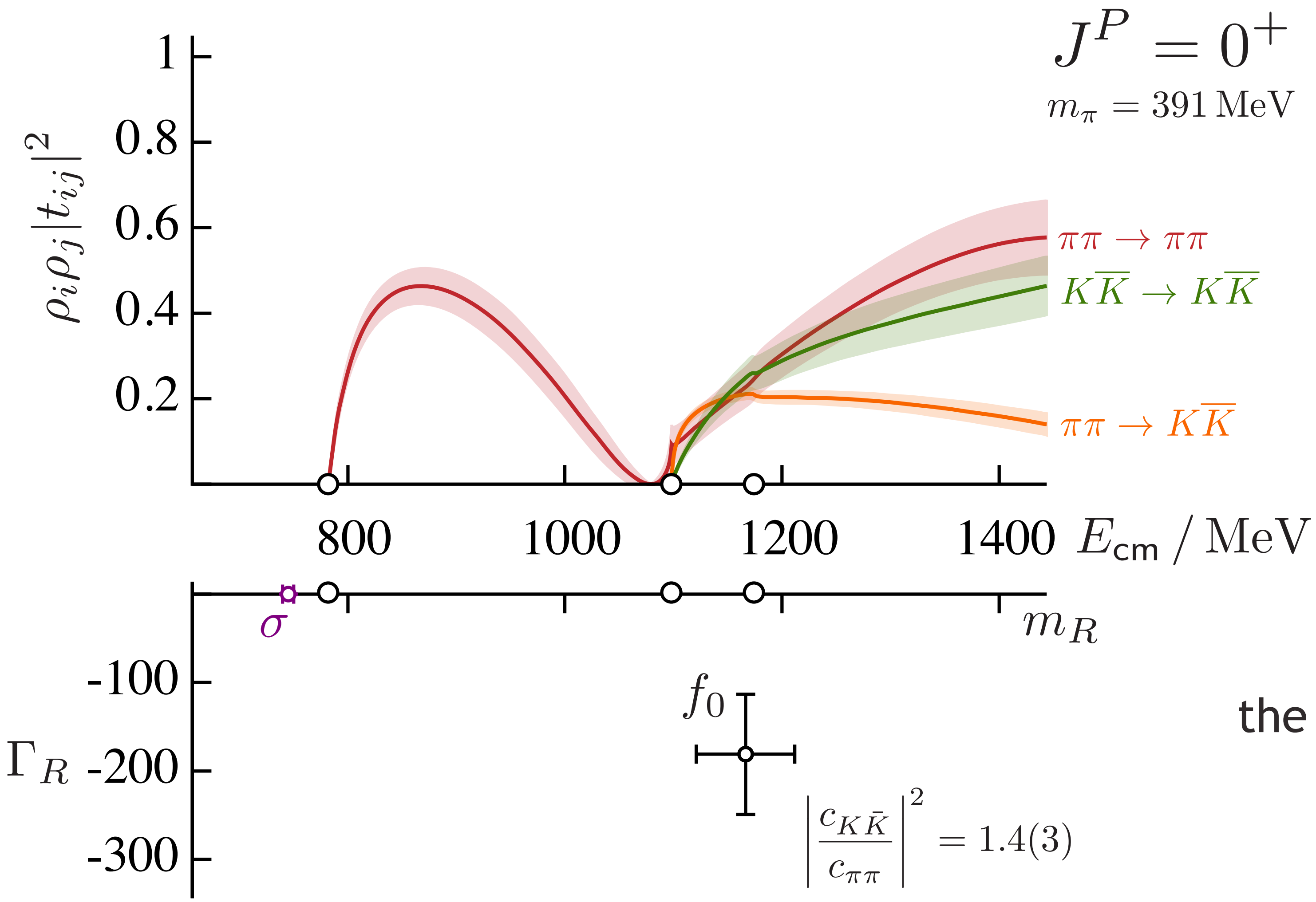

the $f_0($“980”$)$?

f_0(980) $I^G(J^{PC}) = 0^+(0^{++})$

See the review on "Scalar Mesons below 2 GeV."
Mass $m = 990 \pm 20$ MeV
Full width $\Gamma = 10$ to 100 MeV

f_0(980) DECAY MODES	Fraction (Γ_i/Γ)	p (MeV/c)
$\pi\pi$	seen	476
$K\overline{K}$	seen	36
$\gamma\gamma$	seen	495

$\pi\pi$, $K\bar{K}$, $\eta\eta$ scattering with m_π~391 MeV

D-wave amplitudes

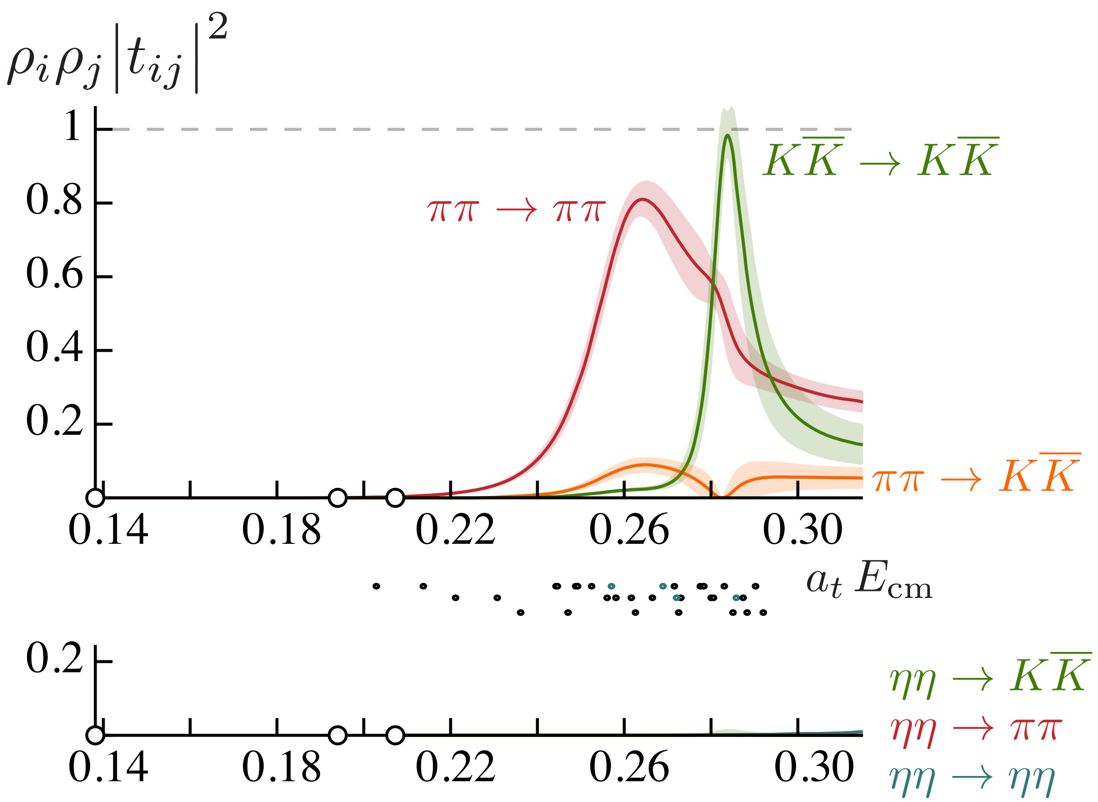

bumps are in the three-channel region ⇒ **8 sheets !**

won't burden you with the sheet details here …

$\pi\pi$, $K\bar{K}$, $\eta\eta$ scattering with m_π~391 MeV

PRD 97 054513 (2018)

D-wave amplitudes

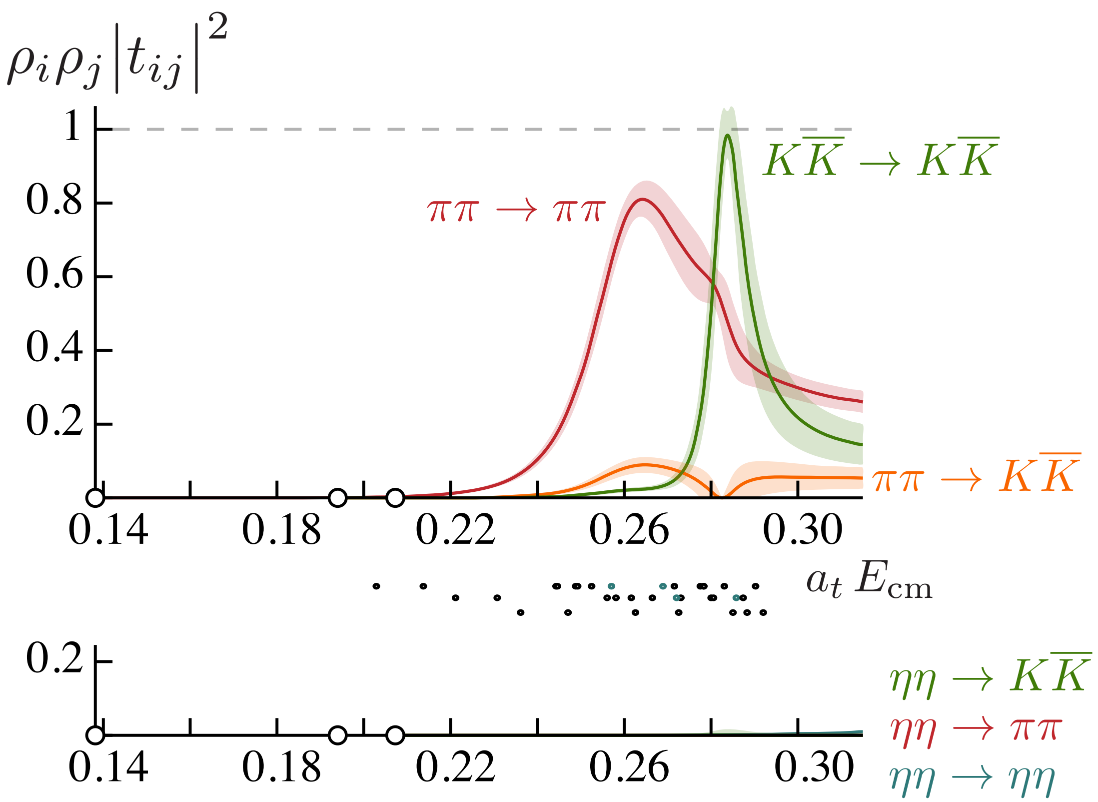

bumps are in the three channel region ⇒ **8 sheets !**

won't burden you with the sheet details here …

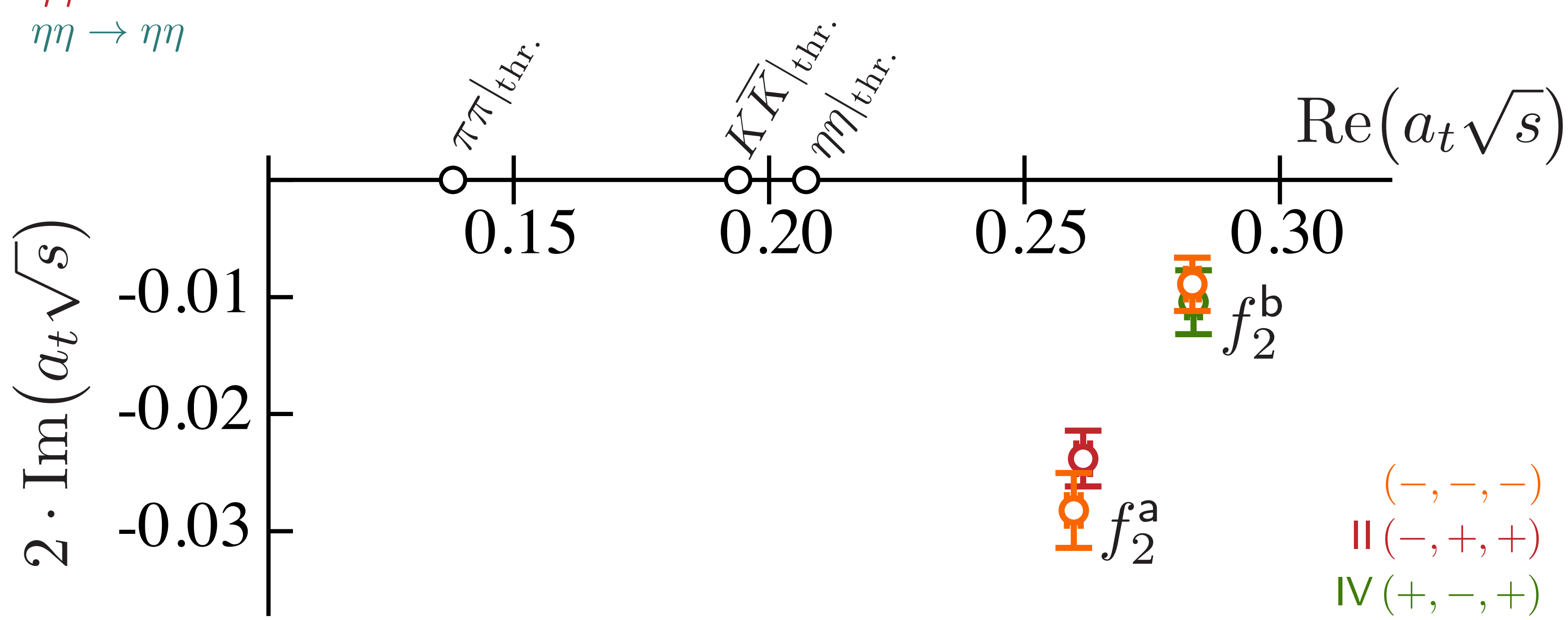

(–,–,–) is 'closest' sheet to physical scattering above all three thresholds

couplings at the poles

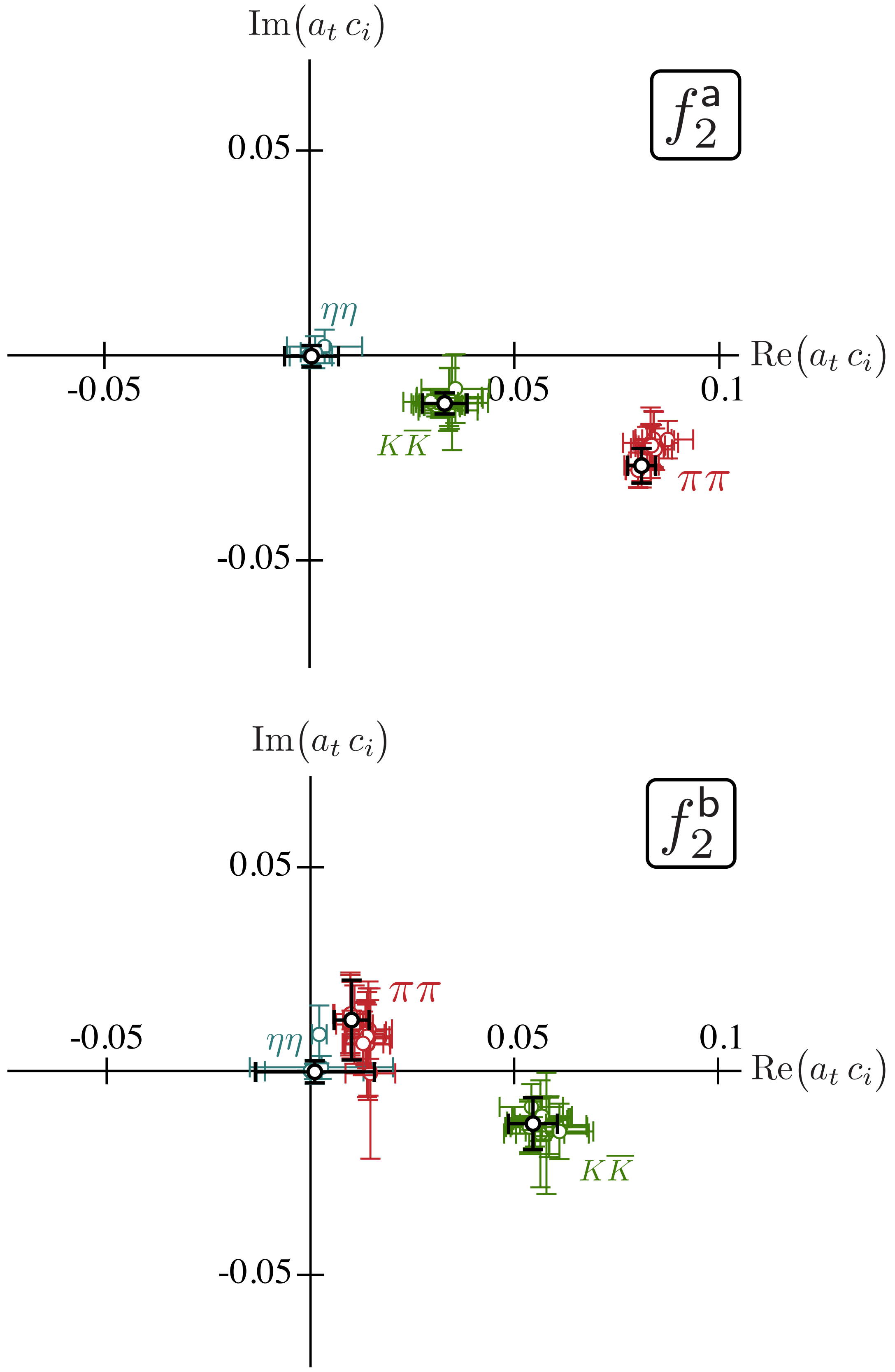

$\pi\pi$, $K\bar{K}$, $\eta\eta$ scattering with m_π~391 MeV

D-wave amplitudes & poles

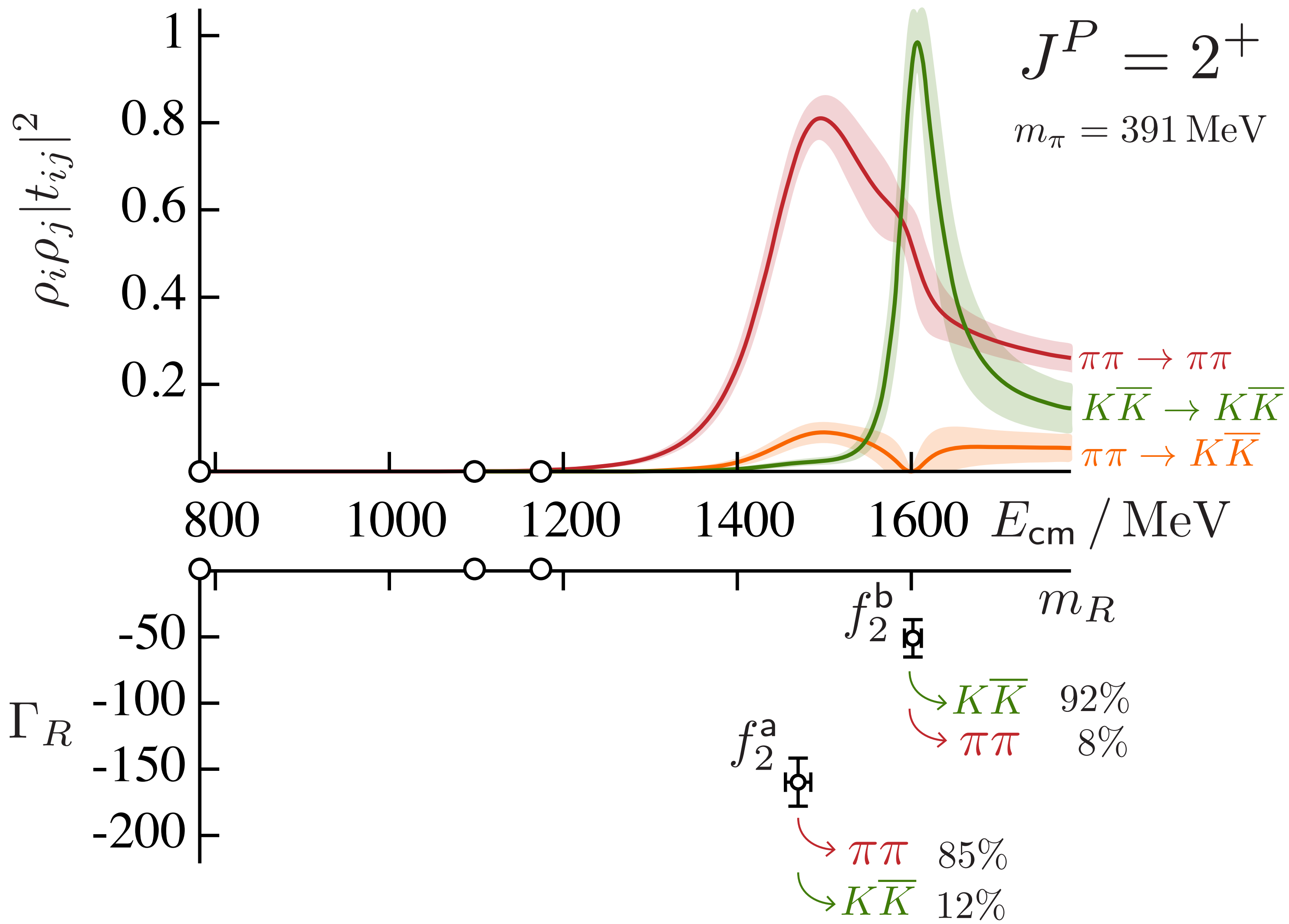

pdg summary

$f_2(1270)$ $I^G(J^{PC}) = 0^+(2^{++})$

Mass $m = 1275.5 \pm 0.8$ MeV
Full width $\Gamma = 186.7^{+2.2}_{-2.5}$ MeV (S = 1.4)

$f_2(1270)$ DECAY MODES	Fraction (Γ_i/Γ)	Scale factor/ Confidence level	p (MeV/c)
$\pi\pi$	$(84.2 \ {}^{+2.9}_{-0.9})$ %	S=1.1	623
$\pi^+\pi^-2\pi^0$	$(7.7 \ {}^{+1.1}_{-3.2})$ %	S=1.2	563
$K\bar{K}$	$(4.6 \ {}^{+0.5}_{-0.4})$ %	S=2.7	404
$2\pi^+2\pi^-$	(2.8 ± 0.4) %	S=1.2	560
$\eta\eta$	$(4.0 \pm 0.8) \times 10^{-3}$	S=2.1	326
$4\pi^0$	$(3.0 \pm 1.0) \times 10^{-3}$		565

$f_2'(1525)$ $I^G(J^{PC}) = 0^+(2^{++})$

Mass $m = 1525 \pm 5$ MeV [l]
Full width $\Gamma = 73^{+6}_{-5}$ MeV [l]

$f_2'(1525)$ DECAY MODES	Fraction (Γ_i/Γ)	p (MeV/c)
$K\bar{K}$	(88.7 ± 2.2) %	581
$\eta\eta$	(10.4 ± 2.2) %	530
$\pi\pi$	$(8.2 \pm 1.5) \times 10^{-3}$	750

singularity structure from lattice calculations — elastic

$\pi\pi$ isospin=0

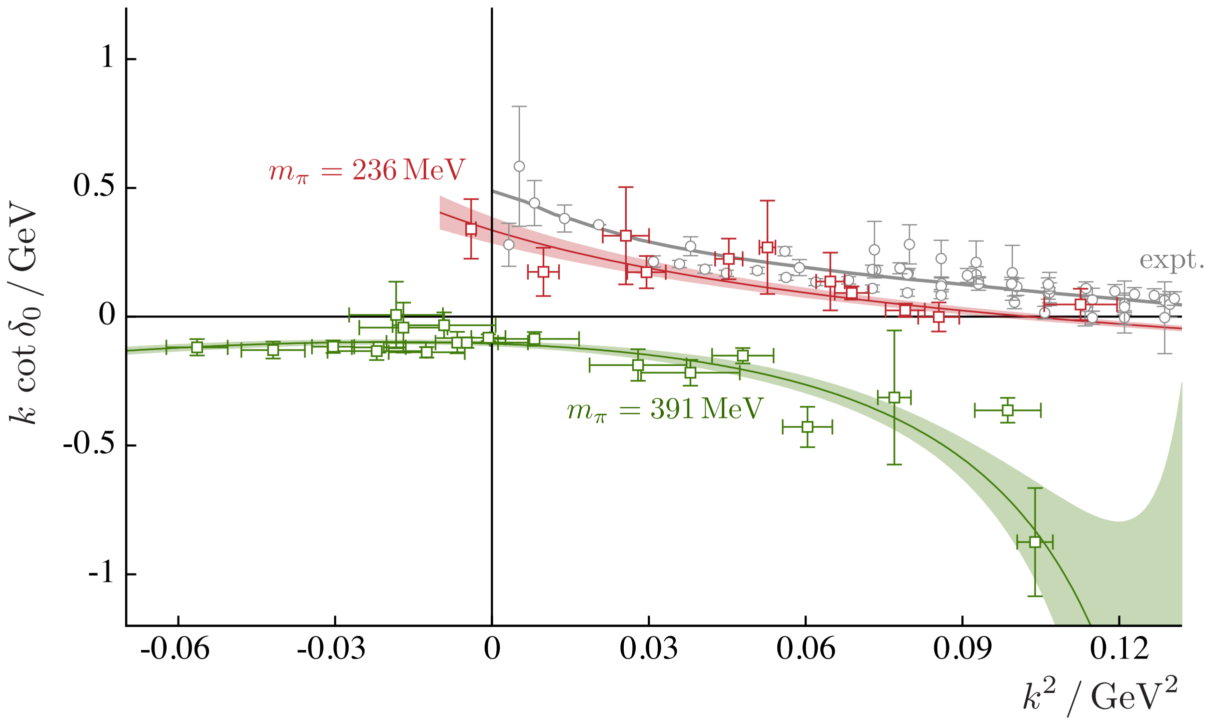

PRL118 022002 (2017)

m_π~391 MeV — a bound-state pole

m_π~236 MeV — a resonance pole

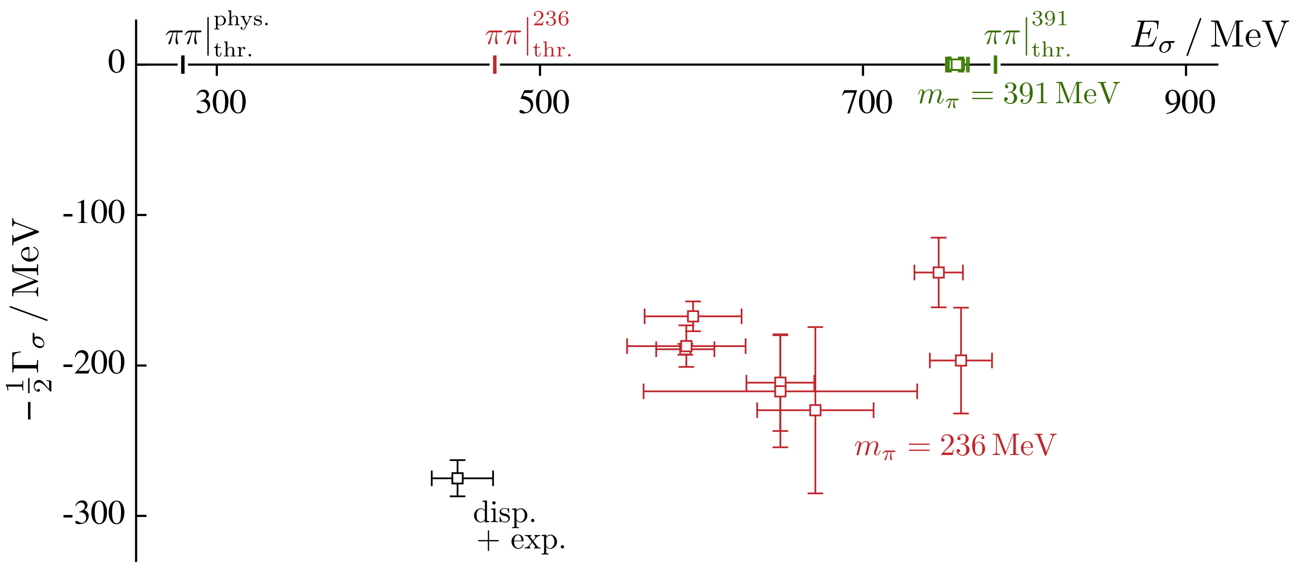

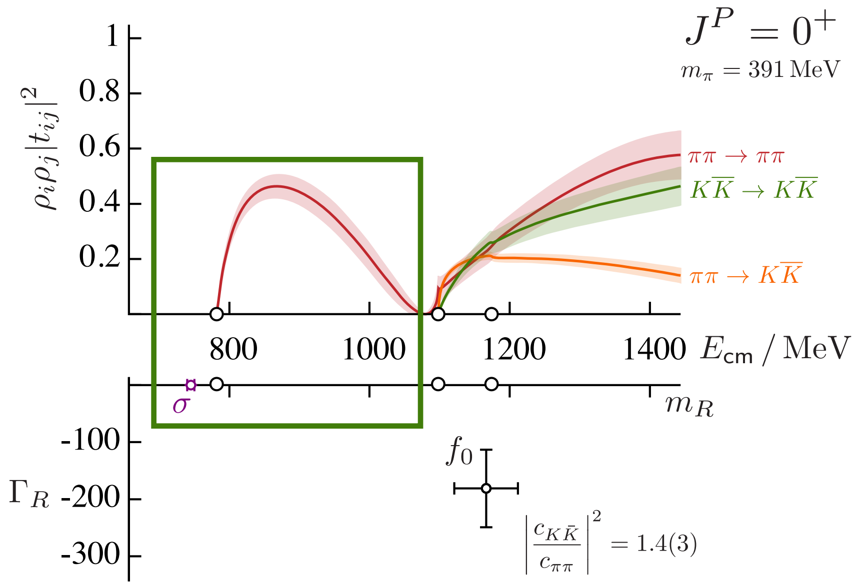

similar calculation in **isospin=1**, **G-parity negative** channel

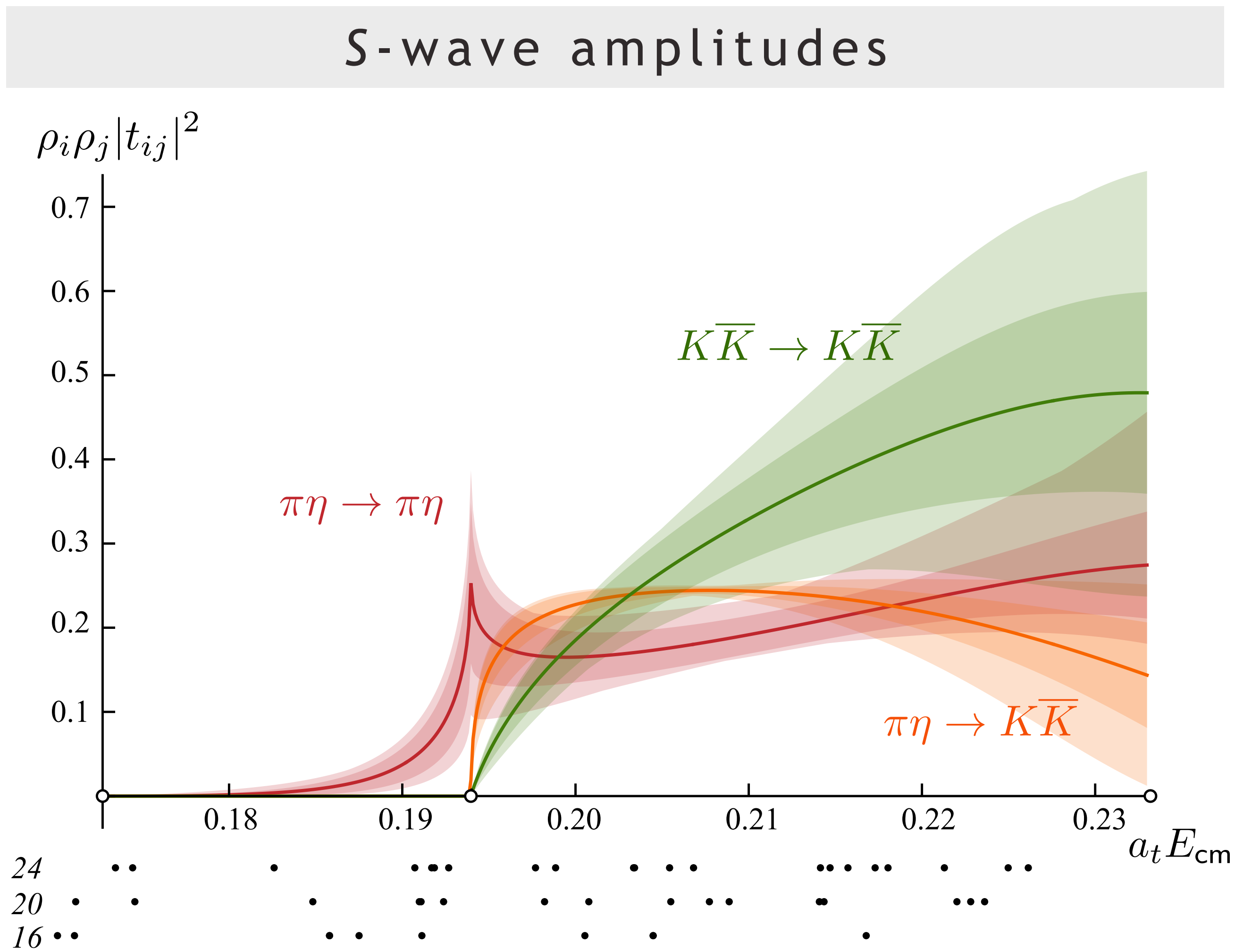

looks very different to isospin=0 case shown before

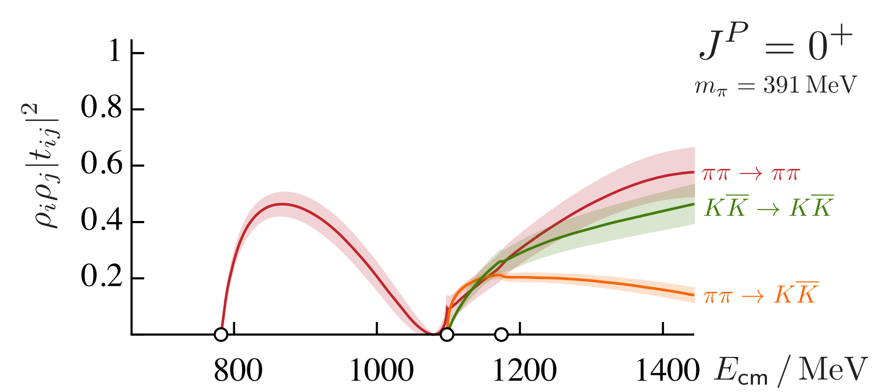

S-wave amplitudes

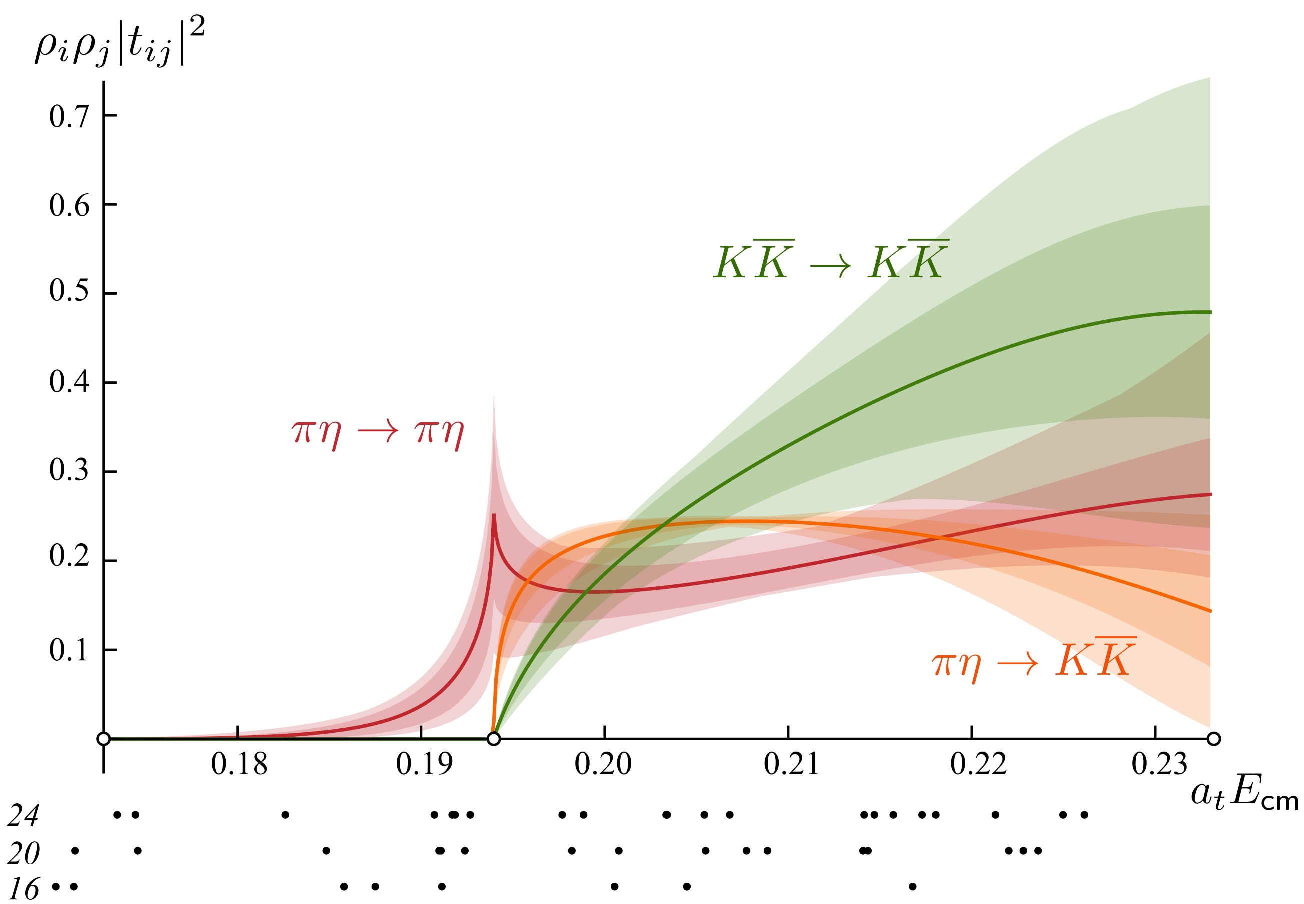

pole singularities

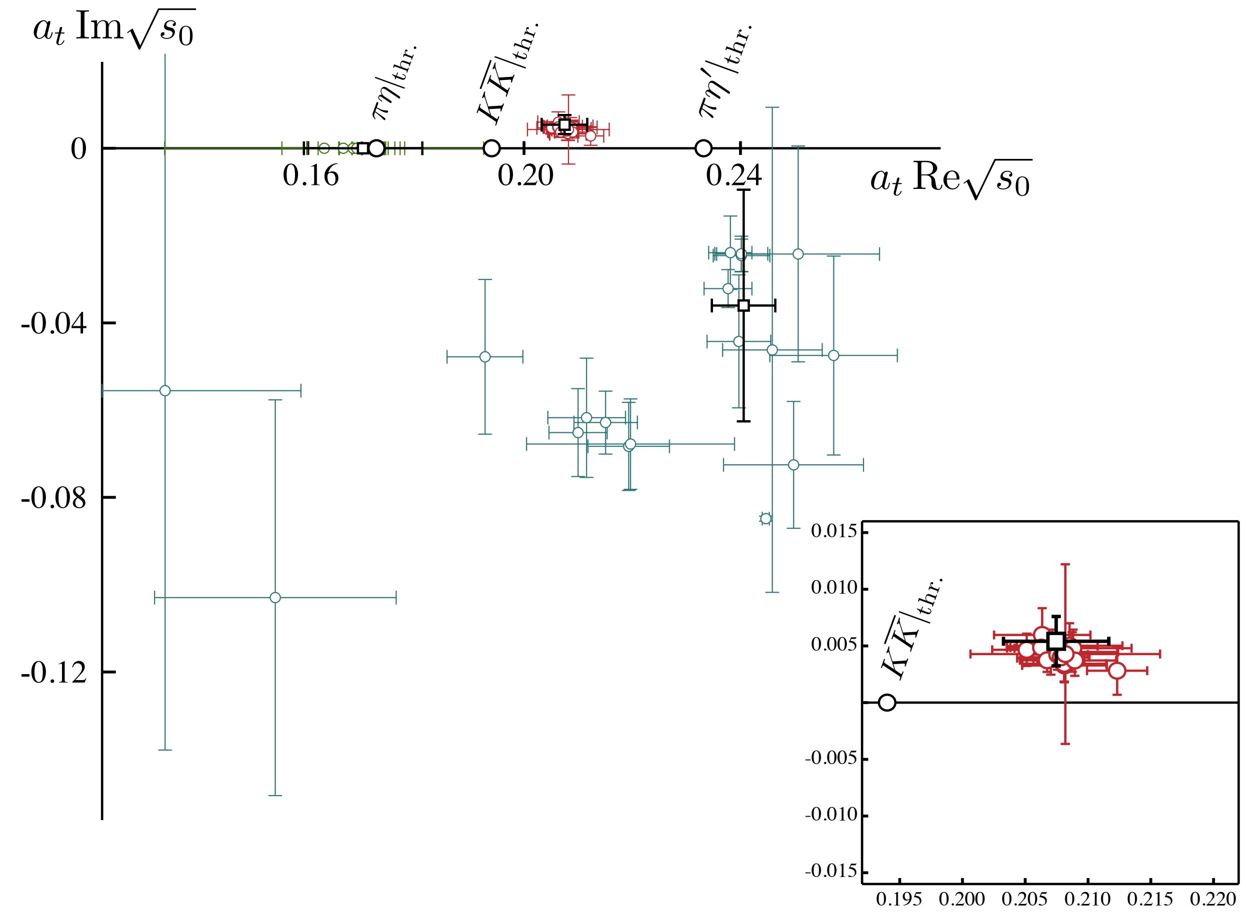

$\pi\eta$, $K\bar{K}$ scattering with m_π~391 MeV

S-wave amplitudes

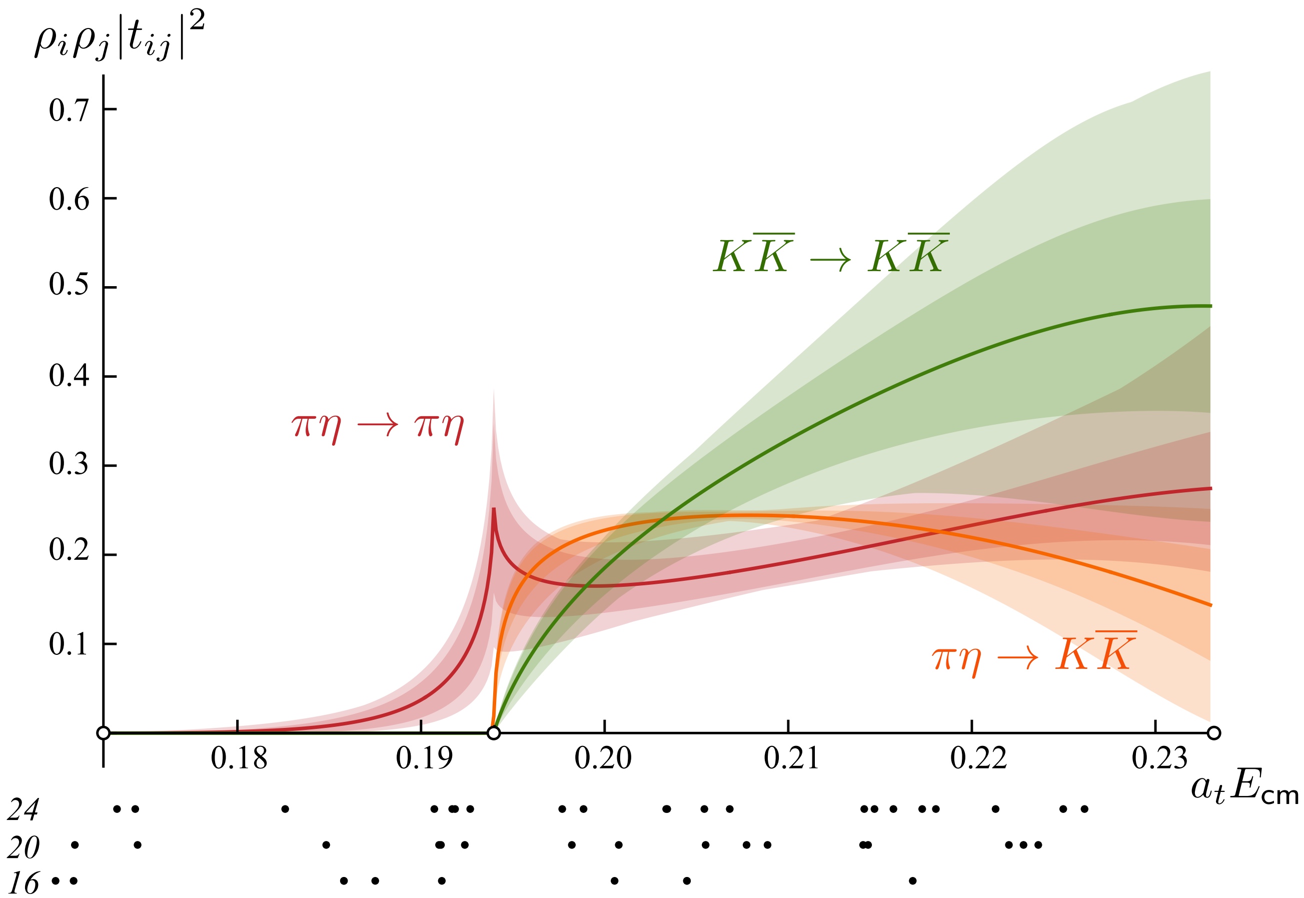

pole singularities

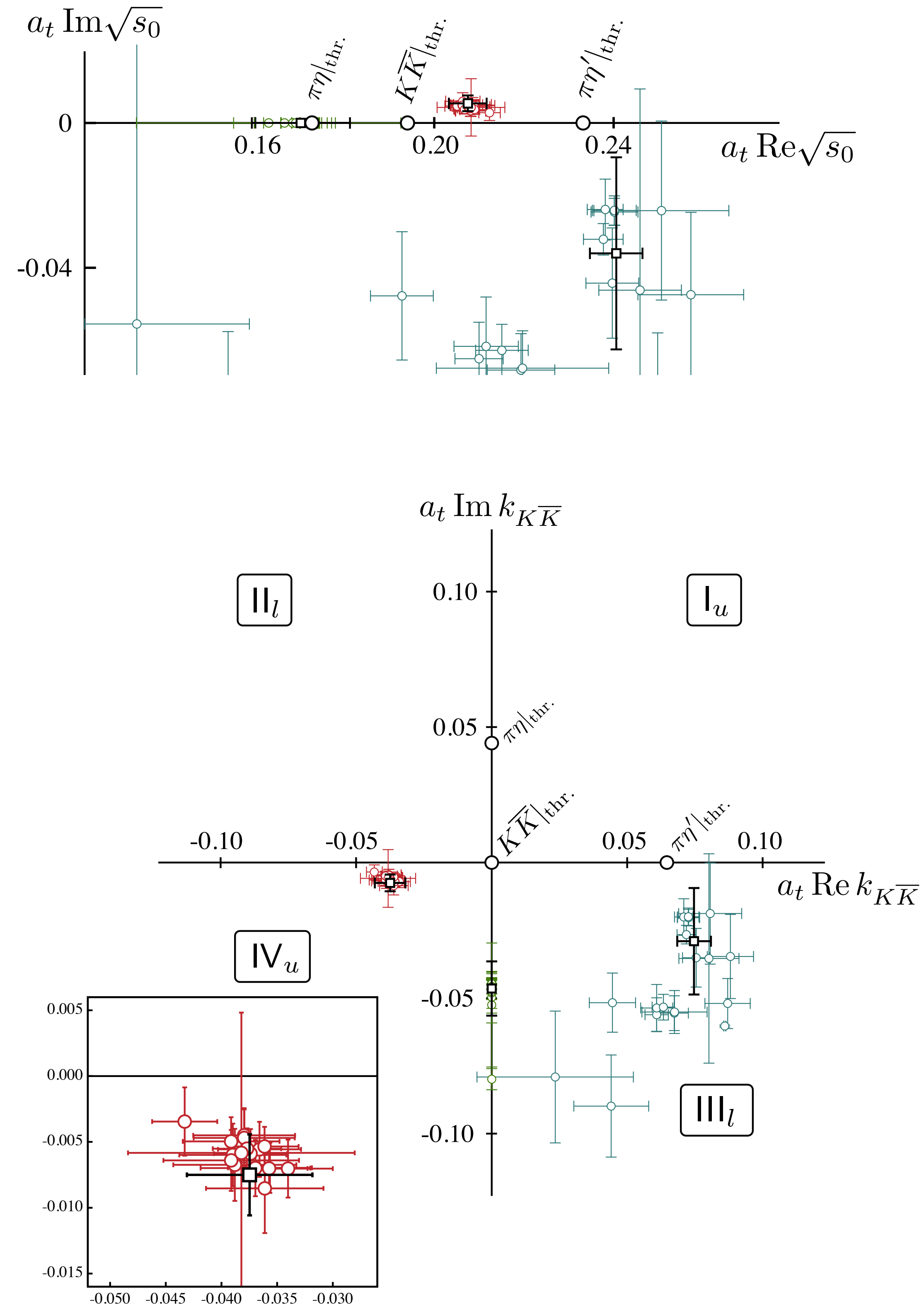

S-wave amplitudes & poles

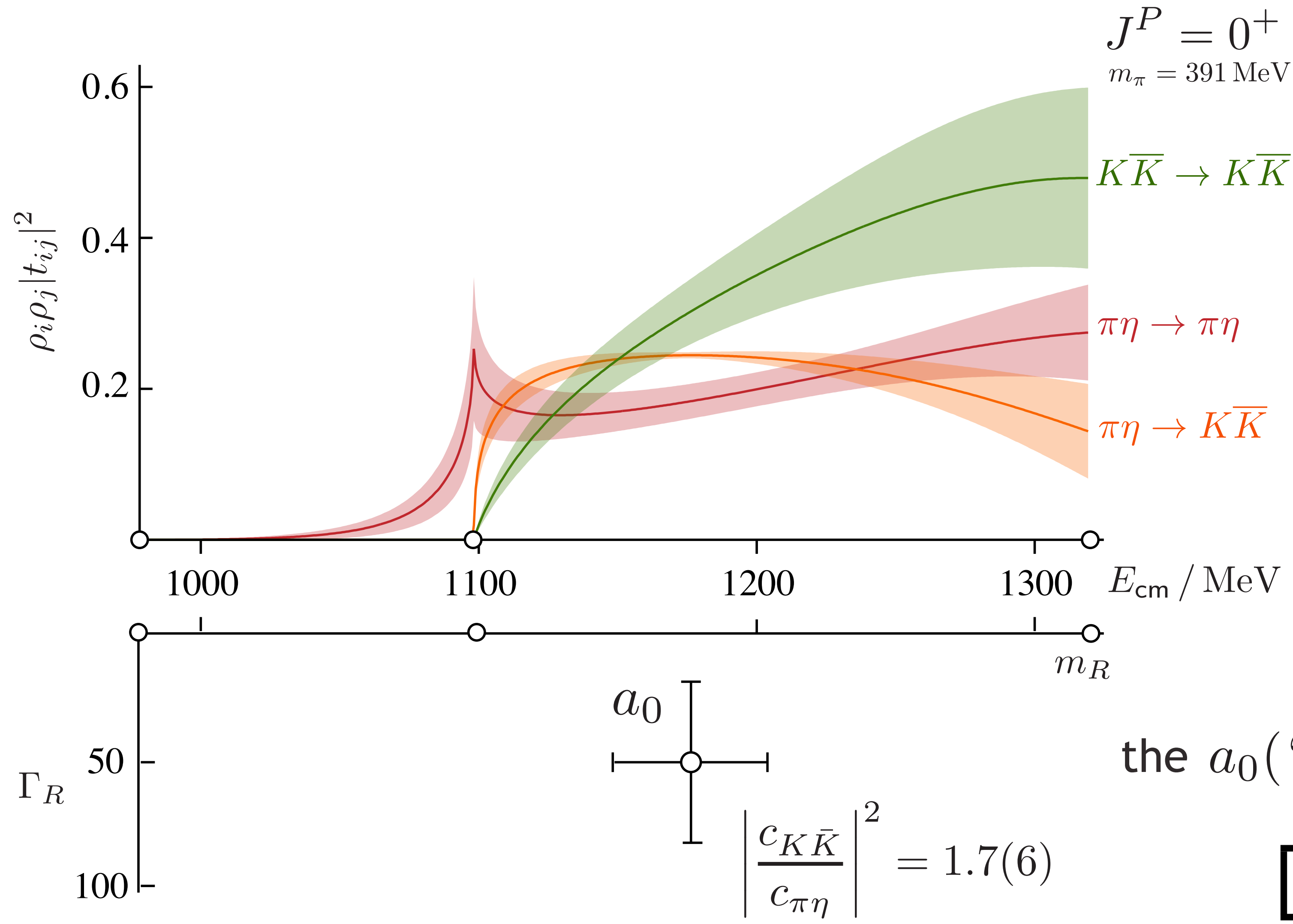

the a_0(“980”) ?

a_0(980) $I^G(J^{PC}) = 1^-(0^{++})$

See the review on "Scalar Mesons below 2 GeV."

Mass $m = 980 \pm 20$ MeV

Full width $\Gamma = 50$ to 100 MeV

a_0(980) DECAY MODES	Fraction (Γ_i/Γ)	p (MeV/c)
$\eta\pi$	seen	319
$K\bar{K}$	seen	†
$\rho\pi$	not seen	137
$\gamma\gamma$	seen	490

vector-pseudoscalar scattering

many-body decays tend to be dominated by **isobars**

e.g. $\pi\pi\pi$ dominated by $\pi\rho$

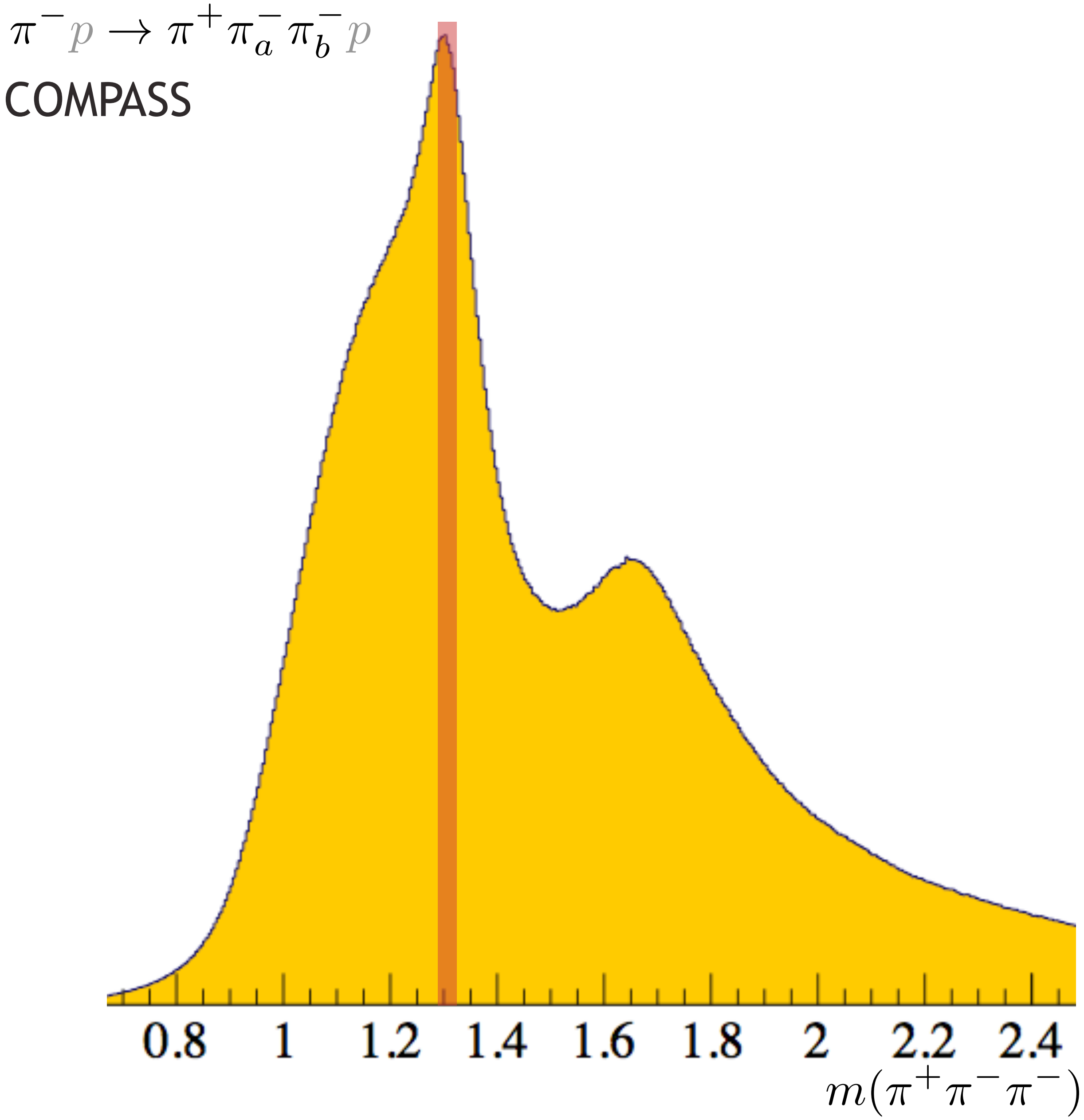

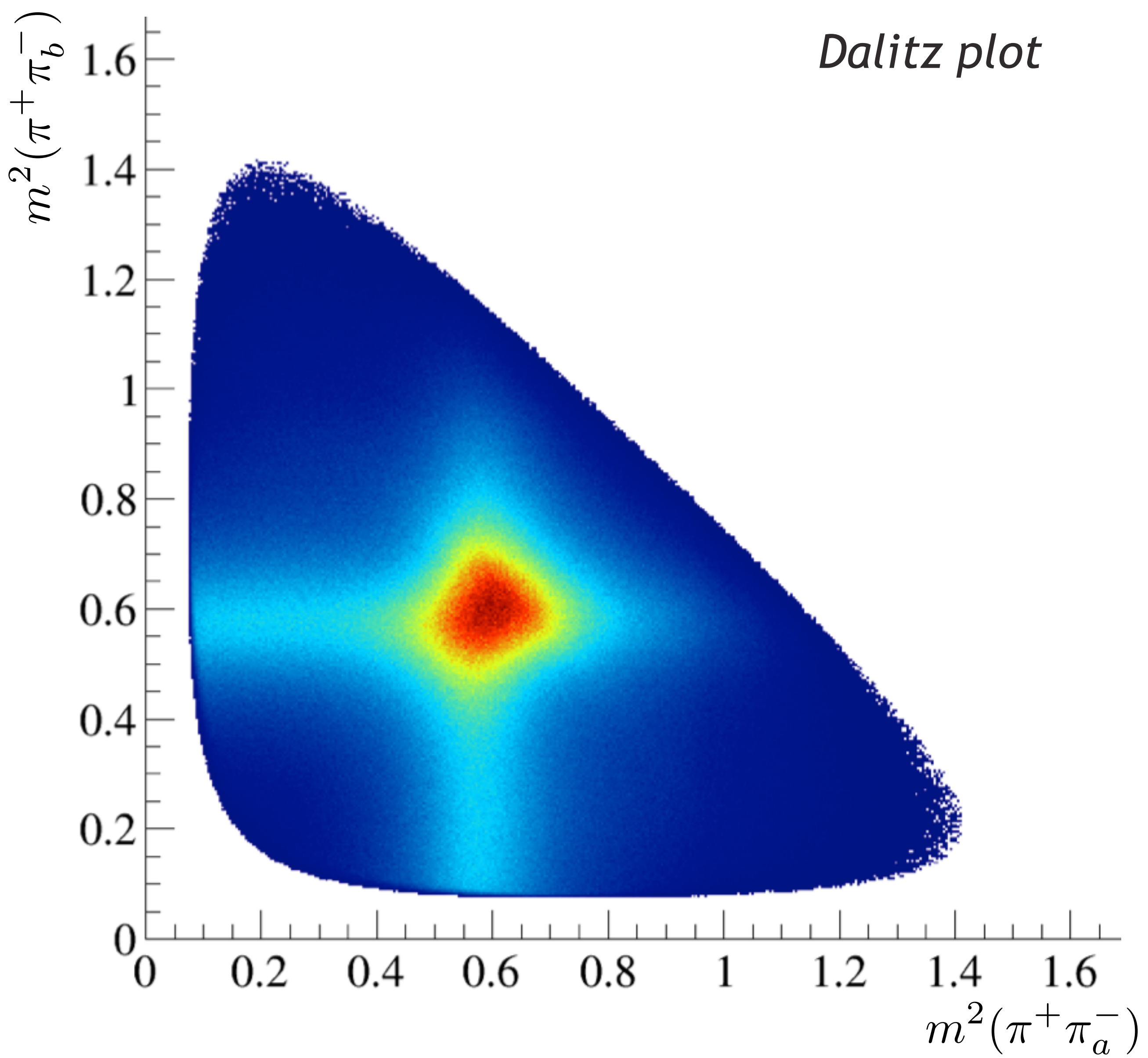

vector-pseudoscalar scattering

many-body decays tend to be dominated by isobars

e.g. $\pi\pi\pi$ dominated by $\pi\rho$

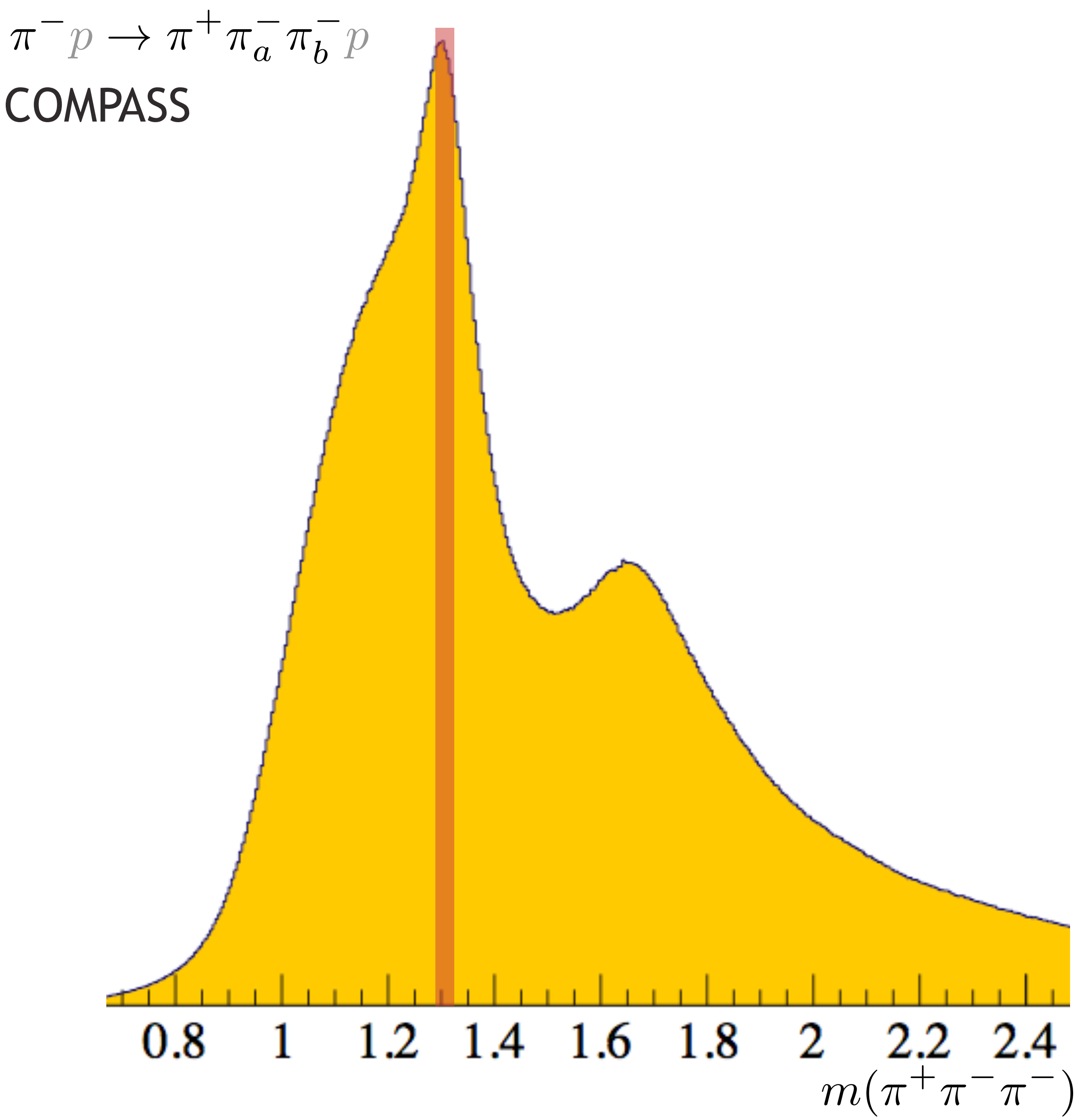

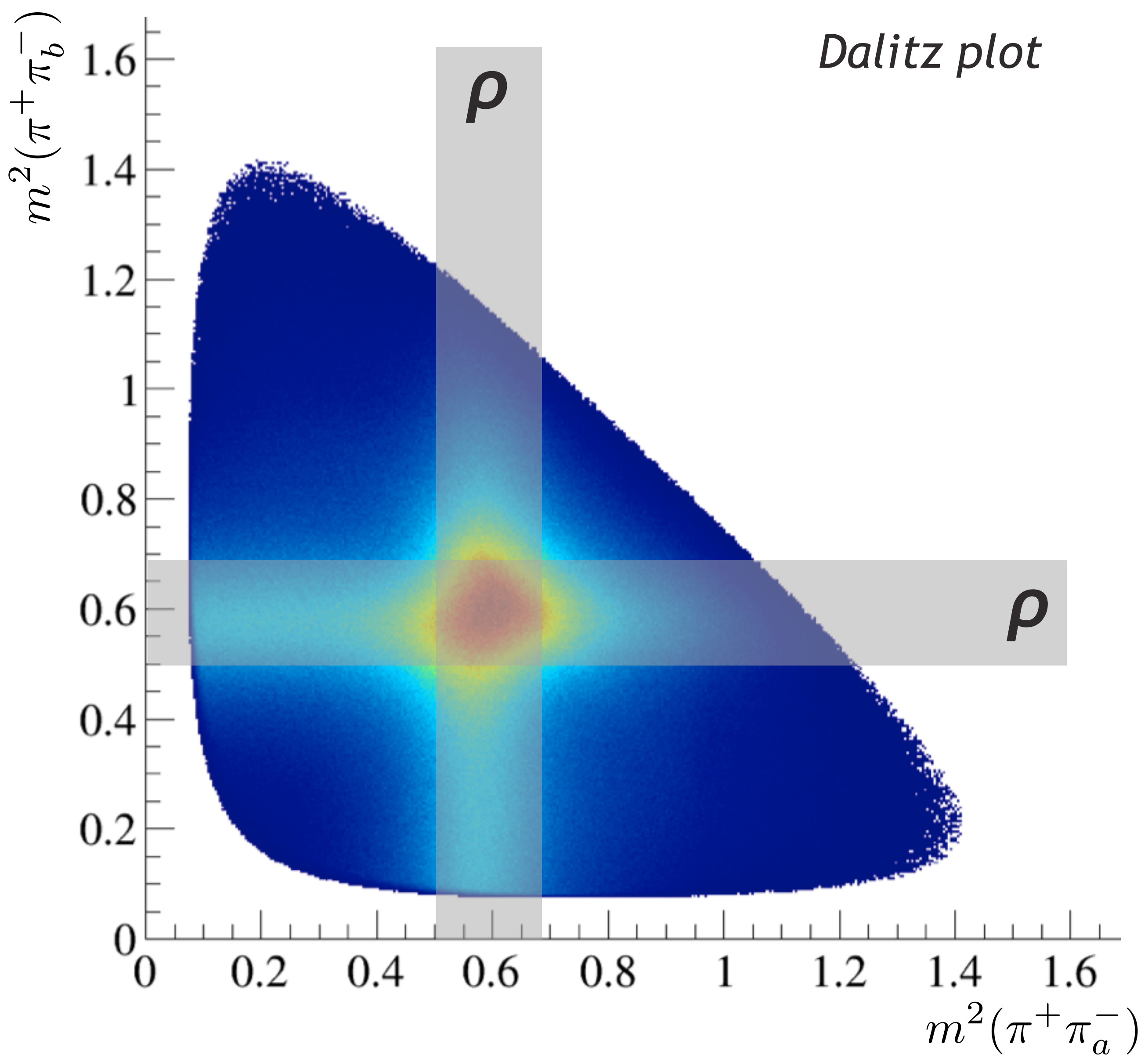

vector-pseudoscalar scattering

for heavier than physical light-quarks,
the $\boldsymbol{\rho}$ resonance becomes **stable**

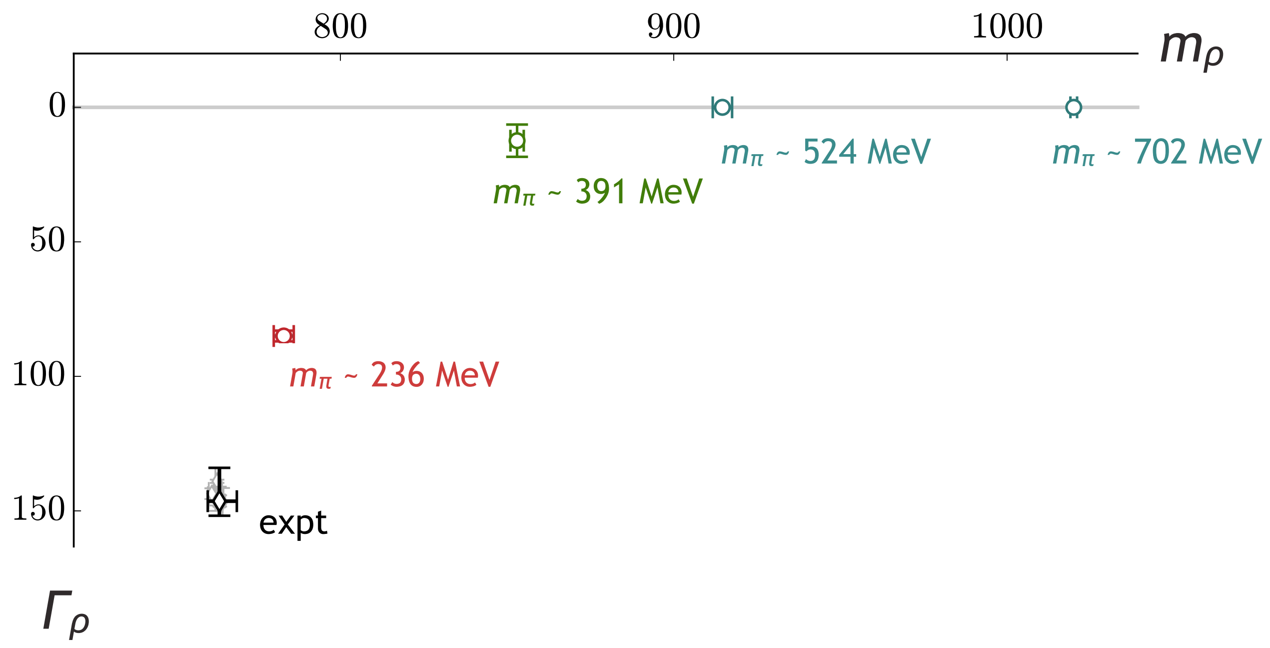

can rigorously study vector-pseudoscalar scattering

complication: need to account for the vector ***ρ* spin**

helicity formalism is common experimental approach,
but **ℓS formalism** more convenient in finite-volume

ℓS formalism

$$\left|J,m\,[\,^{2S+1}\ell_J]\right\rangle = \sum_{m_\ell, m_S} \left\langle \ell m_\ell; S m_S \middle| J m\right\rangle \left|S, m_S\right\rangle \otimes \left|\ell, m_\ell\right\rangle$$

e.g. with S=1 can make J^P=1⁺ in two ways: $^3S_1,\ ^3D_1$

⇒ coupled partial-waves $\quad \boldsymbol{t} = \begin{bmatrix} t(^3S_1|^3S_1) & t(^3S_1|^3D_1) \\ t(^3S_1|^3D_1) & t(^3D_1|^3D_1) \end{bmatrix}$

finite-volume function basis changes too

$$\overline{\mathcal{M}}_{\ell J m, \ell' J' m'} = \sum_{m_\ell, m'_\ell, m_S} \left\langle \ell m_\ell; 1 m_S \middle| J m\right\rangle \left\langle \ell' m'_\ell; 1 m_S \middle| J' m'\right\rangle \mathcal{M}_{\ell m_\ell, \ell' m'_\ell}$$

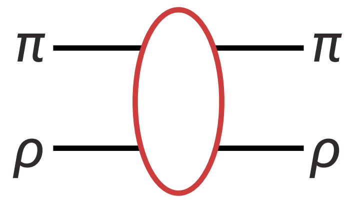
π
π
ρ
ρ

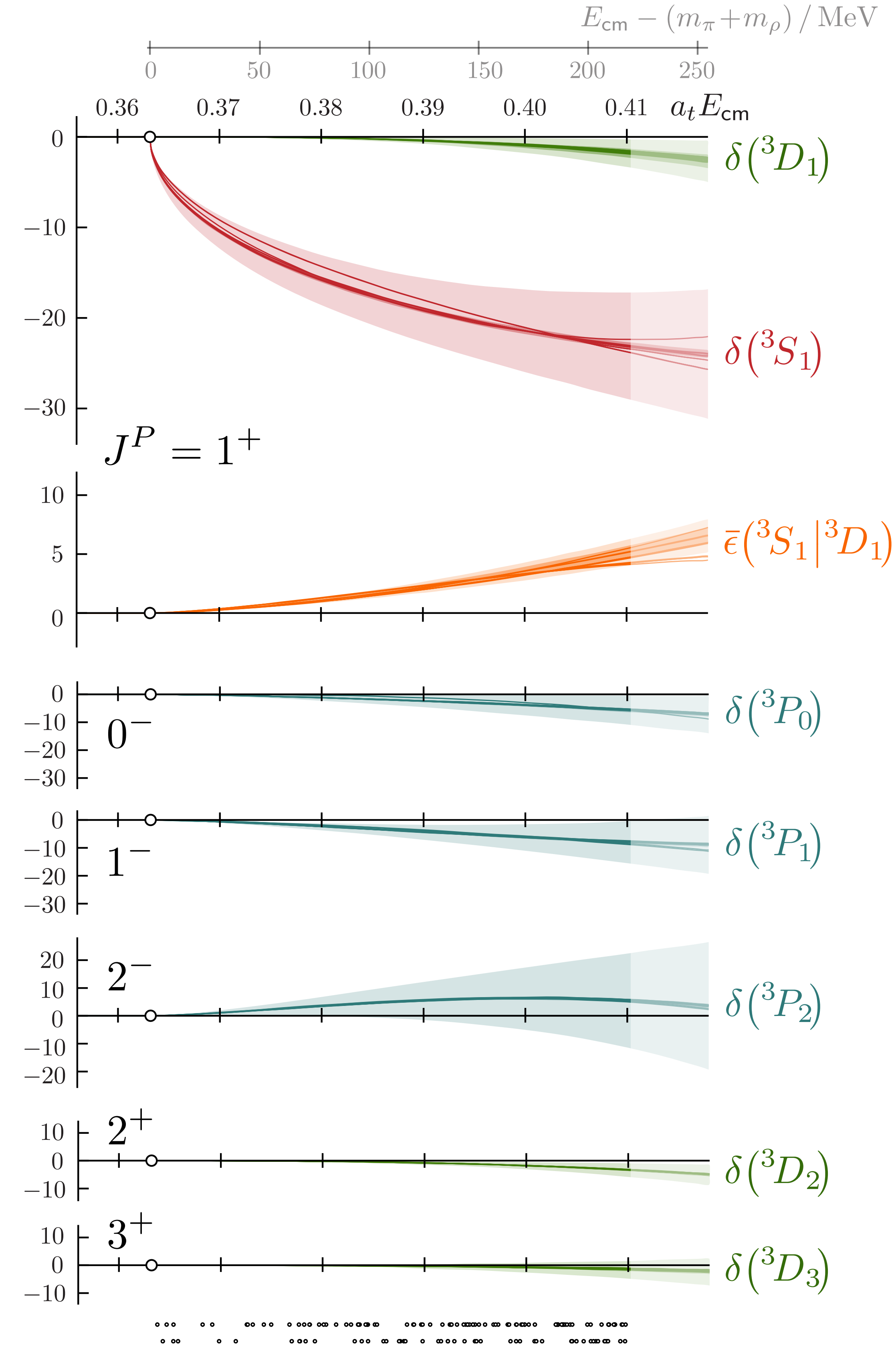
$E_{\rm cm} - (m_\pi + m_\rho)$ / MeV
0
50
100
150
200
250
0.36
0.37
0.38
0.39
0.40
0.41
$a_t E_{\rm cm}$
$\delta(^3D_1)$
$\delta(^3S_1)$
$J^P = 1^+$
$\bar{\epsilon}(^3S_1|^3D_1)$
0^-
$\delta(^3P_0)$
1^-
$\delta(^3P_1)$
2^-
$\delta(^3P_2)$
2^+
$\delta(^3D_2)$
3^+
$\delta(^3D_3)$

$\pi\omega$ isospin=1 — m_π~391 MeV

ω is stable down to quite low quark masses

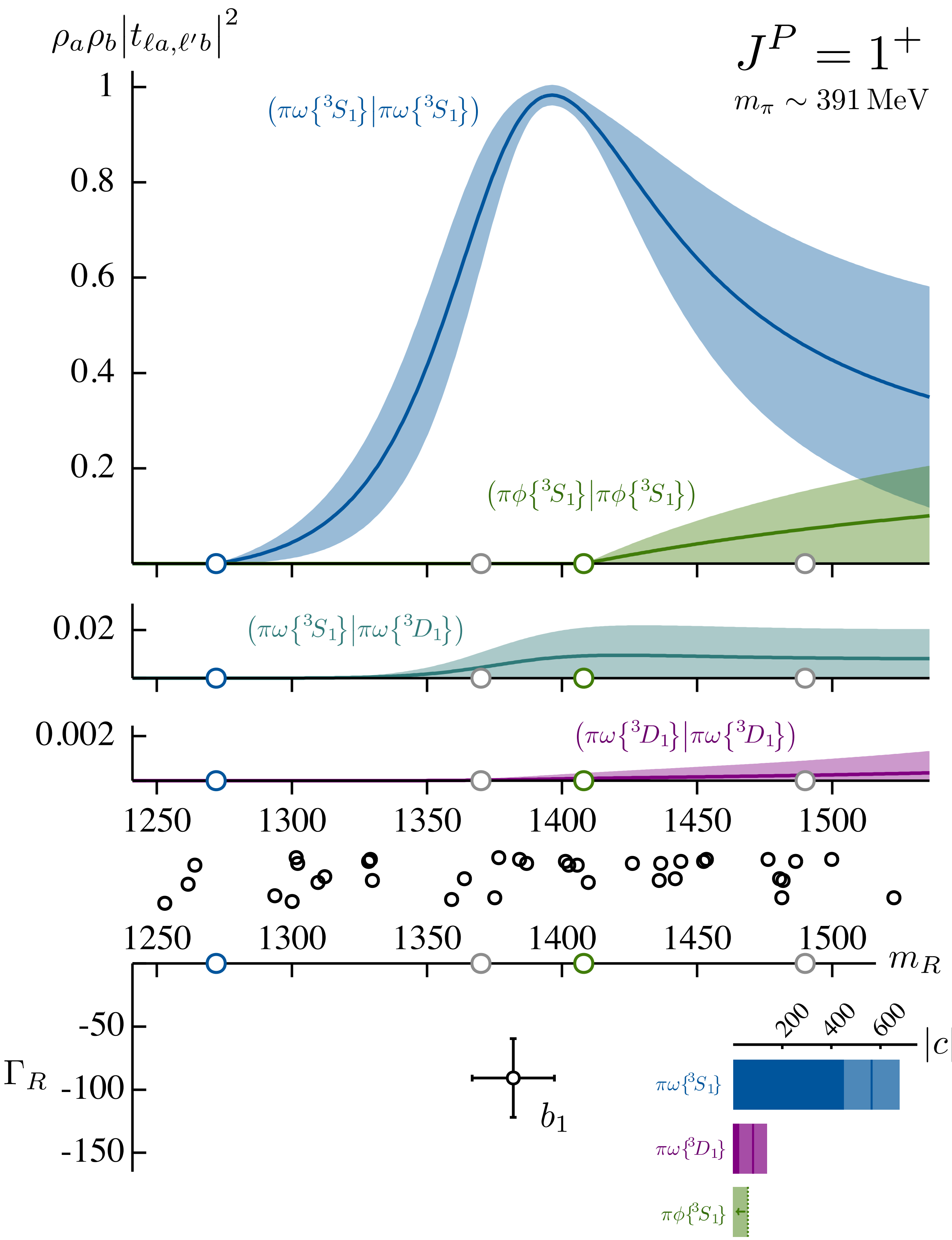

$b_1(1235)$ $\qquad I^G(J^{PC}) = 1^+(1^{+-})$

Mass $m = 1229.5 \pm 3.2$ MeV (S = 1.6)
Full width $\Gamma = 142 \pm 9$ MeV (S = 1.2)

$b_1(1235)$ DECAY MODES	Fraction (Γ_i/Γ)	Confidence level	p (MeV/c)
$\omega\pi$	dominant		348
[D/S amplitude ratio = 0.277 ± 0.027]			

excited J^{--} meson resonances — m_π~700 MeV

exact SU(3) flavor symmetry $\quad \omega_J^{\mathbf{1}} \to \eta^{\mathbf{8}}\omega^{\mathbf{8}}$

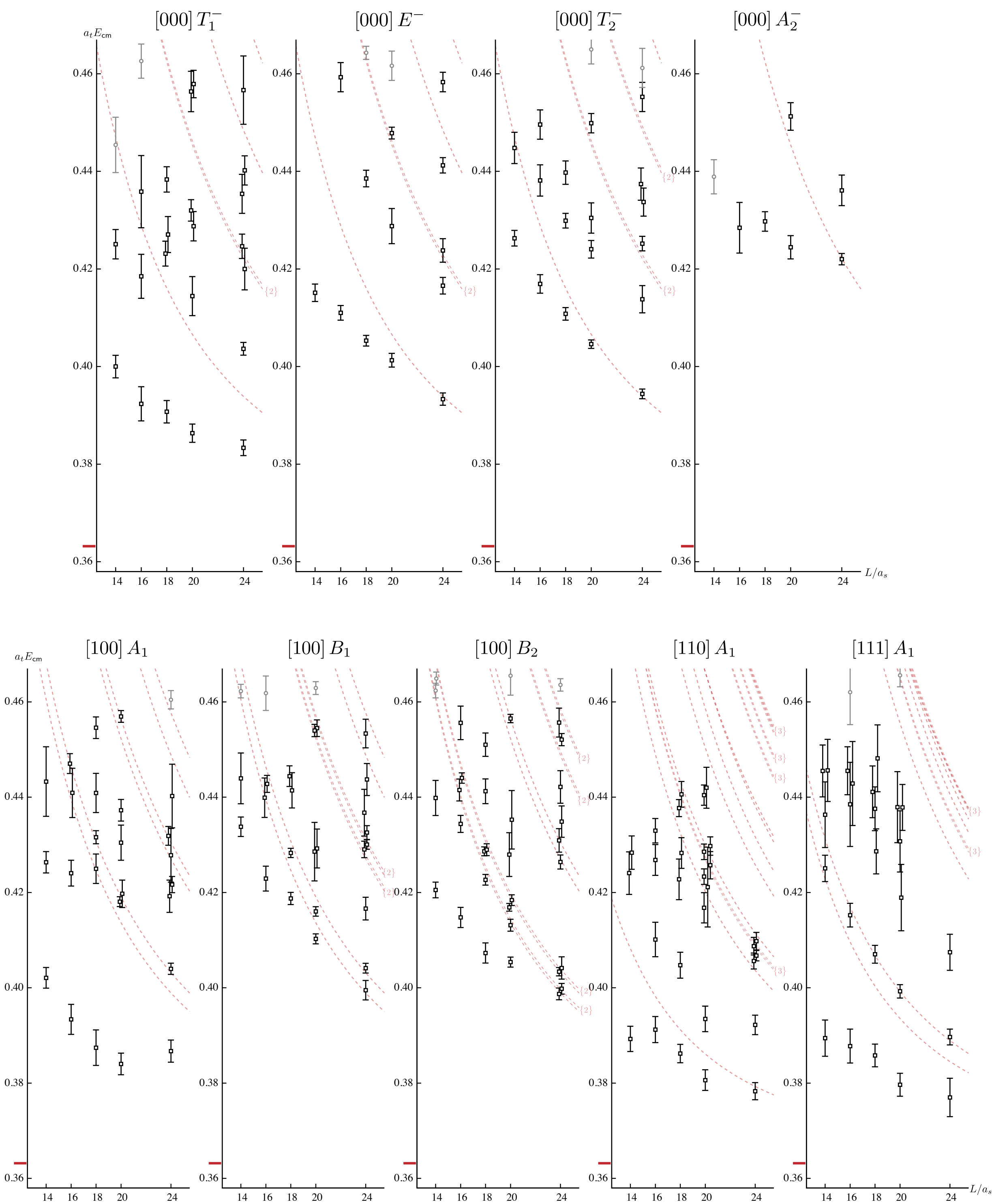

unprecedented number of energy levels

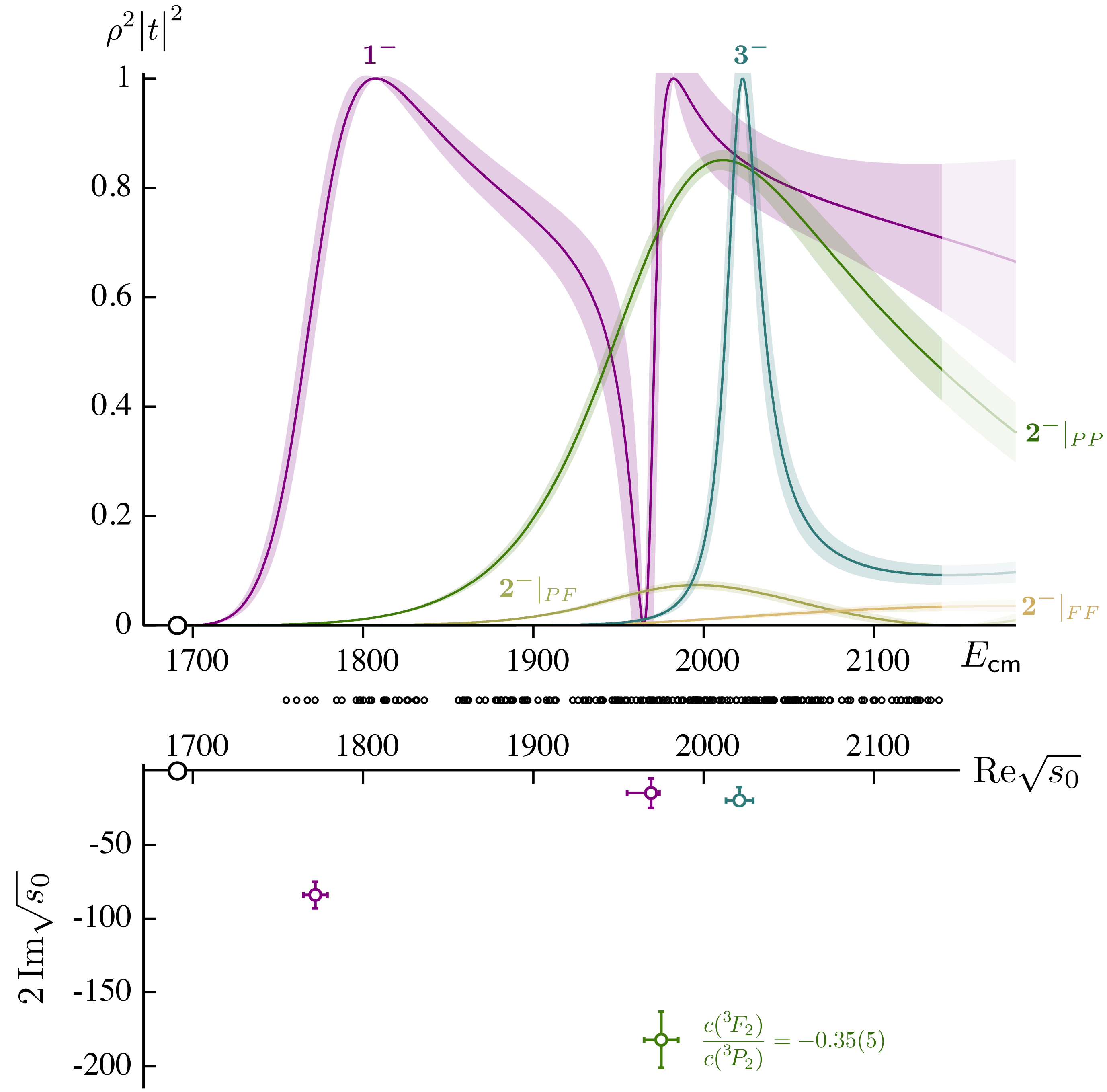

exotic 1^{-+} hybrid meson resonance — m_π~700 MeV

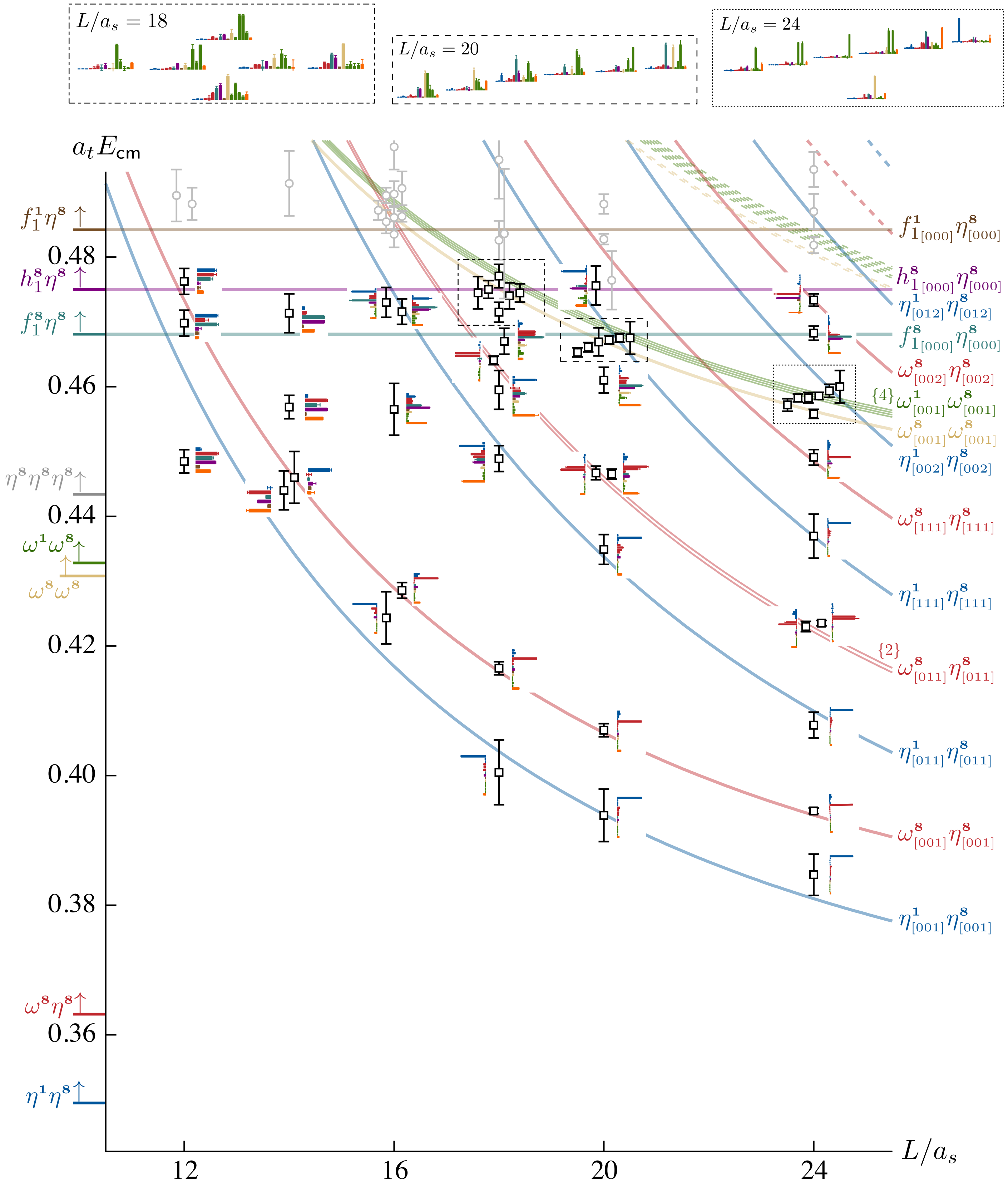

exotic 1^{-+} hybrid meson resonance — m_π~700 MeV

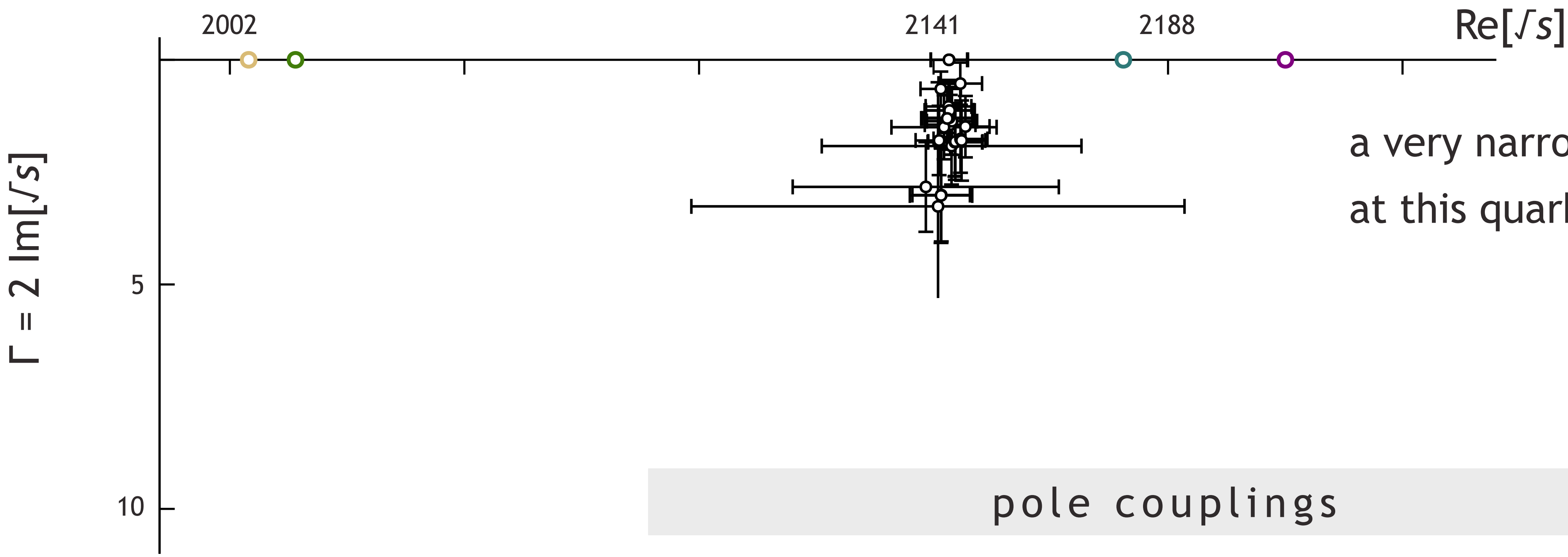

a very narrow resonance
at this quark mass

pole couplings

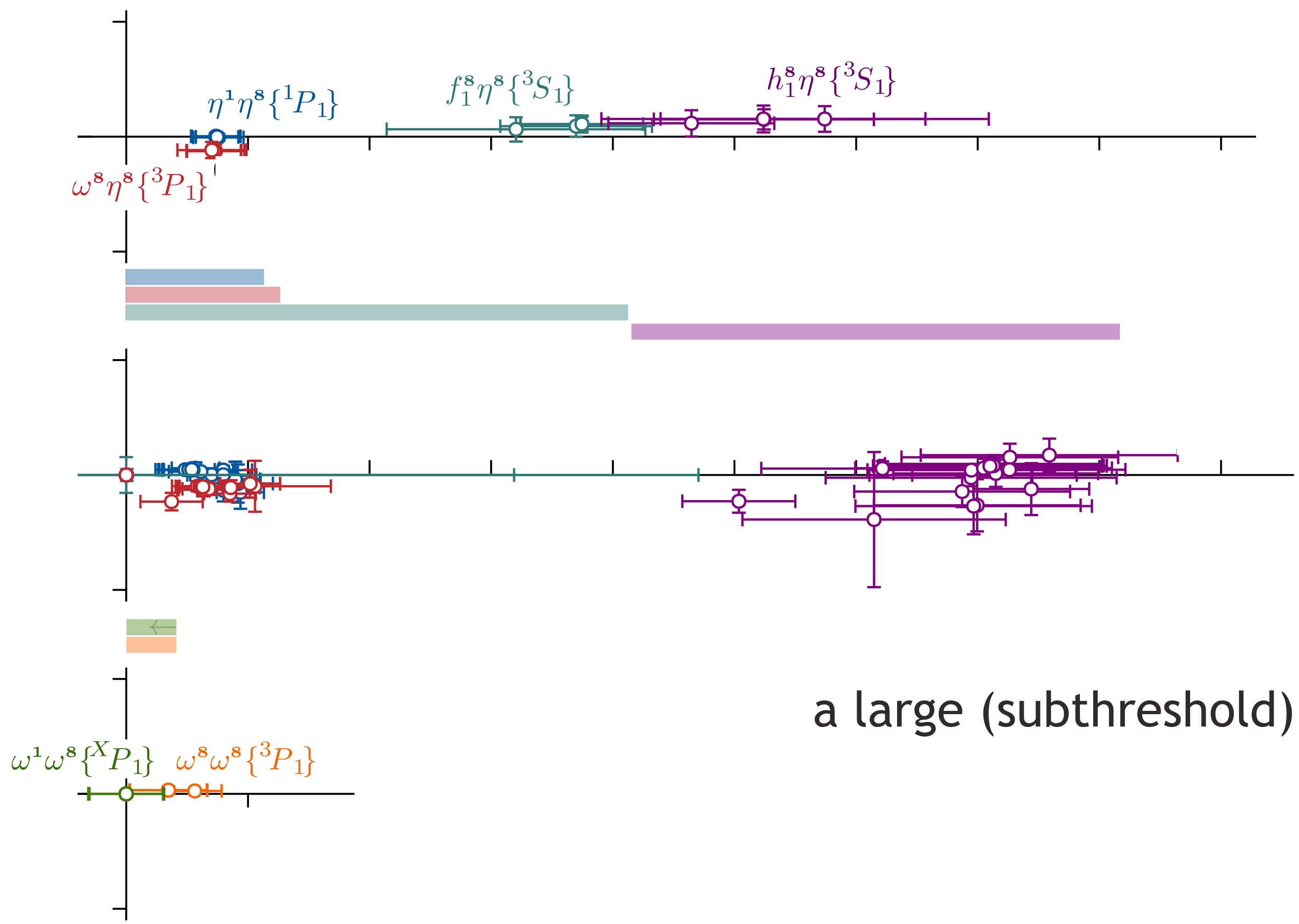

$$t_{ab}(s) \sim \frac{c_a c_b}{s_0 - s}$$

a large (subthreshold) coupling to

$h_1{}^8\eta^8$ ~ πb_1

exotic 1^{-+} hybrid meson resonance — m_π~700 MeV

a very crude extrapolation …

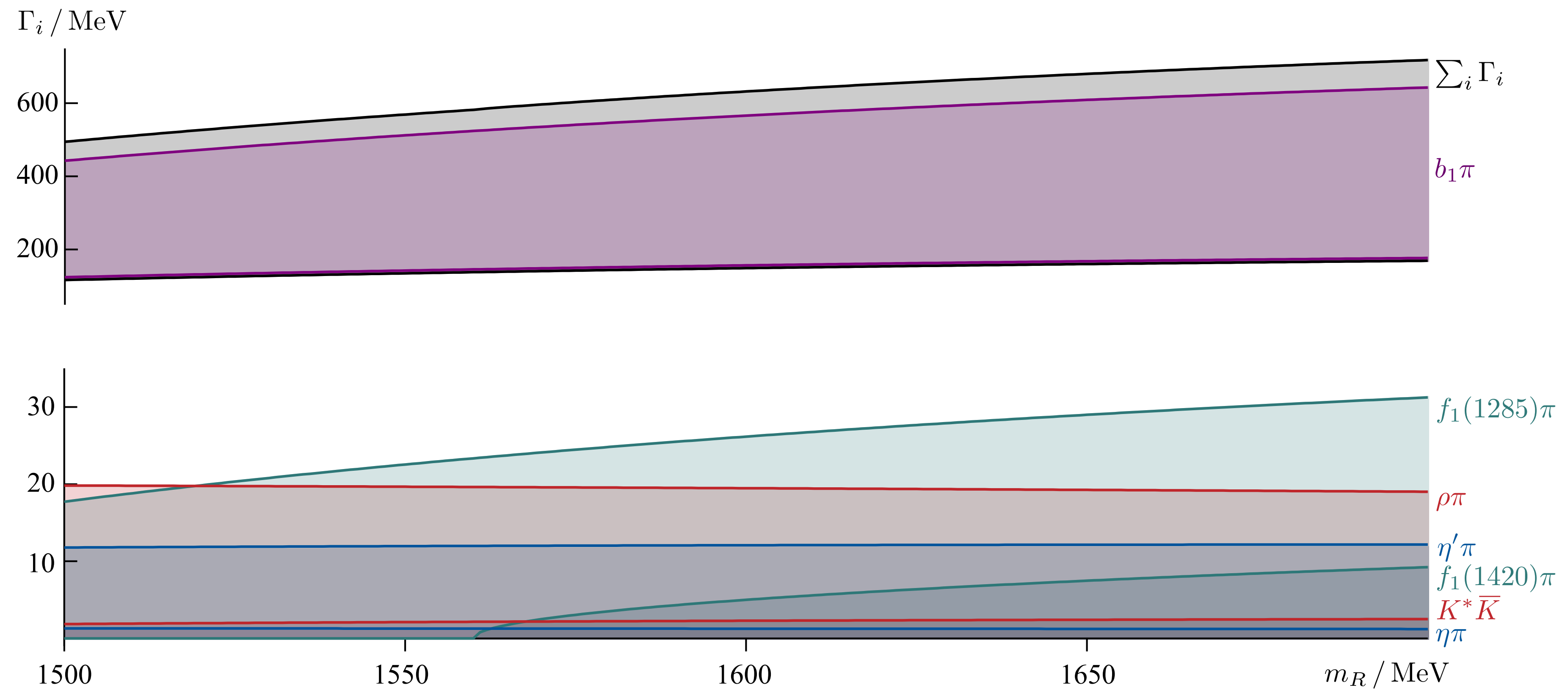

Determination of the Pole Position of the Lightest Hybrid Meson Candidate

A. Rodas,[1,*] A. Pilloni,[2,3,†] M. Albaladejo,[2,4] C. Fernández-Ramírez,[5] A. Jackura,[6,7] V. Mathieu,[2] M. Mikhasenko,[8] J. Nys,[9] V. Pauk,[10] B. Ketzer,[8] and A. P. Szczepaniak[2,6,7]

(Joint Physics Analysis Center)

Poles	Mass (MeV)	Width (MeV)
$a_2(1320)$	$1306.0 \pm 0.8 \pm 1.3$	$114.4 \pm 1.6 \pm 0.0$
$a_2'(1700)$	$1722 \pm 15 \pm 67$	$247 \pm 17 \pm 63$
π_1	$1564 \pm 24 \pm 86$	$492 \pm 54 \pm 102$

Investigation of the Lightest Hybrid Meson Candidate with a Coupled-Channel Analysis of $\bar{p}p$-, π^-p- and $\pi\pi$-Data

B. Kopf, M. Albrecht, H. Koch, J. Pychy, X. Qin,* and U. Wiedner
Ruhr-Universität Bochum, 44801 Bochum, Germany

name	pole mass [MeV/c^2]	pole width [MeV]
$a_2(1320)$	$1308.7 \pm 0.4^{+2.0}_{-4.2}$	$108.6 \pm 0.4^{+1.8}_{-12.9}$
$a_2(1700)$	$1669.2 \pm 1.0^{+20.2}_{-4.6}$	$429.0 \pm 1.7^{+44.4}_{-9.7}$
π_1	$1561.6 \pm 3.0^{+6.6}_{-2.6}$	$388.1 \pm 5.4^{+0.2}_{-14.1}$

why the heavier quark masses ?

we **can** compute spectra at lighter quark masses, but we wouldn't know what to do with them

the problem is three-body and higher channels…

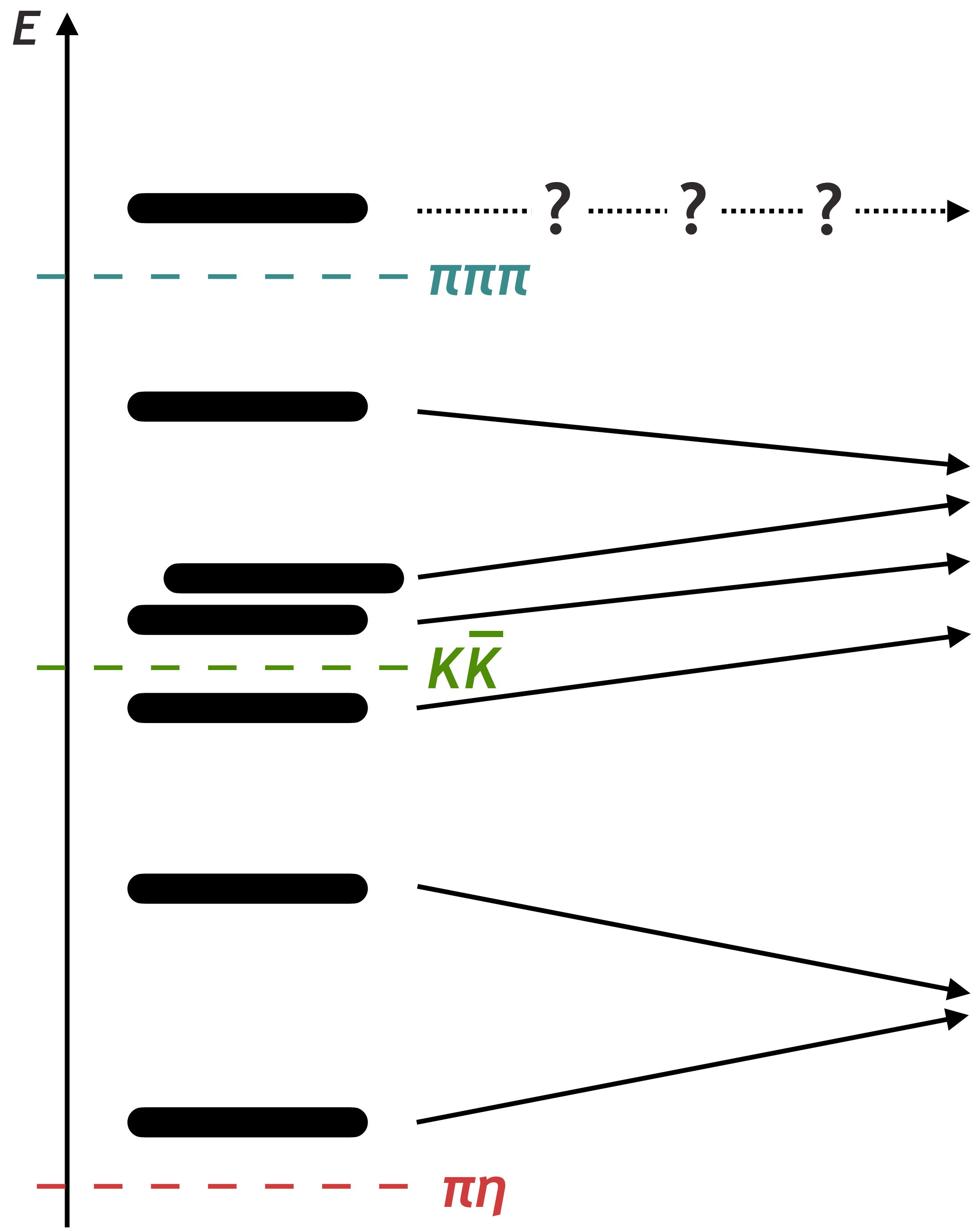

$$\begin{pmatrix} t_{\pi\eta,\pi\eta} & t_{\pi\eta,K\bar{K}} & t_{\pi\eta,\pi\pi\pi} \\ t_{\pi\eta,K\bar{K}} & t_{K\bar{K},K\bar{K}} & t_{K\bar{K},\pi\pi\pi} \\ t_{\pi\eta,\pi\pi\pi} & t_{K\bar{K},\pi\pi\pi} & t_{\pi\pi\pi,\pi\pi\pi} \end{pmatrix}$$

all the complications of infinite-volume three-body (+ more?)

$$\begin{pmatrix} t_{\pi\eta,\pi\eta} & t_{\pi\eta,K\bar{K}} \\ t_{\pi\eta,K\bar{K}} & t_{K\bar{K},K\bar{K}} \end{pmatrix}$$

$$t_{\pi\eta,\pi\eta}$$

physical pion masses = low-lying multipion channels

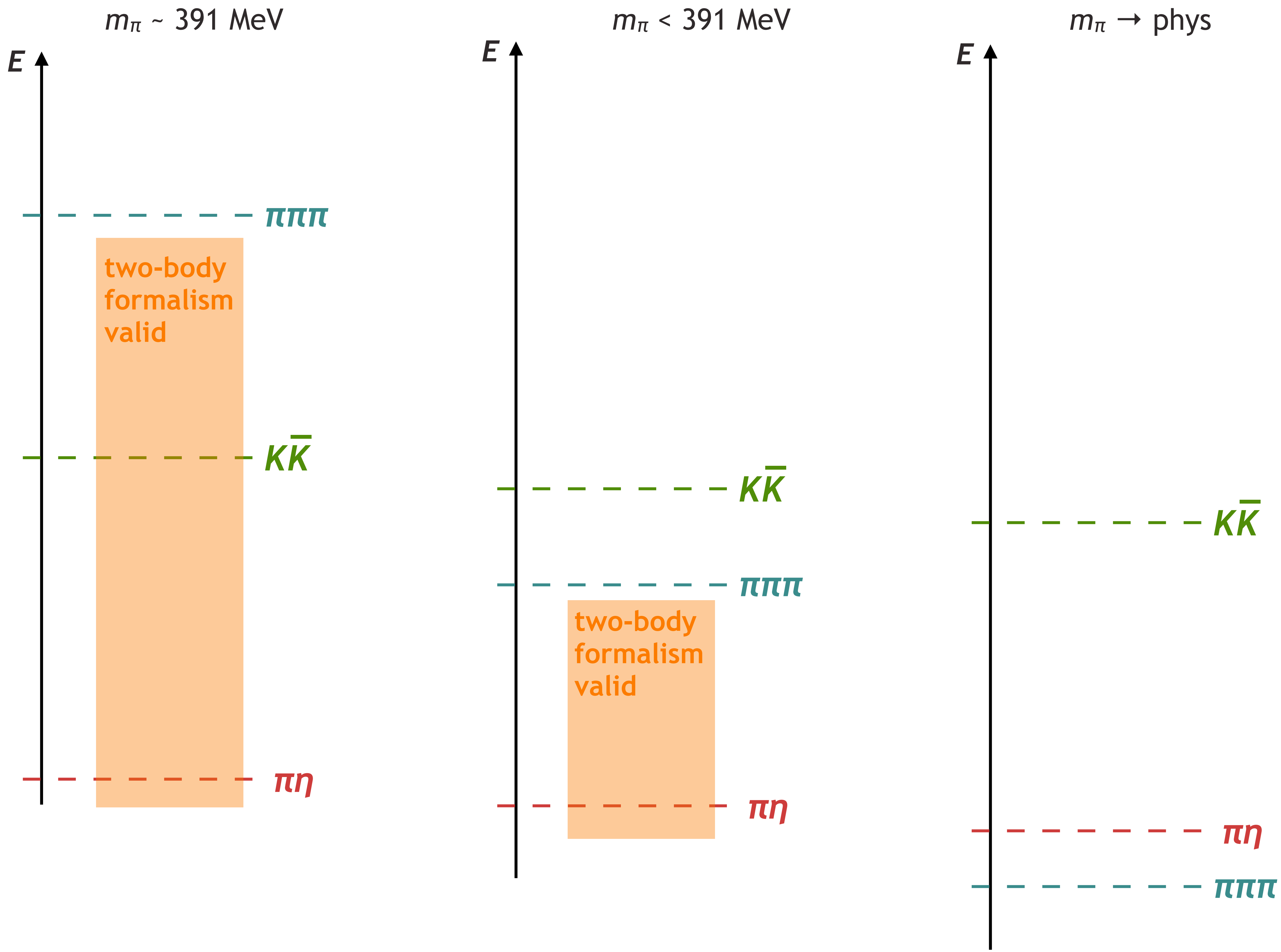

rigorous three body scattering

formalism is significantly more complicated — first applications have appeared

The energy-dependent $\pi^+\pi^+\pi^+$ scattering amplitude from QCD

Maxwell T. Hansen,[1,*] Raul A. Briceño,[2,3,†] Robert G. Edwards,[2,‡] Christopher E. Thomas,[4,§] and David J. Wilson[4,¶]
(for the Hadron Spectrum Collaboration)

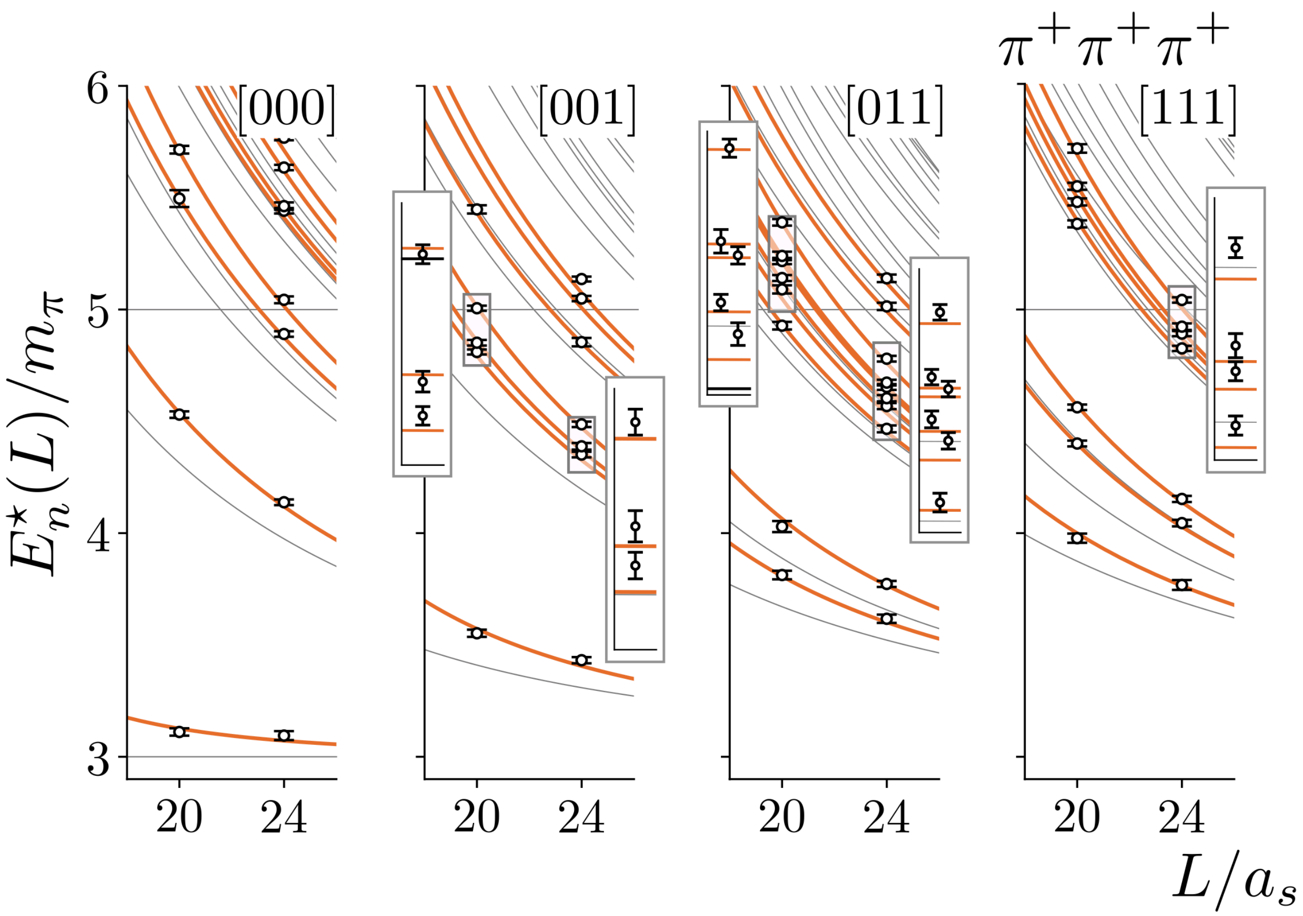

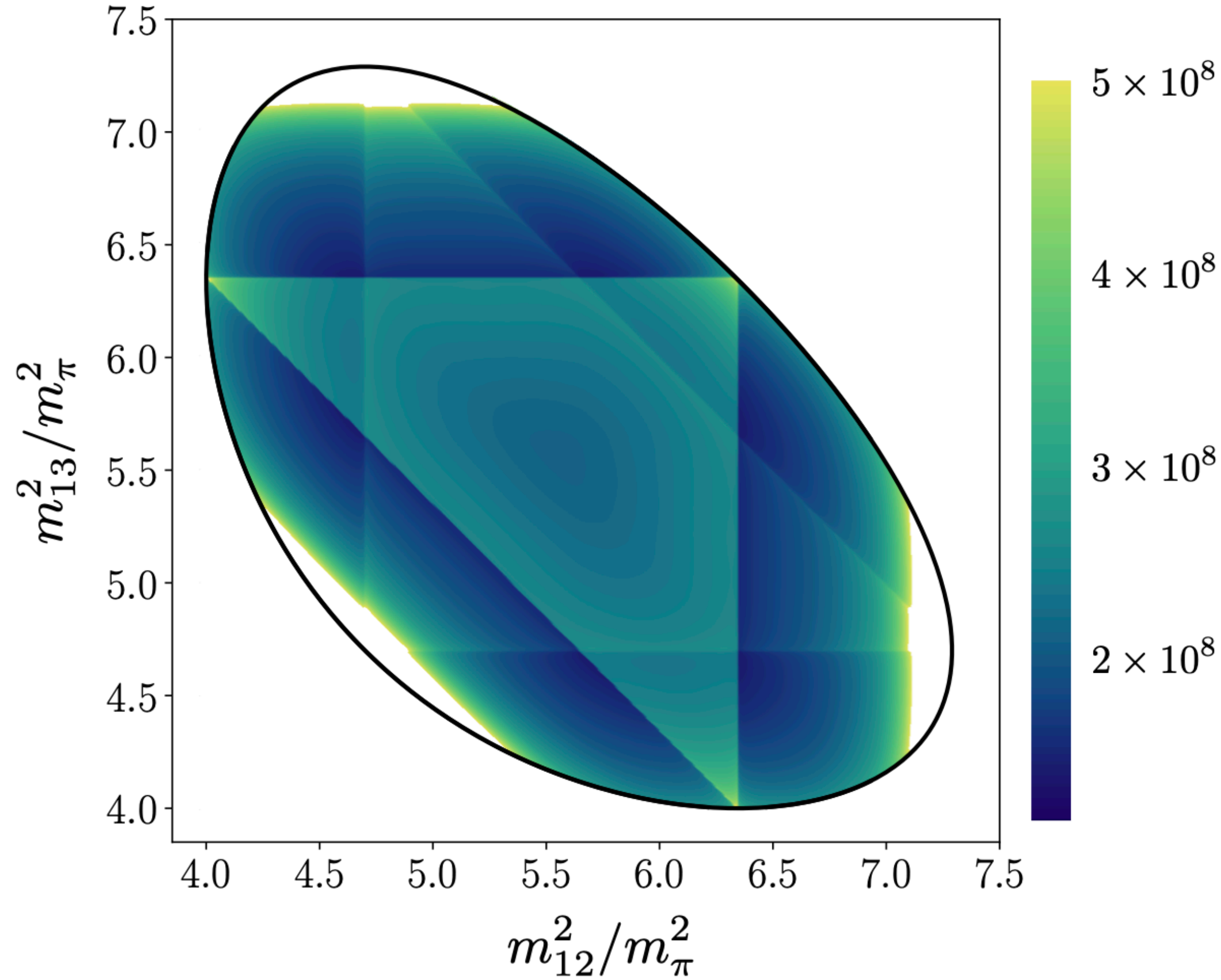

coupling scattering systems to external currents

e.g. consider the process in which
a pion absorbs a photon* to become two pions $\gamma\pi \to \pi\pi$

* could be virtual

in infinite volume, described by a matrix element $\langle \pi\pi(E_{\mathsf{cm}}, \mathbf{P}) | j^\mu(0) | \pi(\mathbf{p}) \rangle$

$\pi\pi$ state can be projected into a partial wave, e.g. ℓ=1

$$\propto F(E_{\mathsf{cm}}, Q^2)$$

after the current produces $\pi\pi$ ... $\pi\pi$ will rescatter strongly

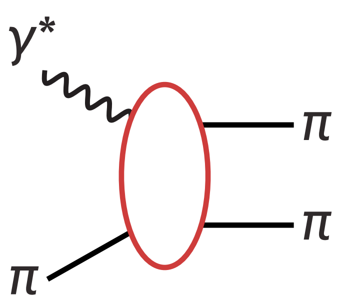

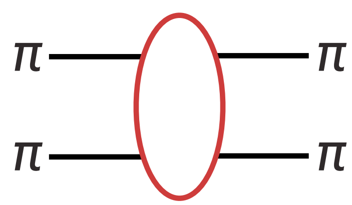

$\Rightarrow$ the matrix element is proportional to $t_\ell(E_{\mathsf{cm}})$

if there's a resonance $t_\ell(s \sim s_0) \sim \dfrac{c^2}{s_0 - s}$ and $F(s \sim s_0, Q^2) \sim \dfrac{c\, f(Q^2)}{s_0 - s}$

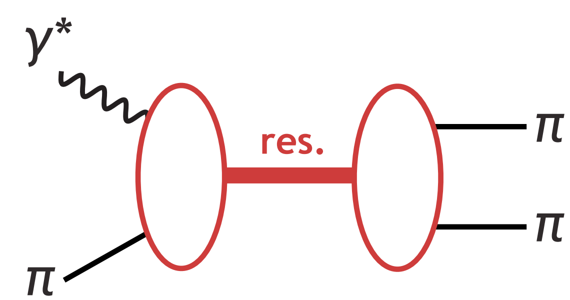

resonance transition form-factor $f(Q^2)$
rigorously defined at the complex pole position

e.g. $\rho \to \pi\gamma$

but what changes in a finite volume ... ?

coupling scattering systems to external currents — fin. vol.

e.g. consider the process in which
a pion absorbs a photon to become two pions

$$\gamma\pi \to \pi\pi$$

infinite volume

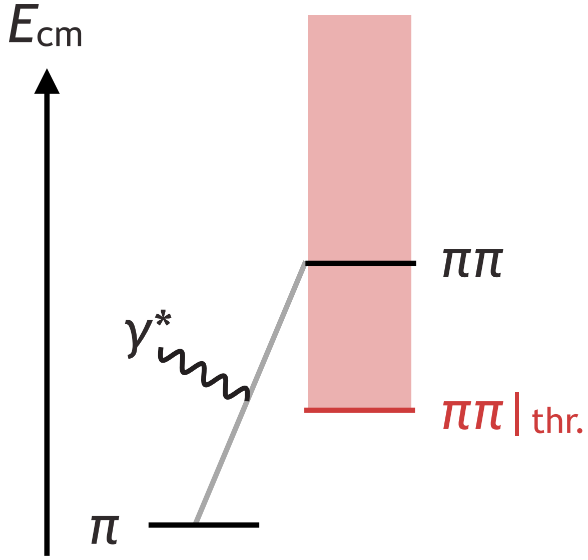

can transition
to any energy
in the $\pi\pi$ continuum

finite volume

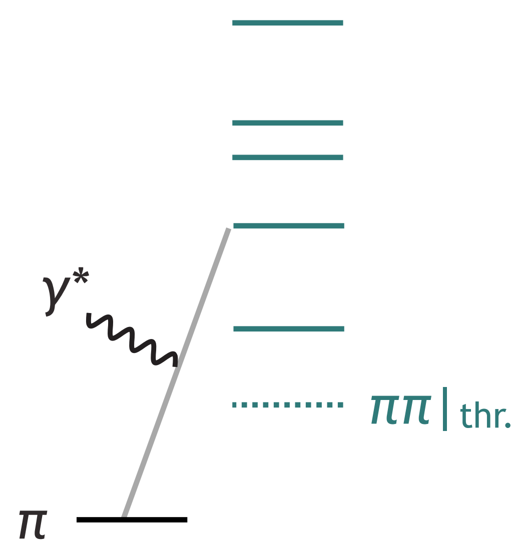

can only transition
to one of the discrete
f.v. eigenstates

finite-volume matrix element

$$_L\big\langle \pi\pi(E_n(L),\mathbf{P})\big| j^\mu(0) \big|\pi(\mathbf{p})\big\rangle_L$$

single hadron state

$$\big|\pi(\mathbf{p})\big\rangle_L = \big|\pi(\mathbf{p})\big\rangle_\infty + O(e^{-m_\pi L})$$

hadron-hadron state

$$\big|\pi\pi(E_n(L),\mathbf{P})\big\rangle_L \sim \sqrt{\mathcal{R}_n}\,\big|\pi\pi(E_{\mathrm{cm}} = E_n(L),\mathbf{P})\big\rangle_\infty$$

effective f.v.
normalization

$$\mathcal{R}_n = 2E_n \lim_{E\to E_n} (E - E_n)\Big(F^{-1}(E,\mathbf{P};L) + M(E)\Big)^{-1}$$

$$F = \tfrac{1}{16\pi}\, i\rho\,(1 + i\mathcal{M})$$

$$M = 16\pi\, t$$

effective f.v. normalization depends
on the hadron-hadron scattering amplitude

$\pi\pi \to \pi\gamma$ lattice QCD calculation

m_π~391 MeV | PRL115 242001 (2015) | PRD93 114508 (2016)

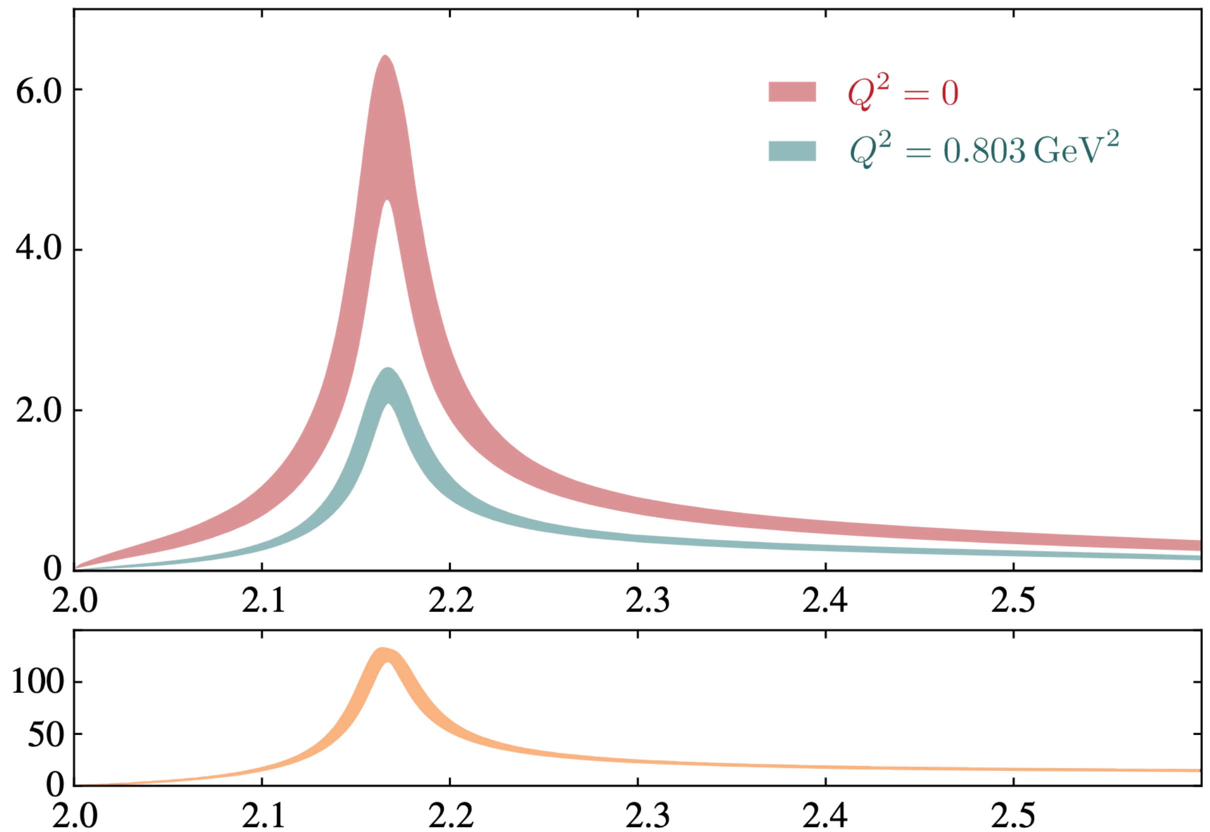

form-factor at the pole

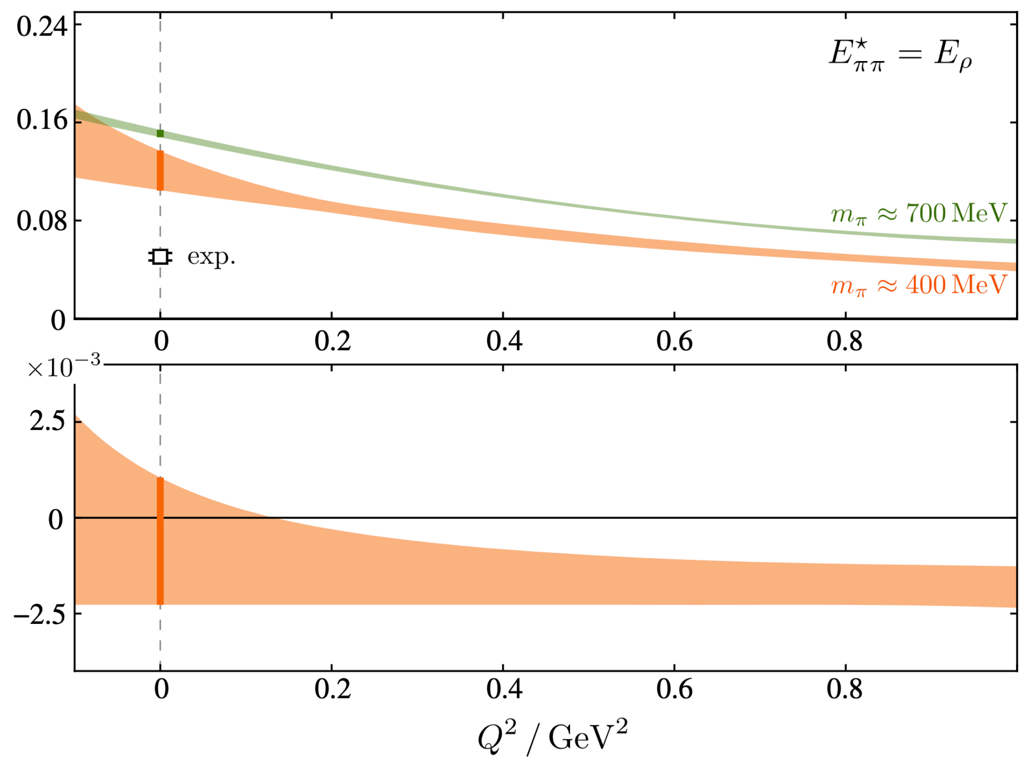

the missing singularity — the 'left-hand cut'

consider the amplitude **before** we partial-wave projected

a function of both ***s*** and ***t***

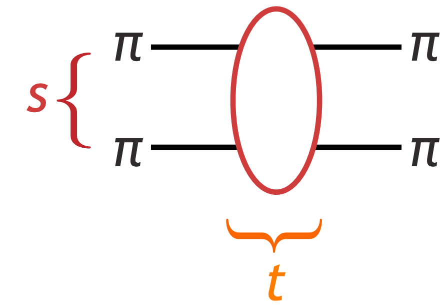

$T(s,t)$

the same amplitude should describe **crossed-channel** scattering

e.g. suppose a stable (scalar) hadron can be exchanged in the ***t*-channel**
what would that imply for the partial-wave amplitude ?

$$T(s,t) = \frac{g^2}{M^2 - t}$$

$$t_\ell(s) = \tfrac{1}{2}\int_{-1}^{1} dx\, P_\ell(x)\, T(s,t(x))$$

$$x = \cos\theta$$
$$t = -2k^2(1-x)$$

S-wave

$$t_0(s) = \tfrac{1}{2} g^2 \int_{-1}^{1} dx\, \frac{1}{M^2 + 2k^2(1-x)}$$

$$t_0(s) = \frac{g^2}{4k^2} \log\left[\frac{s - 4m^2 + M^2}{M^2}\right]$$

branch point at
$s = 4m^2 - M^2$

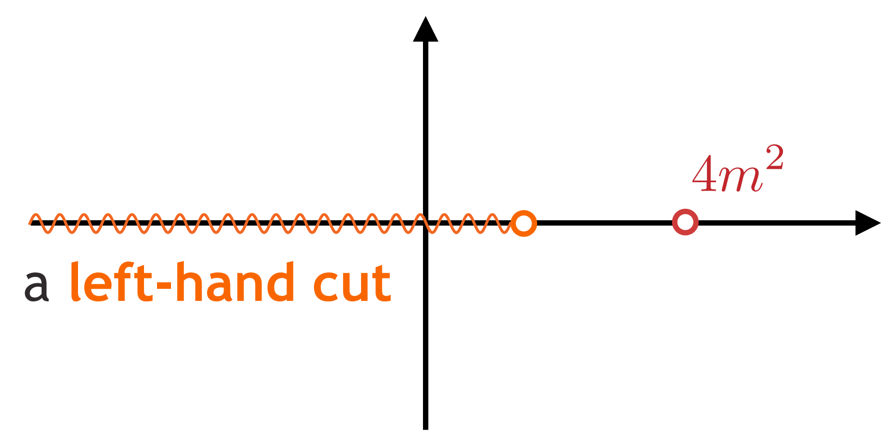

a **left-hand cut**

the missing singularity — the ‘left-hand cut’

consider the amplitude **before** we partial-wave projected

a function of both ***s*** and ***t***

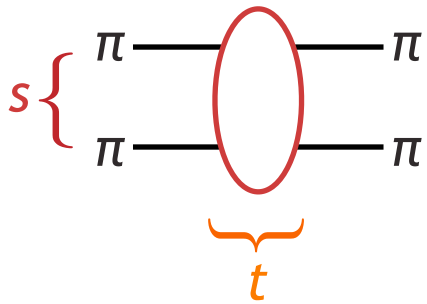

$T(s,t)$

more generally, **unitarity** in the **crossed-channels** demands a **left-hand cut**

dispersion at fixed *s*

$$T(s,t) = \frac{1}{2\pi i}\int_{4m^2}^{\infty} d\bar{t}\,\frac{\mathrm{disc}_t\, T(s,\bar{t})}{\bar{t}-t} + u\text{—channel}$$

$$t_\ell(s) = \tfrac{1}{2}\int_{-1}^{1} dx\, P_\ell(x)\, T(s,t(x))$$

$$x = \cos\theta \qquad t = -2k^2(1-x)$$

$$t_\ell(s) = \frac{1}{4\pi i k^2}\int_{4m^2}^{\infty} d\bar{t}\;\mathrm{disc}_t\, T(s,\bar{t})\; \tfrac{1}{2}\int_{-1}^{1} dx\,\frac{P_\ell(x)}{\left(1+\frac{\bar{t}}{2k^2}\right)-x}$$

$$= Q_\ell\!\left(1+\frac{\bar{t}}{2k^2}\right)$$

Legendre function of the second kind

$Q_\ell(z)$ has branch points at **z=±1**

singularity if $\bar{t} = -4k^2 = 4m^2 - s$

which is in the integration region if $s < 0$

***t*-channel unitarity** generates a **left-hand cut**

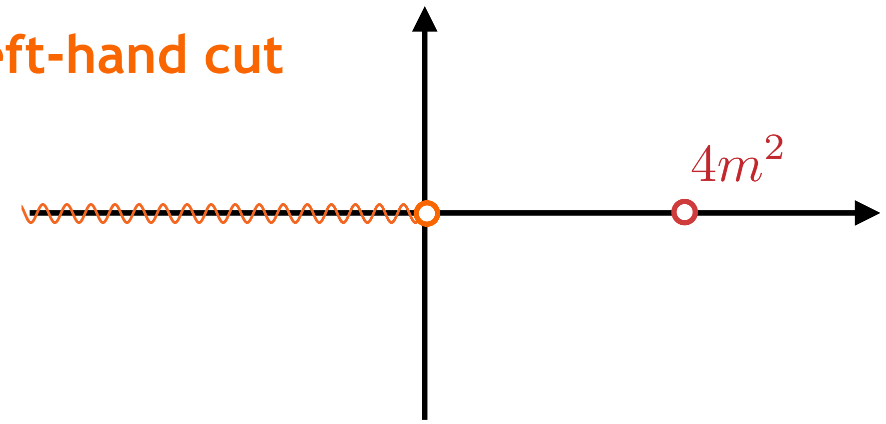

importance of the left-hand cut ?

narrow resonance

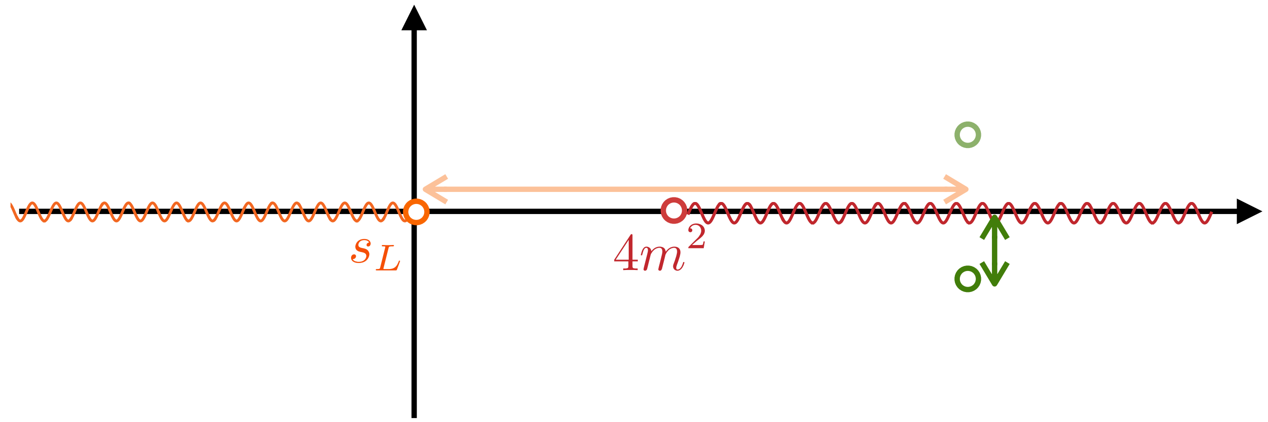

resonance pole nearby
left-hand cut very distant

e.g. can describe scattering near the ρ resonance without describing the left-hand cut

broad resonance

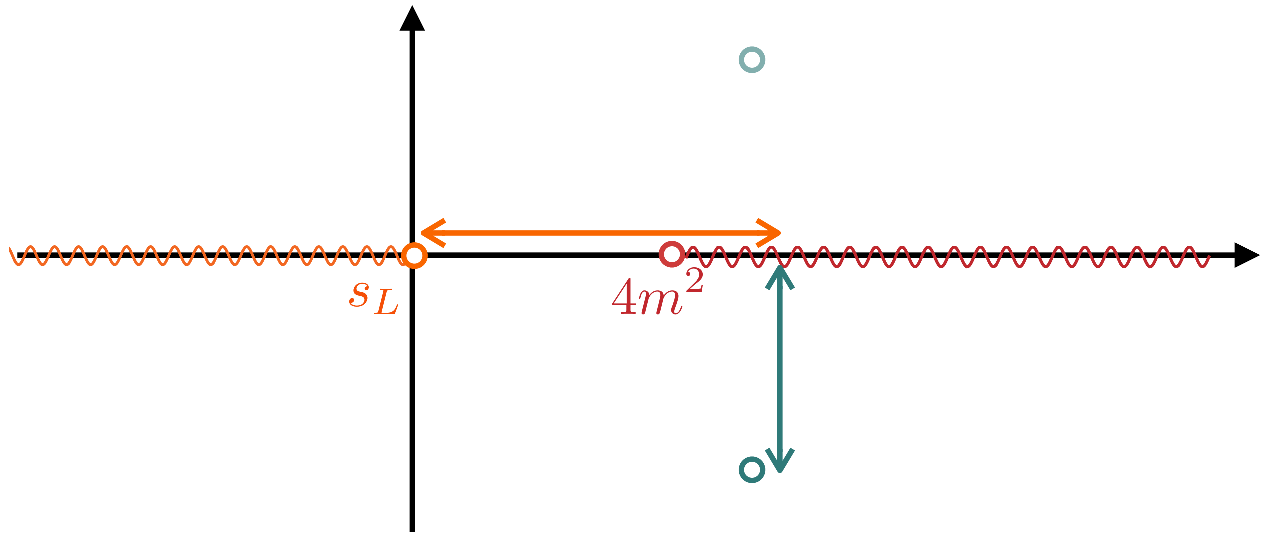

left-hand cut
may be as close as
resonance pole

e.g. the σ resonance in $\pi\pi$ I=0

importance of the left-hand cut ?

narrow resonance

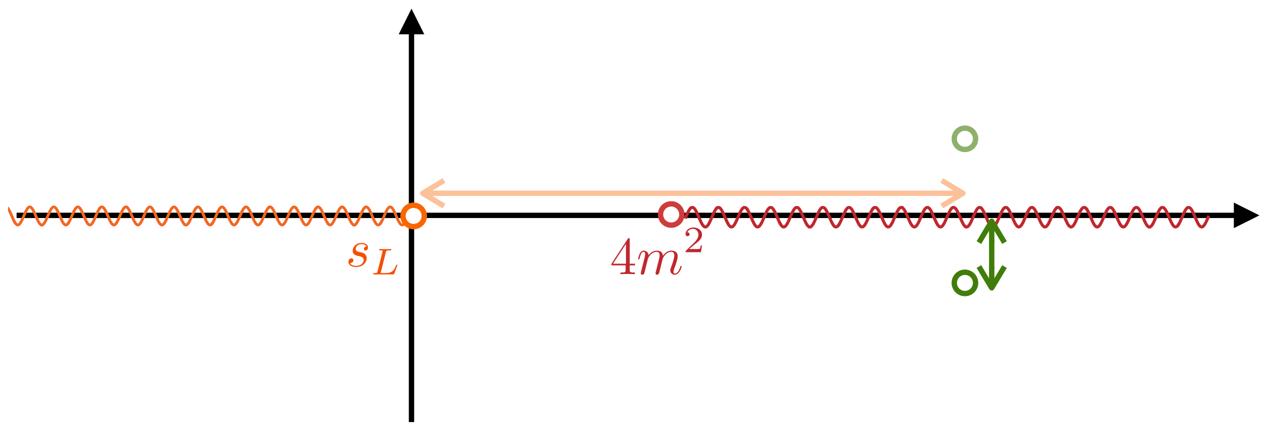

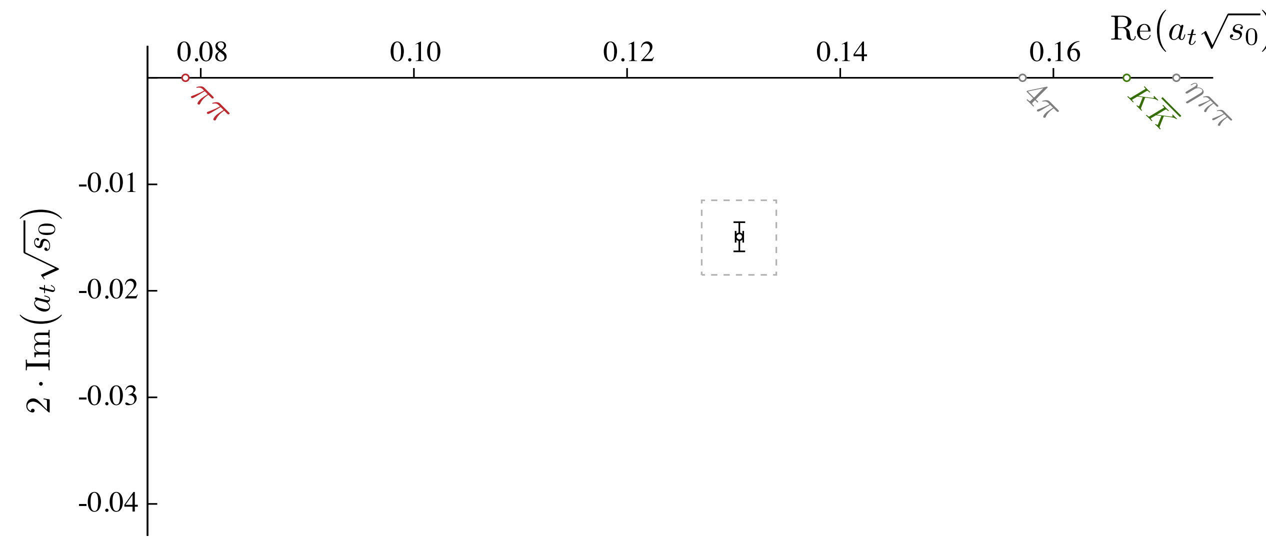

broad resonance

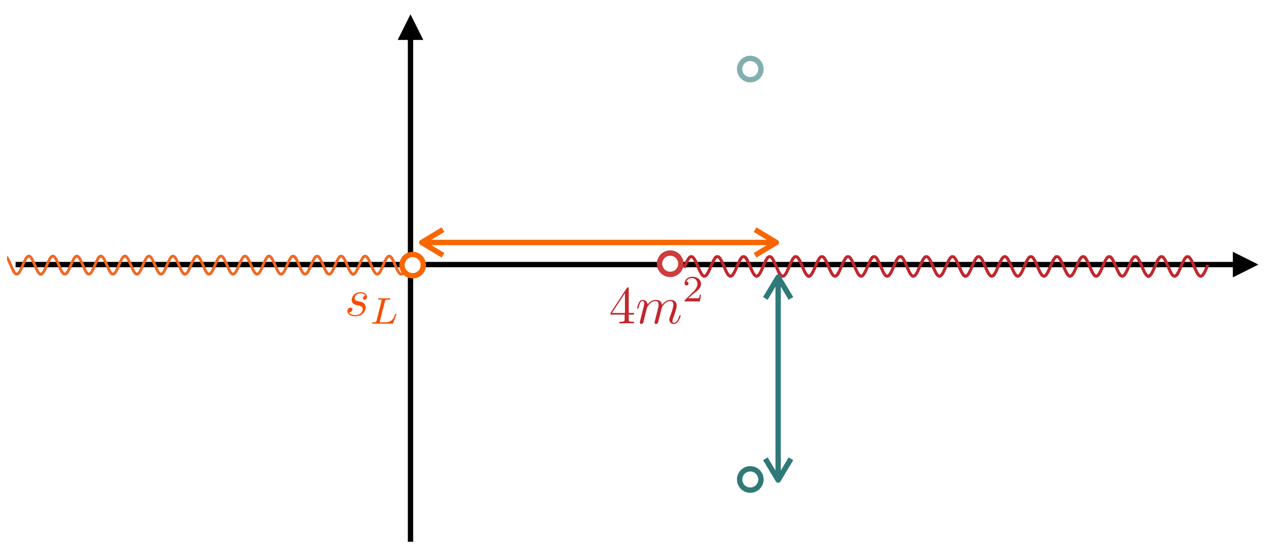

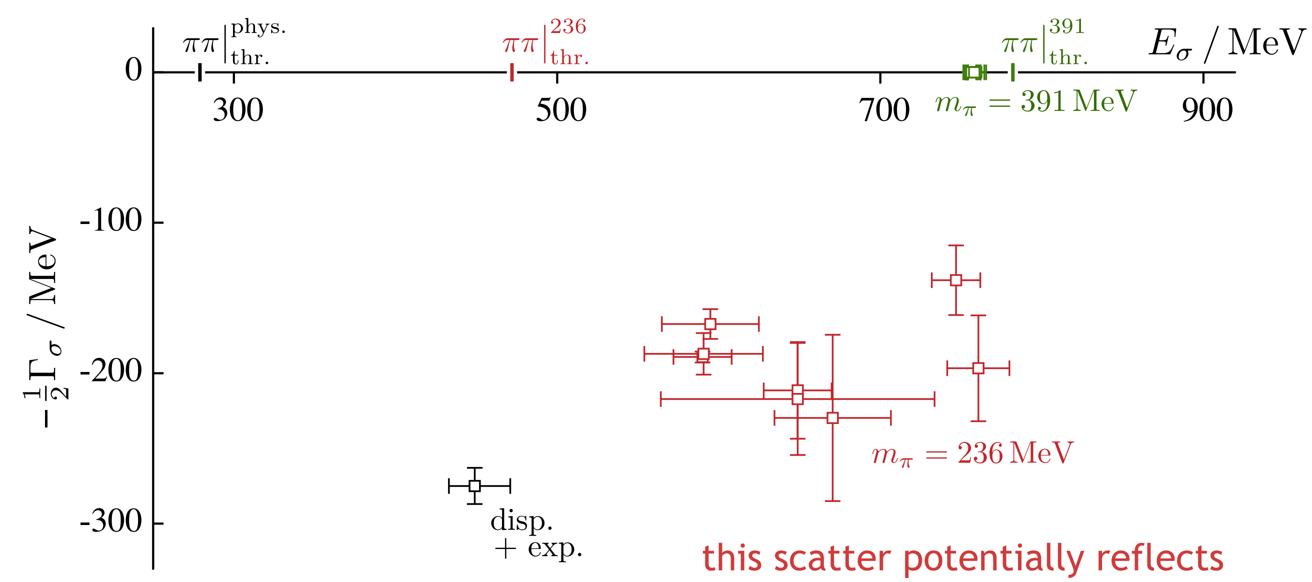

this scatter potentially reflects
the absence of accurate constraint
on the left-hand cut ...

channel decoupling below thresholds

coupled-channel quantization condition $\det\Big[\mathbf{1} + i\boldsymbol{\rho t}\big(\mathbf{1} + i\boldsymbol{\mathcal{M}}\big)\Big] = 0$

e.g. two channels $\boldsymbol{\rho t} = \begin{pmatrix} \rho_1 t_{11} & \rho_1 t_{12} \\ \rho_2 t_{12} & \rho_2 t_{22} \end{pmatrix}$ $\quad \boldsymbol{\mathcal{M}} = \begin{pmatrix} \mathcal{M}(k_1) & 0 \\ 0 & \mathcal{M}(k_2) \end{pmatrix}$

$$\mathbf{1} + i\boldsymbol{\rho t}\big(\mathbf{1} + i\boldsymbol{\mathcal{M}}\big) = \begin{pmatrix} 1 + i\rho_1 t_{11}(1 + i\mathcal{M}_1) & i\rho_1 t_{12}(1 + i\mathcal{M}_2) \\ i\rho_2 t_{12}(1 + i\mathcal{M}_1) & 1 + i\rho_2 t_{22}(1 + i\mathcal{M}_2) \end{pmatrix}$$

e.g. consider the rest-frame A_1 irrep – below threshold: $\mathcal{M}(i\kappa) = i - \frac{i}{\kappa} \sum_{\mathbf{n} \neq \mathbf{0}} \frac{e^{-\kappa |\mathbf{n}| L}}{|\mathbf{n}| L}$

so **far below threshold** $\mathcal{M} \to i$

suppose we're above threshold 1, but well below threshold 2 $\mathbf{1} + i\boldsymbol{\rho t}\big(\mathbf{1} + i\boldsymbol{\mathcal{M}}\big) \to \begin{pmatrix} 1 + i\rho_1 t_{11}(1 + i\mathcal{M}_1) & 0 \\ i\rho_2 t_{12}(1 + i\mathcal{M}_1) & 1 \end{pmatrix}$

quantization condition → $1 + i\rho_1 t_{11}(1 + i\mathcal{M}_1) = 0$

which is the one-channel condition